STUDIES ON PHOTOCHEMICAL REACTIONS OF THREE-COMPONENT SYSTEMS INVOLVING ELECTRON TRANSFER

TETSURO MAJIMA

OSAKA UNIVERSITY
OSAKA, JAPAN

JANUARY, 1980

STUDIES ON PHOTOCHEMICAL REACTIONS OF THREE-COMPONENT SYSTEMS INVOLVING ELECTRON TRANSFER

(電子移動を含む三成分系の光化学反応に関する研究)

TETSURO MAJIMA

OSAKA UNIVERSITY
OSAKA, JAPAN

JANUARY, 1980

PREFACE

This thesis deals with the studies accomplised by the author under the guidance by Professor Hiroshi Sakurai at the Institute of Scientific and Industrial Research, Osaka University.

The author would like to express his sincere thanks to Professor Hiroshi Sakurai for his invaluable guidance and constant encouradgement throughout this investigation since 1977.

The author also would like to express his utmost gratitude To Dr. Chyongjin Pac and Assistant Professor Setsuo Takamuku for their helpful and fruitful suggestions and discussions. Grateful acknowledgements are also made to Dr. Yoshiki Okamoto and Dr. Susumu Toki for their helpful suggestions through stimulating discussions with the author.

The author is also very grateful to Dr. Kazuhiko Mizuno at the Department of Applied Chemistry, College of Engineering, University of Osaka Prefecture for his valuable suggestion and discussion.

It is a real pleasure to express the author's gratitude to Mr. Akira Nakasone, Junichi Kubo, and Hidekazu Miyata for their collaboration in the course of experiment. The author's grateful thanks are also due to all the members in the Institute of Scientific and Industrial Research and in the Faculty of Engineering, who have made γ-irradiations, spectroscopic measurements, and elemental analyses. The author wishes to thank all members of Sakurai Laboratory for their friendship.

Finally the author would like to make grateful acknowledgements to Professor Emeritus Rokuro Okawara, Assistant Professor Yoshikane Kawasaki, Dr. Masanori Wada, and Dr. Hideo Kurosawa at the Department of Petroleum Chemistry, Faculty of Engineering, Osaka University for their inspirous and warm-hearted encouragements.

Suita, Osaka
January, 1980

Tetsuro Majima

Tetsuro Majima

LIST OF PAPERS

The contents of this thesis are composed of the following papers.

(1) Exciplex Quenching by Pyridine, Methylated Pyridines, and Methylated Imidazoles and Termolecular Interaction in the Excited Singlet State
T. Majima, C. Pac, and H. Sakurai,
Bull. Chem. Soc. Jpn., 51, 1811 (1978).

(2) Redox-photosensitised Cleavage of Indene Dimers Using Aromatic Hydrocarbon–Dicyanobenzene Systems; Catalysis by the Cation Radical of Aromatic Hydrocarbons
T. Majima, C. Pac, A. Nakasone, and H. Sakurai,
J. Chem. Soc., Chem. Commun., 490 (1978).

(3) Redox-photosensitized Stereomutation of 1-Phenoxypropene; Catalysis by the Cation Radical of Aromatic Hydrocarbons
T. Majima, C. Pac, and H. Sakurai,
Chem. Lett., 1133 (1979).

(4) Radiation-induced Cycloreversion of Indene Cyclobutane Dimers in n-Butyl Chloride by a Chain Reaction Mechanism
T. Majima, C. Pac, S. Takamuku, and H. Sakurai,
Chem. Lett., 1149 (1979).

(5) Redox-photosensitized Chain Monomerization of *cis,syn*-Dimer of Dimethylthymine; Unusual Effect of Molecular Oxygen
T. Majima, C. Pac, J. Kubo, and H. Sakurai,
Tetrahedron Lett., inpress.

(6) Redox-Photosensitized Ring Cleavage of 1,1a,2,2a-Tetrahydro-7*H*-cyclobut[*a*]indene Derivatives; Mechanism and Structure-Reactivity Relationship
T. Majima, C. Pac, and H. Sakurai,
submitted to J. Am. Chem. Soc..

(7) Redox-Photosensitized Reactions of Electron Donor-Acceptor Pairs by Aromatic Hydrocarbons; Catalysis by the Cation Radical of Aromatic Hydrocarbons and Mechanism
T. Majima, C. Pac, A. Nakasone, and H. Sakurai,
J. Am. Chem. Soc., to be published.

CONTENTS

INTRODUCTION

A great number of photochemical reactions has been studied organic-chemically physicochemically on mostly monomolecular reactions of electronically excited species and/or bimolecular reactions between the excited species and other molecules. However, photochemical reactions involving many components have been scare mainly because of complexity of the reactions. In contrast with these, photobiological reactions[1] such as photosynthesis,[2] photosense,[3] photodamage,[4] and photorepair[4] are evidently photochemical reactions of many-component systems and are phenomena resulting from a photoexcitation and the following dynamic processes involving many components. The mechanisms of dynamic processes on molecular grounds are considered to be common in usual photochemical reactions. Therefore, photochemical reactions of three-component systems are thought of the fundamentals of those of many-component systems. Moreover, one may expect the participation of termolecular interactions in excited states and/or the intermediacy of a triplex and so on characteristic of three-component systems.

Recently, much attention has been paid to photochemical reactions involving electron transfer (or charge transfer) which are current topics of organic photochemistry.[5] One of the particularly interesting reactions is the catalytic nature of chlorophyll a molecules in the reaction center of photosynthesis; electronically excited chlorophyll molecules in the reaction center formed by receiving photoenergies from antenna chlorophylls catalyze the pumping up of electrons from electron donor to electron acceptor by acting as redox carriers, thus converting solar energy into chemical energy.[6] To see whether photochemical reactions involving electron transfer, similar to the roles of chlorophyll a molecules in the reaction center of photosynthesis, occur even in homogeneous systems containing simple organic compounds or not is considered to provide fundamental and significant information regarding the subject of study on the conversion of solar energy to chemical energy using a model reaction of photosynthesis, and contribute to the development of photochemistry in the meaning of a new type of photochemical reactions.

With these in view, the author wishes to describe in this thesis mainly the photochemical reactions of three-component

systems involving electron transfer, especially a novel type of photosensitized reaction; redox-photosensitized reaction.

Chapter 1 deals with the exciplex quenching by pyridine, methylated pyridines, and methylated imidazoles and termolecular interaction in the excited singlet state. On the basis of the kinetic results, the mechanisms will be discussed in terms of the interaction of the n-orbital of the positive charge developed on the electron-donor side of the exciplexes. Chapter 2 deals with the redox-photosensitized reactions of electron donor-acceptor pairs by aromatic hydrocarbonds. On the basis of the kinetic results, the mechanism will be discussed in terms of catalysis of cation radical of aromatic hydrocarbons *via* the π-complex formed between the cation radical and an electron donor without the formation of the discrete cation radical of the electron donor. Chapter 3 deals with the redox-photosensitized ring cleavage of cyclobutane compounds. On the basis of the kinetic results, the chain reaction mechanism will be discussed in terms of catalysis of cation radical of aromatic hydrocarbons *via* a π-complex. From the structure-reactivity relationship, the importance of through-bond interactions between the two π-electron systems of cyclobutane compounds will be discussed. In the redox-photosensitized chain monomerization of *cis,syn*-dimethylthymine cyclobutane dimer, unusual effect of molecular oxygen will be found and discussed in terms of CT-complex between the dimer and molecular oxygen. Chapter 4 deals with the redox-photosensitized stereomutation of 1-phenoxypropene. The mechanism will be discussed in terms of catalysis by the cation radical of aromatic hydrocarbons *via* a π-complex. Chapter 5 deals with radiation-induced chain cycloreversion of indene cyclobutane dimers in n-butyl chloride. The chain reaction mechanism will be discussed in terms of catalysis by cation radical of n-butyl chloride.

References

1 J. Jagger, "Introduction to Research in Ultraviolet Photobiology", Prentice-Hall, Englewood Cliffs, N. J., 1967.

2 G. E. Fogg,"Photosynthesis", 2nd ed., English Univ. Press,

London (1972); J. A. Bassham and M. Calvin, "The Path of Carbon in Photosynthesis", Prentice-Hall, Englewood Cliffs, N. J., 1957; R. K. Clayton, "Molecular Physics in Photosynthesis", Blaisdell, New York, N. Y., 1965; L. P. Vernon and G. R. Seely, "The Chlorophylls", Academic Press, New York, N. Y., 1966.

[3] A. C. Giese, "Photopysiology", Vol. 2, Academic Press, New York, N. J., 1964; H. Mohr, in "An Introduction to photobiology", C. P. Swanson, Ed., Prentice-Hall, Englewood Cliffs, N. J., 1969, p. 99.

[4] H. Harm, in "Photochemistry and Photobiology of Nucleic Acids", Vol. 2, R. C. Wang, Ed., Academic Press, New York, N. Y., 1976, Ch 6; P. C. Hanawalt, in "An Introduction to Photobiology", C. P. Swanson, Ed., Prentice-Hall, Englewood Cliffs, N. J., 1969, p. 53; A. Wirkemann, *ibid.*, p. 81.

[5] R. S. Davidson, in "Molecular Association", R. Foster, Ed., Academic Press, New York, N. Y., 1975, Ch 4; M. Gordon and W. R. Ware, "The Exciplex", Academic Press, New York, N. Y., 1975; N. Mataga, "Kokagakujosetsu", Kyoritsu Publ., Tokyo, 1975.

[6] M. Gibbs *et al.*, organizers, "Proceedings of the Woekshop on Bio-solar Conversion", a Report on a Workshop Held at Bethesda", Maryland, 1973; S. Lein and A. San Pietro, "An inquiry into Biophotolysis of Water to Produce Hydrogen", a Report NSF and RANN, Indiana Univ., 1975.

CHAPTER 1 EXCIPLEX QUENCHING BY PYRIDINE, METHYLATED PYRIDINES, AND METHYLATED IMIDAZOLES AND TERMOLECULAR INTERACTION IN THE EXCITED SINGLET STATE

1-1 INTRODUCTION

Exciplex formation has been recognized to be a general mechanistic pathway in fluorescence quenching[1,2] and has been suggested to precede photocycloadditions in a variety of reaction system.[3-5] Photocycloadditions of furan and olefinic compounds to aromatic nitriles have been also extensively investigated and suggested to occur *via* exciplexes.[6] In some exciplex-formation systems, the increase in the concentration of a precursor results in the formation of a termolecular excited complex (triplex), which arises from the interaction of a precursor with an exciplex.[7,8] This type of termolecular interaction can be considered to be rather general and has been suggested to be important in some photoreactions.[9] Caldwell and his co-workers reported a different type of termolecular interaction in the excited singlet state which occurs by means of the interaction of exciplexes with compounds which are not the precursors of the exciplexes and which possess either an electron-donor or an electron-acceptor nature.[10] In regard with this, it has been reported that pyridine quenches exciplexes which emit very weakly or which are not emissive at all.[11] The exciplex quenching by pyridine provides a convenient method for establishing the existence of the exciplex intermediacy in photocycloadditions of furan and olefinic compounds to aromatic nitriles. In the exciplex quenching, however, pyridine can act as either an n-donor or a π-acceptor, since it is weakly basic as well as π-deficient. In this chapter, the author describes that pyridine, methylated pyridines, and methylated imidazoles quench the exciplexes of aromatic nitrile–2,5-dimethylfuran or 2,5-dimethyl-2,4-hexadiene by acting as n-donors, and that 1-methyl and 1,2-dimethylimidazoles quench the fluorescence of aromatic nitriles by way of a termolecular process.

1-2 RESULTS

Characteristics of Exciplexes. For exciplex-quenching experiments, the exciplexes of 1- and 2-naphthonitriles (1- and 2-NN)–2,5-dimethylfuran (DF) and 9-cyanophenanthrene (9-CP)–2,5-dimethyl-2,4-hexadiene (DHD) were employed, since these exciplexes can be considered to be typical models of the supposed intermediates in photocycloadditions of furan and olefinic compounds to aromatic nitriles and all are fairly emissive. Table 1 lists the lifetimes of the exciplexes in a benzene solution containing 0.3 M in DF or DHD, the exciplex emission maxima in benzene and ethyl acetate solutions containing 0.3 M in DF or DHD, the calculated dipole moments, and the apparent rate constants ($\gamma_0 k_e$) of the quenching of the aromatic nitrile fluorescence by DF or DHD.

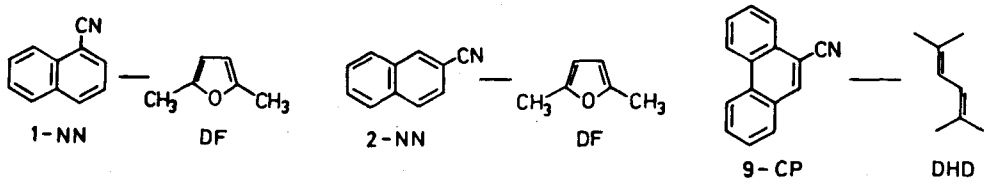

Table 1. Characteristics of Exciplexes

		Exciplex		
		1-NN–DF	2-NN–DF	9-CP–DHD
λ_{max}[a]/nm	C_6H_6	435	413	440
	AcOEt	445	435	460
τ_{EX}[b]/ns		32[c] (15)	28[c] (14)	21[d] (12)
Dipole moment[e]/D		~10	~10	~10
$\gamma_0 k_e$[f]/$\times 10^{-9}$ $M^{-1}s^{-1}$		8.1	2.6	8.1

[a] Emission maxima of the exciplexes; 5×10^{-4} M in aromatic nitrile and 0.3 M in DF or DHD; ±2 nm. [b] Lifetimes in degassed benzene; the numbers in parentheses are the lifetimes in air-saturated benzene; ±0.5 ns. [c] Oxygen-quenching method. [d] Determined by an N_2 laser-flash method. [e] Calculated from the solvent shifts of the emission maxima. [f] Apparent rate constants for the quenching of the aromatic nitrile fluorescence by DF or DHD.

The lifetime of the 9-CP–DHD exciplex was directly determined by monitoring the decay of the exciplex fluorescence at 440 nm

using an N_2 laser. When the decay of the residual 9-CP fluorescence was monitored at 375 nm, two decays were observed; the lifetimes of the slow and rapid decay components were calculated to be 17 ns and less than 2 ns respectively. The slow-decay component apparently arises from the reversible dissociation of the exciplex into an excited singlet 9-CP and a ground-state DHD. However, the reversible dissociation can be considered to be not so significant, since the quenching of the 9-CP fluorescence by DHD occurred at a diffusion-controlled rate. The lifetimes of the 1-NN– and 2-NN–DF exciplexes were determined by the oxygen-quenching method proposed by Caldwell.[12]

These exciplexes are charge-transfer complexes in nature, as is shown by the dipole moment, which was obtained by a usual method using plots of the wave numbers of the emission maxima in various solvents *vs.* $[(\varepsilon - 1)/(2\varepsilon - 1) - (n^2 - 1)/2(2n^2 - 1)]$,[13] where ε and n represent the dielectric constant and the refractive index of the solvent respectively. The slopes of the plots are commonly $(10 \pm 1)\times10^3$ cm^{-1}, which corresponds to ca. 10 Debey units of the dipole moment. The 9-CP–DHD exciplex crosses over a $2\pi + 2\pi$ cycloadduct,[6f] while the 1- and 2-NN–DF exciplexes do not result in the formation of any stable products at room temperature. The UV spectra showed no indication of the formation of charge-transfer complexes in the ground state.

Exciplex Quenching by Pyridine and Imidazole Compounds. For the exciplex quenching, pyridine (1a), 2-, 3-, and 4-methylpyridines (1b, 1c, and 1d), 2,6- and 3,5-dimethylpyridines (1e and 1f), 1-methylimidazoles (2a), and 1,2-dimethylimidazole (2b) were used as quenchers. The exciplex-quenching experiment were carried

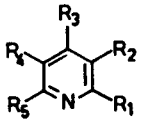

1

1a: $R_1=R_2=R_3=R_4=R_5=$ H
1b: $R_1=CH_3$, $R_2=R_3=R_4=R_5=$ H
1c: $R_2=CH_3$, $R_1=R_3=R_4=R_5=$ H
1d: $R_3=CH_3$, $R_1=R_2=R_4=R_5=$ H
1e: $R_1=R_5=CH_3$, $R_2=R_3=R_4=$ H
1f: $R_2=R_4=CH_3$, $R_1=R_3=R_5=$ H

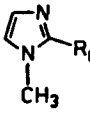

2

2a: $R_6=$ H
2b: $R_6=CH_3$

out as usual. Figure 1, for example, shows the spectral change in the fluorescence from a benzene solution containing 5×10^{-4} M in 9-CP and 0.3 M in DHD on the addition of 1a. The exciplex

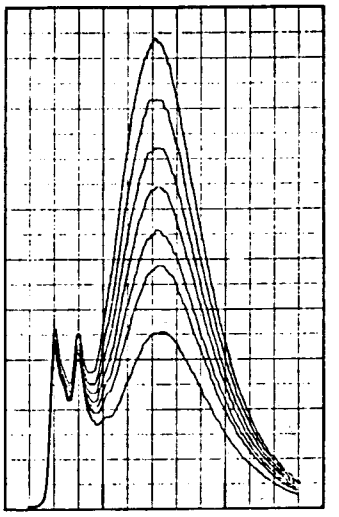

Figure 1. Quenching of 9-CP—DHD exciplex by 1a in deoxygenated benzene: $k_q\tau_{EX} = 1.5\ M^{-1}$.

emission with the maximum at 440 nm was significantly quenched. The plot of the relative intensities at 440 nm in the absence of and in the presence of 1a (I^0_{EX}/I^Q_{EX}) *vs.* the concentrations of 1a gave a linear line, the slope of which was 1.5 M^{-1} (Figure 5); the rate constant (k_q) of the exciplex quenching was calculated to be $7.1\times10^7\ M^{-1}s^{-1}$ by applying the slope to eq 1, where τ_{EX} and Q represent the lifetimes of an exciplex and an exciplex quencher

$$I^0_{EX}/I^Q_{EX} = 1 + k_q\tau_{EX}[Q] \qquad (1)$$

respectively. Similarly, the rate constants of the quenching of the 1- and 2-NN—DF exciplexes by pyridine were calculated to be 3.5×10^8 and $2.6\times10^8\ M^{-1}s^{-1}$ respectively.

As is shown in Figure 1, the residual 9-CP fluorescence at 360-380 nm was also slightly quenched by pyridine. Similarly, a slight quenching of the residual 1- and 2-NN fluorescence was also observed in the quenching of the 1- and 2-NN—DF exciplexes by pyridine. In contrast, the 2-NN or 9-CP fluorescence in the absence of DF or DHD was not quenched at all by pyridine, while the quenching of the 1-NN fluorescence by pyridine was relatively efficient, the rate constant being $3\times10^8\ M^{-1}s^{-1}$. Therefore, the the quenching of the residual 2-NN or 9-CP fluorescence can be

ascribed to the decrease in the reversible dissociation of the exciplex because of the exciplex quenching. In the case of the 1-NN–DF exciplex, however, the singlet quenching of the residual 1-NN fluorescence would be caused by either the exciplex quenching or the direct quenching of the excited singlet 1-NN by pyridine.

Table 2 lists the quenching constants ($k_q\tau_{EX}^{air}$) for each exciplex-quencher pair; they were obtained by the usual Stern-Volmer plots for air-saturated benzene and ethyl acetate solutions, using eq 1 but replacing τ_{EX} by τ_{EX}^{air}, the lifetime in air-saturated solutions. In order to avoid the quenching of excited-singlet aromatic nitrile, the concentrations of the quenchers were kept as low as the quenching of excited-singlet aromatic nitrile, which was negligible expect for the exciplex quenching by 1b and 1e. There was no indication of the formation of any charge-transfer complexes between A or D and Q in the ground state.

Table 2. Quenching of Exciplex Emission by Exciplex Quenchers[a]

Quencher	$k_q\tau_{EX}^{air}/M^{-1}$					
	1-NN–DF		2-NN–DF		9-CP–DHD	
	C_6H_6	AcOEt	C_6H_6	AcOEt	C_6H_6	AcOEt
1a	5.6(11.3)[b]	9.6	3.6(7.2)[b]	7.7	0.9(1.5)[b]	2.6
1c	-	10.5	-	8.5	1.1	-
1d	8.0	11.0	-	9.3	1.4	3.3
1f	-	11.0	-	12.0	-	-
1b	0.8	~1.0	-	~0.5	<0.2	<0.2
1e	-	~0.3	-	<0.1	<0.1	-
2a	37.5	-	20.5	-	4.9	9.0
2b	12.2	-	12.0	-	-	-

[a] In air-saturated solutions; 5×10^{-4} M in aromatic nitriles and 0.3 M in DF or DHD. [b] In degassed benzene.

Quenching of Aromatic Nitrile Fluorescence by 2a and 2b. The fluorescence of 1- and 2-NN was quenched by 2a. Interestingly, the Stern-Volmer plots were not linear (Figure 2). In the fluorescence quenching, very weak exciplex emission appeared, but no isoemissive points could be observed. 9-CP fluorescence was not quenched by 2a at all. The quenching of the 2-NN and 9-CP fluorescence by 2b gave, again, slightly curved Stern-Volmer plots, while that of the 1-NN fluorescence was efficient and gave a linear

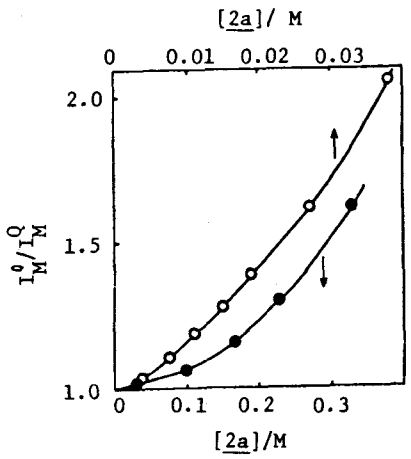

Figure 2. Stern-Volmer plots for the quenching of 1-NN (-○-) and 2-NN (-●-) fluorescence by 2a in air-saturated benzene, [1- and 2-NN] = 5×10^{-4} M.

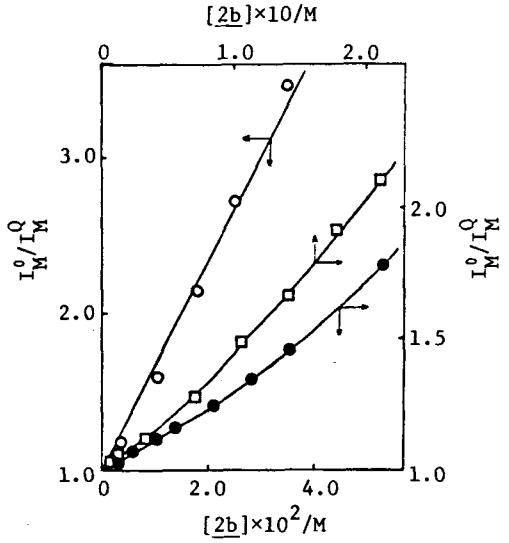

Figure 3. Stern-Volmer plots for the quenching of 1-NN (-○-), 2-NN (-●-), and 9-CP (-□-) fluorescence by 2b in air-saturated benzene, [aromatic Nitrile] = 5×10^{-4} M.

Stern-Volmer plot (Figure 3). In the latter quenching, a fairly strong exciplex emission with the maximum at 408 nm appeared without an iso-emissive point; it revealed its maximum intensity at the concentration of 1.8×10^{-2} M of added 2b. A further increase in the 2b concentration resulted in a decrease in the exciplex emission (Figure 4). Table 3 summarizes the relative intensities of 1-NN fluorescence at 340 nm (I_M^0/I_M^Q) and those of the exciplex emission at 408 nm ($\phi_{EX}/\phi_{EX}^{max}$), the latter of which are corrected by

Table 3. Quenching of 1-NN Fluorescence by 2b[a]

[2b]×10²/M	0.36	1.1	1.8	2.5	3.6	5.4	7.2	10.8
I_M^0/I_M^Q[b]	1.16	1.58	2.14	2.72	3.47	-	-	-
$\phi_{EX}/\phi_{EX}^{max}$[c,d]	0.47	0.92	1.00	0.99	0.93	0.80	0.69	0.54
L_{max}/L[d]	0.77	0.9	1.0	1.11	1.32	1.48	1.79	2.28

[a] In air-saturated benzene, 5×10^{-4} M in 1-NN. [b] Relative intensities of the 1-NN fluorescence at 340 nm in the absence and in the presence of 2b. [c] Relative intensities of the exciplex emission at 408 nm. [d] See the text.

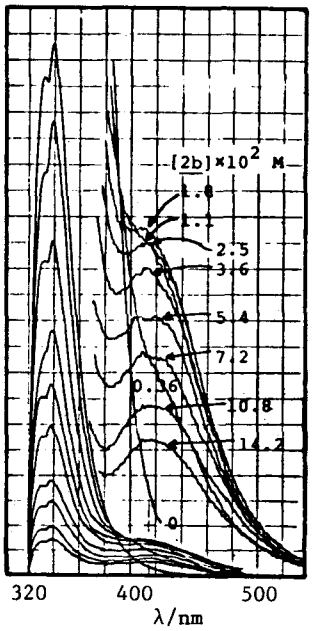

Figure 4. Quenching of 1-NN fluorescence by 2b in air-saturated benzene, [1-NN] = 5×10^{-4} M.

subtracting the intensity of the 1-NN fluorescence at 408 nm from the total intensity at this wavelength. The curved Stern-Volmer plots could be caused by the formation of charge-transfer complexes in the ground state. However, UV measurements eliminated this posibility.

Quenching of 1-NN–2b Exciplex by 1. The emission of 1-NN–2b exciplex with the maximum at 408 nm was quenched significantly quenched by 1. The spectral changes in the fluorescence and the exciplex emission on the addition of 1 were measured in a benzene solution containing 5×10^{-4} M in 1-NN and 1.8×10^{-2} M in 2b. Table 4, for example, in the case of 1a, summarizes the relative intensities of 1-NN fluorescence at 340 nm ($I_M^0/I_M^{Q+Q'}$) and those of the exciplex emission at 408 nm ($\phi_{EX}^{Q+Q'}/\phi_{EX}^{max}$), the latter of which are corrected by subtracting the intensity of the 1-NN fluorescence at 408 nm from the total intensity at this wavelength.

Table 4. Quenching of 1-NN–2b Exciplex by 1a[a]

[1a]×10²/M	0.0	0.41	1.24	2.1	2.9	4.1	6.2	8.2
$I_M^0/I_M^{Q+Q'}$[b]	2.43	2.45	2.48	2.53	2.55	2.61	2.73	2.75
$\phi_{EX}^{Q+Q'}/\phi_{EX}^{max}$[c,d]	1.00	0.97	0.93	0.89	0.84	0.79	0.71	0.64
$L_{max}/L^{Q+Q'}$[d]	1.00	1.02	1.06	1.09	1.13	1.16	1.26	1.37

[a] In air-saturated benzene, 5×10^{-4} M in 1-NN and 1.8×10^{-2} M in 2b. [b] Relative intensities of the 1-NN fluorescence at 340 nm in the absence and in the presence of 2b and 1a. [c] Relative intensities of the exciplex emission at 408 nm. [d] See the text.

1-3 DISCUSSION

Mechanism of Exciplex Quenching. Scheme 1 shows the reaction processes involving the exciplex formation and the quenching of the exciplex, where A, D, $[A^-D^+]^*$, and Q represent the aromatic nitriles, DF or DHD, the exciplexes, and the exciplex quenchers respectively. Processes 2 and 5 involve all the unimolecular physical decays of A and $[A^-D^+]^*$ respectively. Equations 8 and 9 are the Stern-Volmer equations for the quenching of the monomer (A) fluorescence by D in the absence of Q and of exciplex emission at a constant concentration of D (0.3 M) by Q respectively.

$$A \xrightarrow{h\nu} {}^1A^* \tag{1}$$

$${}^1A^* \xrightarrow{1/\tau_M} A + h\nu' \text{ (or heat)} \tag{2}$$

$${}^1A^* + Q \xrightarrow{k_q'} A + Q \tag{3}$$

$${}^1A^* + D \underset{k_{-e}}{\overset{k_e}{\rightleftharpoons}} [A^-D^+]^* \tag{4}$$

$$[A^-D^+]^* \xrightarrow{k_d} A + D + h\nu'' \text{ (or heat)} \tag{5}$$

$$[A^-D^+]^* \xrightarrow{k_p} \text{Product(s)} \tag{6}$$

$$[A^-D^+]^* + Q \xrightarrow{k_q} A + D + Q \tag{7}$$

Scheme 1.

$$I_M^0/I_M^Q = 1 + \gamma_0 k_e \tau_M [D] \tag{8}$$

$$\gamma_0 = (k_d + k_p)/(k_{-e} + k_d + k_p) \sim 1$$

$$I^0_{EX}/I^Q_{EX} = (1 + \frac{k_q'\tau_M[Q]}{1 + k_e\tau_M[D]})(1 + k_q\tau_{EX}[Q]) \qquad (9)$$

The value of γ_0 is unity, since the fluorescence of A was quenched by D at a diffusion-controlled rate i.e., $k_{-e} << k_d + k_p$; the exciplexes are almost irreversibly formed. In the presence of 0.3 M in D, therefore, eq 9 can be reduced to eq 1, since $1 >> k_q'\tau_M[Q]/(1 + k_e\tau_M[D])$. The calculated k_q values for the quenching of the exciplexes by pyridine are one or two orders lower than the diffusion-controlled rate, showing that pyridine is an inefficient quencher for the exciplexes. Significantly, however, pyridine does not quench the 2-NN and 9-CP fluorescence at all; thus, it can be used as a selective quencher for the exciplexes involving nitriles.[11] The photocycloaddition of DHD to 9-CP[6f] was also quenched by pyridine; the Stern-Volmer plot gave the $k_q\tau_{EX}$ value of $1.95 \times 0.5\ M^{-1}$, which is very similar to that obtained from exciplex-emission quenching experiments (Figure 5). The results clearly demonstrate the intermediacy of the exciplex in the photocycloaddition.

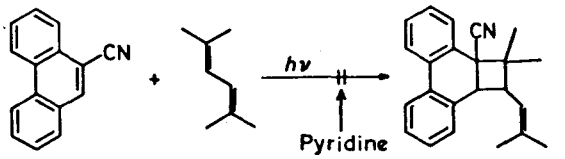

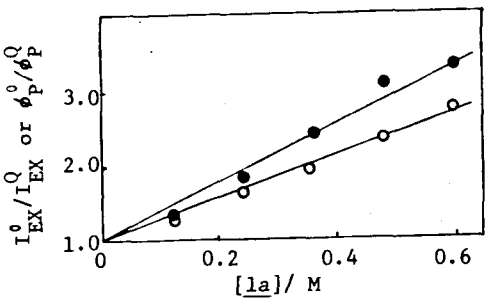

Figure 5. Stern-Volmer plots for the quenching of 9-CP–DHD exciplex by 1a in degassed benzene; fluorescence quenching (-○-) and product quenching (-●-) runs, 9-CP = 5×10^{-4} M and [DHD] = 0.3 M.

According to Caldwell's generalization of exciplex quenching,[10] an exciplex quencher possessing an electron-donor or electron-acceptor nature (Q_D or Q_A) interacts with an exciplex $[A^-D^+]^*$ on the D or A side i.e., $A^{\delta-}\cdots D\cdots Q_D{}^{\delta+}$ or $Q_A{}^{\delta-}\cdots A\cdots D^{\delta+}$. This termolecular interaction results in exciplex quenching. Therefore, if pyridine acts as an n-donor in the exciplex quenching, the n-orbital of pyridine must perpendicularly approach to the molecular plane of the D side of exciplexes (I in Scheme 2). On the other hand, the pyridine which acts as π-acceptor can interact with the A side of exciplexes with a sandwich type of configuration (II).

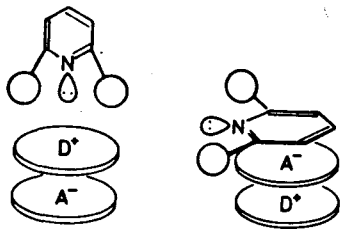

I II

Scheme 2.

As is shown in Table 2, methylsubstitution at the 2- and 2,6-positions of the pyridine ring commonly leads to a marked decrease in the quenching ability of the three exciplexes, while substitution at the other positions instead slightly enhances the quenching rate. The effect of the methyl groups at the 2- and 2,6-positions demonstrates the dominant n-donor character in the exciplex quenching. The methyl group of 1b and 1e would sterically inhibit the approach of the n-orbital to the exciplexes within an effective distance for the quenching. In the case of the other methylated pyridines, such steric hindrance can not occur in the attack of the n-orbital on the exciplexes. Moreover, this mechanism is supported by the observation that the $k_q\tau_{EX}^{air}$ values increase in the base strength of the quenchers; methyl substitution in the pyridine ring enhances the basic strength, and imidazole is much more strongly basic, but less π-defficient, than pyridine.[14] In line with this mechanism, 2a is a much more efficient quencher than 1a. Methyl substitution at the 2-position of the imidazole ring results, again, in a decrease in the quenching efficiency to some extent, though the steric effect is much smaller than that of the methyl group of 1b; the difference in the

steric effects can be easily predicted by molecular model. In conclusion, the exciplex quenching occurs by means of the attack of the n-orbital of the quenchers on the positive charge developed on the D side because of a high degree of charge-transfer contribution to the exciplexes. The ionic or charge-transfer nature of the exciplex quenching is supported by the observation that the $k_q\tau_{EX}^{air}$ values in ethyl acetate are grater than those in benzene.

Quenching of Aromatic Nitrile Fluorescence by 2a and 2b. The quenching the 1- and 2-NN fluorescence by 2a gave curved Stern-Volmer plots, which, it may be suggested, occur by way of a termolecular process involving the exciplexes of 1- and 2-NN–2b. The termolecular mechanism is further suggested by the observation that the emission of the 1-NN–2b exciplex increases up to the concentration of 1.8×10^{-2} M in 2b, but decreases upon a further increase in the concentration of 2b. In Scheme 3, therefore, the reaction processes are shown, where A, Q, and [AQ]* denote the aromatic nitriles, 2a, or 2b, and the exciplexes respectively.

$$A \xrightarrow{h\nu} {}^1A^* \tag{10}$$

$${}^1A^* \xrightarrow{1/\tau_M} A + h\nu' \text{ (or heat)} \tag{11}$$

$${}^1A^* + Q \underset{k_{-e}}{\overset{k_e}{\rightleftharpoons}} [AQ]^* \tag{12}$$

$$[AQ]^* \xrightarrow{k_f} A + Q + h\nu'' \tag{13}$$

$$[AQ]^* \xrightarrow{k_d} A + Q + \text{heat} \tag{14}$$

$$[AQ]^* + Q \xrightarrow{k_q} A + 2Q \tag{15}$$

Scheme 3.

The process for the formation of stable products, [AQ]* and/or [AQ]* + Q ⟶ Products, can be discarded, since no products could be detected. Equation 15 represents the Stern-Volmer equation for the quenching of the aromatic nitrile fluorescence by Q, whereas eq 16 shows the quantum yield of the 1-NN–2b exciplex emission at a given concentration of Q.

$$I_M^0/I_M^Q = 1 + \left\{\frac{1 + k_q\tau_{EX}^0[Q]}{1 + (k_{-e} + k_q[Q])\tau_{EX}^0}\right\}k_e\tau_M[Q] \tag{16}$$

$$\tau_{EX}^0 = 1/(k_d + k_f)$$

$$\phi_{EX} = (\frac{I_M^Q}{I_M^0})\{\frac{k_f\tau_{EX}^0}{1 + (k_{-e} + k_q[Q])\tau_{EX}^0}\}k_e[Q] \qquad (16)$$

If the reversible dissociation of the exciplex into $^1A^*$ and Q can be neglected (i.e., $k_{-e} << k_d + k_f$), eq 15 can be reduced to a usual Stern-Volmer equation; thus, the fluorescence quenching would give a linear Stern-Volmer plot. The quenching of the 1-NN fluorescence by 2b fits the case (Figure 3); the k_e value was calculated to be $(9.3\pm1.0)\times10^9$ $M^{-1}s^{-1}$ from the slope of the Stern-Volmer plot (71.0 M^{-1}) and the lifetime of the excited singlet 1-NN in air-saturated benzene (7.5±0.5 ns). The occurrence of a diffusion-controlled fluorescence quenching demonstrates the negligible importance of the reversible dissociation.

If the reversible dissociation can not be neglected, eq 15 predicts non-linear Stern-Volmer plots (Figures 2 and 3). Equation 15 can be transformed into eq 17; thus, the plots of $(I_M^0/I_M^Q - 1)/[Q]$ *vs.* [Q] are shown in Figures 6 and 7, using the data in Figures 2 and 3. Equation 17 predicts that the plots will be linear at

$$(I_M^0/I_M^Q - 1)/[Q] = \frac{k_e\tau_M}{1 + (k_{-e} + k_q[Q])\tau_{EX}^0} + \frac{k_e\tau_M k_q\tau_{EX}^0[Q]}{1 + (k_{-e} + k_q[Q])\tau_{EX}^0} \qquad (17)$$

lower concentrations of Q, provided $k_q[Q] << k_d + k_f + k_{-e}$, while a deviation from the linearity occurs at higher concentrations of Q. The results are in good accord with this prediction. When the slopes and intercepts in Figures 6 and 7 applied to eq 17, one can obtain the values of $\{1/(1/\tau_{EX}^0 + k_{-e})\tau_{EX}^0\}k_e$ and $k_q\tau_{EX}^0$ listed in Table 5. The former is the apparent rate constant for the formation of the exciplex, in which the reversible dissociation of the exciplex is taken into account. In the case of the 2-NN–2a exciplex, the rate constant is three orders lower than the diffusion-controlled rate, suggesting the dominant dissociation; the exciplex formation must be isothermal or only slightly exothermic. In the case of all the other exciplexes except the 1-NN–2b exciplex, the dissociation is also important. The curved Stern-Volmer plots arise from the quenching of the exciplexes by 2a or 2b. The $k_q\tau_{EX}^0$ values can be obtained by dividing the slopes by the intercepts in Figures 6 and 7.

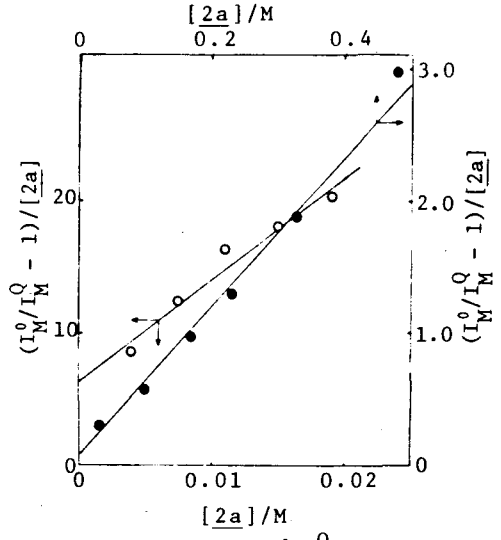

Figure 6. Plots of $(I_M^0/I_M^Q - 1)/[2a]$ *vs.* [2a] for 1-NN (-O-) and 2-NN (-●-) using the data in Figure 2.

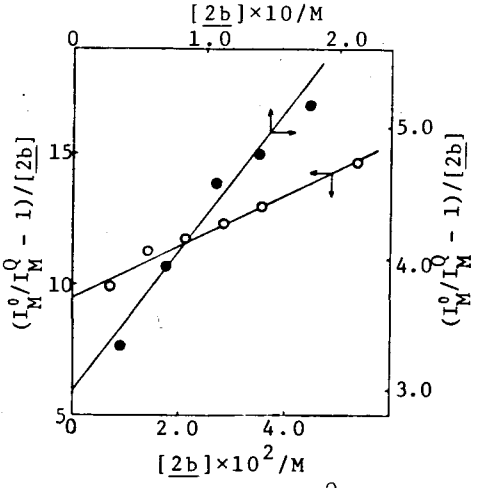

Figure 7. Plots of $(I_M^0/I_M^Q - 1)/[2b]$ *vs.* [2b] for 2-NN (-O-) and 9-CP (-●-) using the data in Figure 3.

Table 5. Rate Constants for Quenching of Aromatic Nitrile Fluorescence by 2a and 2b[a]

	2a		2b		
	1-NN	2-NN	1-NN	2-NN	9-CP
τ_M[b]/ns	7.5	10.0	7.5	10.0	10.0
$\{1/(1/\tau_{EX}^0 + k_{-e})\tau_{EX}^0\}k_e\tau_M$ /M^{-1}	6.1	0.06	71.0	9.5	3.0
$k_e/(1/\tau_{EX}^0 + k_e)\tau_{EX}^0$ /$M^{-1}s^{-1}$	8.1×10^8	6×10^6	9.3×10^9	9.5×10^8	3×10^8
$k_q\tau_{EX}^0$ /M^{-1}	179	93.3	22.0	10.0	4.4

[a] In air-saturated benzene, 5×10^{-4} M in aromatic nitriles. [b] Lifetimes of air-saturated benzene; ±0.5 ns.

In the case of the 1-NN–2b exciplex, the $k_q\tau_{EX}^0$ value should be calculated by anothor method, since the Stern-Volmer plot for the quenching of the 1-NN fluorescence by 2b gives a linear line. If eq 18 represents the maximum quantum yield of the 1-NN–2b exciplex emission observed in the presence of 1.8×10^{-2} M in 2b ($[Q]_{max}$), eq 19 can be finally obtained by dividing eq 18 by eq 16 and by a subsequent transformation. Since the 1-NN–2b exciplex is almost irreversibly formed, k_{-e} was omitted in eqs 16, 18, and

$$\phi_{EX}^{max} = \left(\frac{I_M^Q}{I_M^0}\right)_{max} \left(\frac{k_f \tau_{EX}^0}{1 + k_q \tau_{EX}^0 [Q]_{max}}\right) k_e [Q]_{max} \qquad (18)$$

$$L_{max}/L = \left(\frac{\phi_{EX}^{max}}{\phi_{EX}}\right) \left(\frac{[Q]}{[Q]_{max}}\right) \left\{\frac{(I_M^Q/I_M^0)}{(I_M^Q/I_M^0)_{max}}\right\}$$

$$= \left(\frac{1}{1 + k_q \tau_{EX}^0 [Q]_{max}}\right) (1 + k_q \tau_{EX}^0 [Q]) \qquad (19)$$

19. Thus, L_{max}/L was plotted *vs.* [Q] using the data in Table 3; a good linear line was thus obtained (Figure 8). The $k_q \tau_{EX}^0$ value

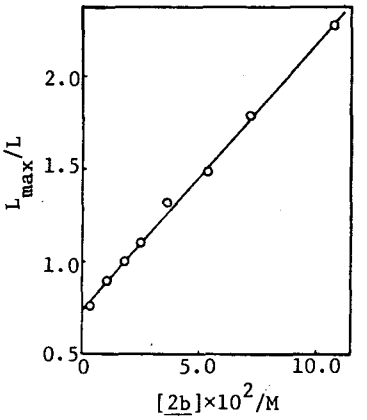

Figure 8. Plots of L_{max}/L *vs.* [2b], using the data in Table 3.

was calculated to be 22.0 M^{-1} by dividing the slope by the intercept, or 24.1 M^{-1} from the intercept. Although the latter must include a greater error than the former, the agreement between the calculated values is good within the limits of experimental error.

The apparent rate constants for the formation of the 1- and 2-NN–2a exciplexes are much lower than those for the exciplexes of 2b. This suggests that 2a and 2b act as π-donors in the exciplex formation, since 2b is apparently a stronger π-donor than 2a. In contrast, the $k_q \tau_{EX}^0$ values for 1- and 2-NN–2a system are about ten times greater than those for the 1- and 2-NN–2b system respectively. The difference between the $k_q \tau_{EX}^0$ values for 2a and 2b suggests that 2a and 2b act as n-donors in process 14,

as is illustrated as III; the methyl group at the 2-position of 2b sterically inhibits the interaction of the n-orbital with the 1- and 2-NN-2b exciplexes, leading to lower k_q values than those for 2a, as has been discussed in the foregoing section.

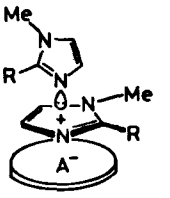

III

In the case of the 1-NN–2b exciplex quenching by 1, processes 20 and 21 should be added into Scheme 3, where Q′ represents 1.

$$^1A^* + Q' \xrightarrow{k_q'} A + Q' \qquad (20)$$

$$[AQ]^* + Q' \xrightarrow{k_q^{Q'}} A + Q + Q' \qquad (21)$$

Instead of eqs 15 and 16, therefore, eqs 22 and 23 are obtained respectively, which represent the Stern-Volmer equation for the quenching of 1-NN fluorescence by Q and Q′ and the quantum yield of the 1-NN–2b exciplex emission at a given concentration of Q′ respectively, in the presence of 1.8×10^{-2} M in 2b ($[Q] = [Q]_{max}$):

$$\frac{I_M^0}{I_M^{Q+Q'}} = 1 + k_q'\tau_M[Q'] + \{\frac{1 + (k_q[Q]_{max} + k_q^{Q'}[Q'])\tau_{EX}^0}{1 + (k_{-e} + k_q[Q]_{max} + k_q^{Q'}[Q'])\tau_{EX}^0}\}k_e\tau_M[Q]_{max} \qquad (22)$$

$$\phi_{EX}^{Q+Q'} = (\frac{I_M^{Q+Q'}}{I_M^0})\{\frac{k_f\tau_{EX}^0}{1 + (k_{-e} + k_q[Q]_{max} + k_q^{Q'}[Q']\tau_{EX}^0}\}k_e[Q]_{max} \qquad (23)$$

As k_{-e} can be omitted, eq 24 can be obtained by dividing eq 18 by eq 23 and by a subsequent transformation, in place of eq 19:

$$L_{max}/L^{Q+Q'} = (\frac{\phi_{EX}^{max}}{\phi_{EX}^{Q+Q'}})\{\frac{(I_M^{Q+Q'}/I_M^0)}{(I_M^Q/I_M^0)_{max}}\} = 1 + \frac{k_q^{Q'}\tau_{EX}^0[Q']}{1 + k_q\tau_{EX}^0[Q]_{max}} \qquad (24)$$

The plot of $L_{max}/L^{Q+Q'}$ *vs.* [Q′] (Q′ = 1a) using the data in Table 4

gave a good linear line (Figure 9). The $k_q^{Q'}\tau_{EX}^0$ value was calculated to be 6.1 M^{-1} from the slope, since the $k_q\tau_{EX}^0$ value for 2b was determined to be 22.0 M^{-1}. Similarly, the $k_q^{Q'}\tau_{EX}^0$ values were determined for each Q'; the plots of $L_{max}/L^{Q+Q'}$ *vs.* [Q'] were linear. Table 6 lists the slopes of the plots and the $k_q^{Q'}\tau_{EX}^0$ values.

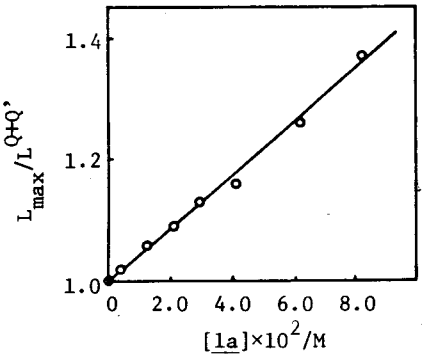

Figure 9. Plots of $L_{max}/L^{Q+Q'}$ *vs.* [1a], using the data in Table 4.

Table 6. Rate Constants for Quenching of 1-NN–2b Exciplex by Q'[a]

	Q'				
	1a	1b	1d	1e	1f
Slope[b]/M^{-1}	4.4	0.91	8.1	0.31	9.5
$k_q^{Q'}\tau_{EX}^0$/M^{-1}	6.1	~1.3	11.2	~0.4	13.3

[a] In air-saturated benzene, 5×10^{-4} M in 1-NN and 1.8×10^{-2} M in 2b. [b] The slopes of linear plots of $L_{max}/L^{Q+Q'}$ *vs.* [Q'].

There is the same tendency for the change of the $k_q^{Q'}\tau_{EX}^0$ values by Q' (Table 6), as has been seen in Table 2: (1) The quenching ability of 1b and 1e are remarkably less than 1a, while (2) 1d and 1f are more efficient quenchers than 1a. Moreover, (3) 2b is a much more efficient quencher than 1. These results suggest that 1 acts as an n-donor in process 21, similarly to 2b, as is illustrated as IV.

Unfortunately, the k_q values which are essential for the discussion can not be calculated, since the τ_{EX}^0 values are not

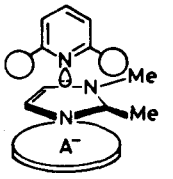

IV

available. However, the participation of the n-orbital of Q and Q' in processes 14 and 21 respectively is further supported by the fact that DF and 1-methylpyrrole, which are strong π-donors but are very weakly basic, do not interact with the respective exciplexes of 1- or 2-NN up to 0.1 M, though they do quench the 1- and 2-NN fluorescence at a diffusion-controlled rate.[15]

1-4 CONCLUSION

The termolecular interactions in the quenching of aromatic nitrile–DF, DHD, or 2 exciplexes by 1 and 2 and the quenching of aromatic nitrile fluorescence by 2a and 2b occur upon the attack of 1 and 2 as the n-donor, Q_n, on the exciplexes, $[A_\pi^- D_\pi^+]^*$ or $[A_\pi^- Q_\pi^+]^*$, giving rise to a purturbation of the exciplexes, by which non-radiative decays may be assisted. The interaction of triplexes, $[A_\pi D_\pi Q_n]^*$ or $[A_\pi Q_\pi Q_n]^*$, provokes an interesting speculation, though triplex emission could not be observed; the triplexes may rapidly collapse into the precursors in the ground state without emission and/or into triplet-state species. Alternatively, the interaction of Q_n with the exciplexes may cause a complete electron transfer from D_π or Q_π to A_π, leading to such ion-pairs as $[A_\pi^- \cdots (D_\pi Q_n)^+]_{solv}$ or $[A_\pi^- \cdots (Q_\pi Q_n)^+]_{solv}$; the electron reversal in the ion-pairs may exclusively occur to result in the collapse into the precursors in the ground-state or triplet-state species because of the low polarity of the solvent. However, it should be pointed out that the decay channels are still open to question.

1-5 EXPERIMENTAL

The 1- and 2-naphthonitriles (Tokyo Kasei Co., Ltd.) were distilled under a high vacuum, chromatographed on silica gel, and recrystallized three times from hexane. The 9-cyanophenanthrene was prepared by a known method,[16] distilled under a high vacuum,

and recrystallized three times from methanol. The 2,5-dimethylfuran and 2,5-dimethyl-2,4-hexadiene (Tokyo Kasei Co., Ltd.) were distilled from sodium under a pure nitrogen stream before use. The pyridine, methylated pyridines, 1-methylimidazole, and 1,2-dimethylimidazole (Tokyo Kasei Co., Ltd.) were all distilled from anhydrous potassium hydroxide under a pure nitrogen stream before use. The benzene and ethyl acetate (spectrograde, Nakarai Chemicals) were distilled before use.

The measurements of the fluorescence spectra and the fluorescence-quenching experiments were carried out with a Hitachi MPF-2A spectrofluorometer. The product analyses were carried out with a Shimadzu GC-2C gas chromatograph using a column of SE-30 (5% on Celite 545, 0.75 m) at 140-170°C, a Hitachi R-24 (60 MHz) NMR spectrometer, and a Hitachi 124 UV spectrometer.

1-6 ACKNOWLEDGEMENT

The author wishes to thank Professor Noboru Mataga and Dr. Tadashi Okada, Osaka University, for their help and guidance in the determination of the lifetime of the 9-CP—DHD exciplex. The author is also indebted to Professor Haruo Shizuka, Gunma University, for the fluorescence lifetimes of 1- and 2-NN.

1-7 REFERENCES AND NOTE

[1] A. Weller, Pure Appl. Chem., 16, 115 (1968); T. B. Birks, "Photophysics of Aromatic Molecules," Wiley, New York, N.Y. (1970).

[2] L. M. Stephenson and G. S. Hammond, Pure Appl. Chem., 16, 125 (1968); D. A. Labianca, G. N. Taylor, and G. S. Hammond, J. Am. Chem. Soc., 94, 3687 (1972); "The Exciplex," Ed by M. Gordon and W. R. Ware, Academic Press, New York (1975); P. Froehlich and E. L. Wehry, in "Modern Fluorescence Spectroscopy," ed by E. L. Wehry, Plenum Press, Vol. 2, New York (1976), p. 319.

[3] R. S. Davidson, in "Molecular Association," Ed by R. Foster, Academic Press, Vol. 1, New York (1975), p. 215; A. Lablache-Combier, Bull. Chim. Soc. Fr., 1972, 4792.

[4] T. S. Cantrell, J. Am. Chem. Soc., 94, 5929 (1972); J. J. McCullough, R. C. Miller, D. Fung, and W.-S. Wu, *ibid.*, 97, 5942 (1975); R. A. Caldwell and L. Smith, *ibid.*, 96, 2994 (1974); N. C. Yang and K. Srinivasachar, J. Chem. Soc., Chem. Commun.,

1976; 48; N. C. Yang, K. Srinivasachar, B. Kim, and J. Libman, J. Am. Chem. Soc., 97, 5006 (1975).

[5] K. E. Wilzbach and L. Kaplan, J. Am. Chem. Soc., 93, 2073 (1971); J. Cornelisse, V. Y. Merritt, and R. Srinivasan, *ibid.*, 95, 6197 (1973); R. M. Bowman, T. R. Chamberlain, C.-W. Huang, and J. J. McCullough, *ibid.*, 96, 692 (1974); T. Sasaki, K. Kanematsu, and K. Hayakawa, *ibid.*, 95, 5632 (1973); O. L. Chapman and R. D. Lura, *ibid.*, 92, 6352 (1970); P. P. Wells and H. Morrison, *ibid.*, 97, 154 (1975); F. D. Lewis and C. E. Hoyle, *ibid.*, 98, 4338(1976).

[6] a) C. Pac, T. Sugioka, and H. Sakurai, Chem. Lett., 1972, 39; b) C. Pac, T. Sugioka, K. Mizuno, and H. Sakurai, Bull. Chem. Soc. Jpn., 46, 238 (1973); c) T. Sugioka, C. Pac, and H. Sakurai, Chem. Lett., 1972, 791 and 667; d) K. Mizuno, C. Pac, and H. Sakurai, *ibid.*, 1973, 309; e) C. Pac, K. Mizuno, T. Sugioka, and H. Sakurai, *ibid.*, 1973, 187; f) K. Mizuno, C. Pac, and H. Sakurai, J. Am. Chem. Soc., 96, 2993 (1974); g) K. Mizuno, C.Pac, and H. Sakurai, J. Chem. Soc., Perkin Trans. 1, 1974, 2350; h) K. Mizuno, C. Pac, and H. Sakurai, J. Chem. Soc., Chem. Commun., 1974, 648; i) K. Mizuno, C.Pac, and H. Sakurai, J. Chem. Soc., Perkin Trans. 1, 1975, 2221.

[7] H. Beens and A. Weller, Chem. Phys. Lett., 2, 140 (1968).

[8] J. Saltiel, D. E. Townsend, B. D. Watson, and P. Shannon, J. Am. Chem. Soc., 97, 5688 (1975).

[9] a) J. Saltiel and D. E. Townsend, J. Am. Chem. Soc., 95, 6140 (1973); b) R. O. Campbell and R. S. H. Liu, Mol. Photochem., 6, 207 (1974); c) N. C. Yang, D. M. Shold, and B. Kim, J. Am. Chem. Soc., 98, 6587 (1976); d) J. Saltiel, D. E. Townsend, B. D. Watson, P. Shannon, and S. L. Finson, *ibid.*, 99, 884 (1977).

[10] a) R. A. Caldwell and L. Smith, J. Am. Chem. Soc., 96, 2994 (1974); b) D. Creed and R. A. Caldwell, *ibid.*, 96, 7369 (1974); c) R. A. Caldwell, D. Creed, and H. Ohta, *ibid.*, 97, 3246 (1975); d) D. Creed, R. A. Caldwell, H. Ohta, and D. C. DeMarco, *ibid.*, 99, 277 (1977).

[11] C. Pac and H. Sakurai, Chem. Lett., 1976, 1067.

[12] The lifetimes were determined from the effect of aeration on the exciplex-emission intensity.[10c]

[13] H. Beens, H. Knibbe, and A. Weller, J. Chem. Phys., 47, 1183 (1967).

[14] L. A. Paquette, "Principles of Modern Heterocyclic Chemistry," W. A. Benjamin, New York (1968), pp. 183 and 222.

[15] Unpublished results.

[16] J. E. Callen, C. A. Dornfeld, and G. H. Coleman, Org. Synth., Coll. Vol. 3, 212 (1955).

CHAPTER 2 REDOX-PHOTOSENSITIZED REACTIONS OF ELECTRON DONOR-ACCEPTOR PAIRS BY AROMATIC HYDROCARBONS; CATALYSIS BY THE CATION RADICAL OF AROMATIC HYDROCARBONS

2-1 INTRODUCTION

Photosensitization is particularly of importance in photochemistry, in view of solar energy utilization, usually occurring in exothermic energy transfer[1]; almost, triplet energy transfer.[1,2] Recently, photosensitized reactions which are endothermic in classical energy transfer have been discussed in terms of exciplexes.[3] In some photoreactions of electron donor-acceptor pairs, the final products arise only from the electron donor, showing a different type of "photosensitization" by the electron acceptor.[4-7] This reaction is shown to be initiated by photochemical electron transfer from the electron donor to the acceptor,[4-7] and therefore, can provide a general and elegant method for the steady genaration of ion radicals. In this regard, it should be noted that the chemistry of cation radicals has been left almost unsolved to be lack of convenient methods for their generation, though they are believed to be very important reactive species in organic reactions as well as biological systems.[8]

In this chapter, the author describes a novel type of photosensitization by aromatic hydrocarbons (S); redox-photosensitized reaction, in which excited singlet aromatic hydrocarbons ($^1S^*$) catalyze electron transfer from an electron donor (D) to an electron acceptor (A) and the initiation process in the photoredox reaction from S to A.

2-2 RESULTS

Products in Redox-Photosensitized Reactions Using Aromatic Hydrocarbons (S)-Electron Acceptor (A)-Electron Donor (D) Systems. D= Furan and Methylated Furans. Irradiation of a 4:1-acetonitrile–methanol solution containing furan (F), 2-methylfuran (MF), or 2,5-dimethylfuran (DF) as D, *p*-dicyanobenzene (DCNB) as A, and phenanthrene (P) as S gave the corresponding products (1-5) in good yields with 70-80% recovery of P; the products are evidently formed *via* cation radicals of D.

Chromatography of 1 and 2 on silica gel or basic alumina gave 6 and 7 respectively, in 20-50% yields with 30-50% recovery of 1

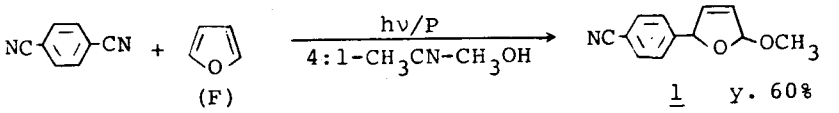

(F)

1 y. 60%

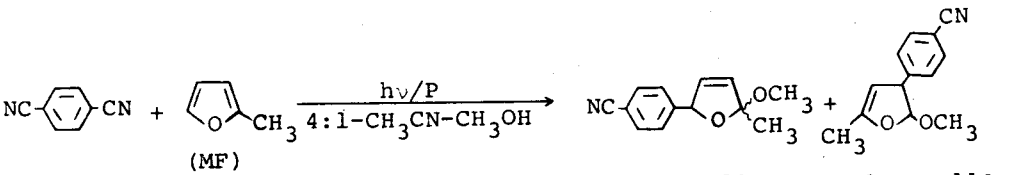

(MF)

2 y. 53% 3 y. 11%

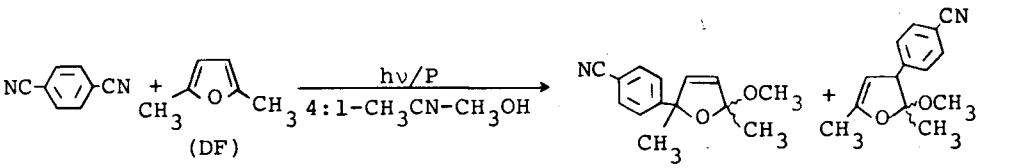

(DF)

4 y. 36% 5 y. 27%

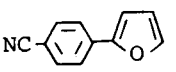

6

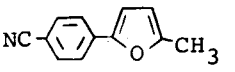

7

and 2; the compounds 6 and 7 are evidently formed by elimination of methanol and following aromatization.

In control runs, it was confirmed that the recovery of P and yields of 1-5 were quantitative; irradiation at >300 nm in the absence of P did not give 1-5 at all. The quantum yield for the formation of 1([F]= 1.0 M) was 0.1 ± 0.01 at 313 nm.

D= 1,1-Diphenylethylene (DPE). Irradiation of a acetonitrile solution containing DPE, P, and DCNB at >300 nm gave 8 in 85% isolated yield. In the presence of 25% methanol, the photoreaction gave 9 and 10 in 70% and 9% isolated yields respectively.

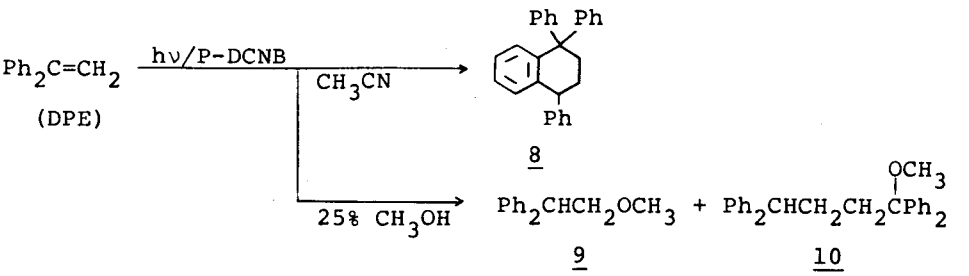

On the other hand, P and DCNB were recovered in 70% and 95% yields respectively. In the absence of P, the formation of 9 occurred less than one-tenth as efficiently as in the presence of P. In place of DCNB, *o*- and *m*-dicyanobenzene can be used.

D= Indene (IN). In the similar way to the case of DPE, the photodimerization of IN was sensitized by P to give *cis,syn*- and *trans,syn*-indene cyclobutane dimers in ~5:95 ratio. In the presence of 25% methanol, the photoreaction gave 11 and 12 in 44% and 12% isolated yields respectively, at the expense of the dimers. On the other hand, P and S were recovered in ca. 80-85% yields. In the absence of either P or DCNB, no photoreaction occurred. In place of DCNB, *o*- and *m*-dicyanobenzene can be used.

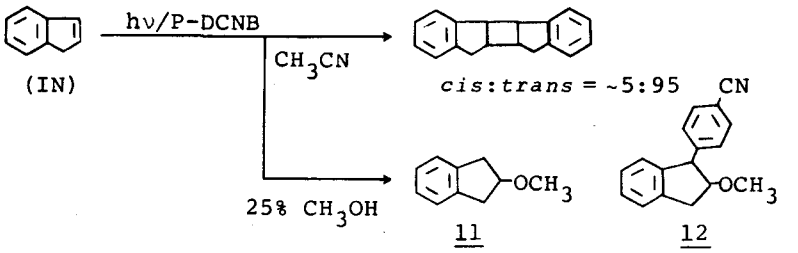

These redox-photosensitized reactions were quenched perfectly by cation radical quenchers such as triethylamine and *p*-dimethoxybenzene possessing low oxidation potentials (Table 6), but not by 1.0 M isoprene.

Redox-Photosensitized Reactions Using Other Aromatic Hydrocarbons. The photosensitized reactions were effected by the other aromatic hydrocarbons involving triphenylene (TR), naphthalene (NT), and chrysene (CR), while pyrene (PR) and anthracene (AN) were not effective. Quantum yields for formation of each product were determined for each effective hydrocarbons. Table 1 summarizes the results together with oxidation potentials of S ($E^{ox}_{1/2}$(S)) and D ($E^{ox}_{1/2}$(D)).

Quantum Yield for 9 formation in Redox-Photosensitized Reaction of DPE. For mechanistic investigation, the anti-Markownikoff addition of methanol to DPE by the redox-photosensitization using P as S and DCNB as A in 4:1-acetonitrile–methanol solutions was employed as the typical reaction.

The formation of 9 increased linearly with irradiation time

Table 1. Redox-Photosensitized Reactions of D and Quantum Yields for Products Formation[a]

S	$E^{ox}_{1/2}$(S)/V	D ($E^{ox}_{1/2}$(D)/V)				
		F (1.40)	MF (1.14)	DF (0.93)	DPE (1.32)	IN (1.17)
Triphenylene (TR)	1.29	0.21[b]	ND[c]	ND[c]	0.41[d]	ND[c]
Naphthalene (NT)	1.22	0.15[b]	ND[c]	ND[c]	0.38[d]	ND[c]
Phenanthrene (P)	1.17	0.10[b]	0.16[e]	ND[c]	0.36[d]	0.25[f]
Chrysene (CR)	1.05	0.049[b]	ND[c]	ND[c]	0.14[d]	ND[c]
Pyrene (PR)	0.78	×	×	×	×	×
Anthracene (AN)	0.75	×	×	×	×	×

[a]Quantum yields (ϕ) were determined for 4:1-acetonitrile–methanole solutions; 313 nm irradiation; [S]= 0.01 M, [DCNB]= 0.1 M, and [D]= 0.1 M. Oxidation otentials were determined *vs.* Ag/Ag^+ in acetonitrile by cyclic voltammetry. The cross mark indicates the lack of the reaction. [b] $\phi_{\underline{1}}$. [c] The photosensitized reaction occurred but the quantum yields were not determined. [d] $\phi_{\underline{9}}$. [e] $\phi_{\underline{2}}$. [f] $\phi_{\underline{11}}$.

up to ca. 8% conversion (Figure 1). Quantum yields for 9 formation ($\phi_{\underline{9}}$) were determined at less than 7% conversion (Table 2), in which formation of 8 and 10 was negligible small. The plot of $\phi_{\underline{9}}^{-1}$ *vs.* reciprocals of concentration of DPE is linear and independent of the intensity of the incidnet light at 313 nm (Figure 2). It was found that $\phi_{\underline{9}}$ depends on concentration of methanol (Table 3 and Figure 3), but not on concetration of P (Table 4).

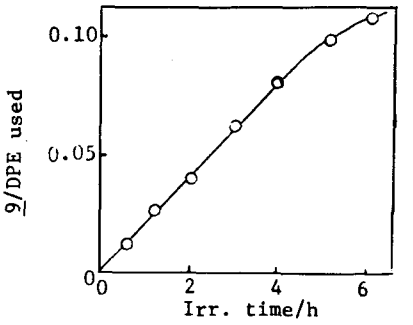

Figure 1. Formation of 9 [mol per mol of DPE] *vs.* irradiation time in the redox-photosensitized reaction of DPE. Degassed 4:1-acetonitrile–methanol solutions; 313 nm irradiation; [DPE]= 0.1 M, [P]= 0.01 M, and [DCNB]= 0.1 M.

Table 2. Dependence of Quantum Yields (ϕ_9) on Concentration of DPE and Light Intensity[a]

[DPE]×10^3/M	ϕ_9 Light intensity[b]	
	2.3×10^{-8}	6.1×10^{-8}
11.4	-	0.238
12.8	0.256	-
14.5	-	0.244
16.0	0.246	-
20.0	-	0.286
40.0	0.294	0.328
76.0	0.370	0.318
∞[c]	0.36	
Intercept[d]	2.8	
Slope[d]×10^2/M	1.8	

[a] Degassed 4:1-acetonitrile-methanol solution; [P]= 0.01 M and [DCNB]= 0.1 M; at 313 nm. [b] Einstein/min. [c] Extraporated value (ϕ_9^∞); see Figure 2. [d] Intercept and slope of the linear plot in Figure 2.

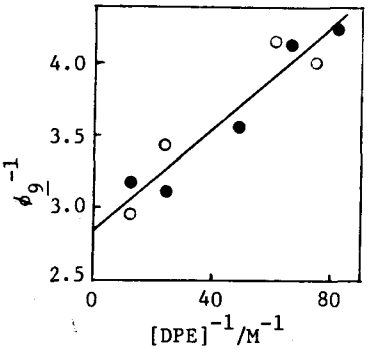

Figure 2. Plots of ϕ_9^{-1} *vs.* $[DPE]^{-1}$ with least-squares fit; 313 nm irradiation with light intensities of 2.3×10^{-8} (-●-) and 6.1×10^{-8} (-○-) einstein/min; see footnotes in Table 2.

Table 3. Dependence of Quantum Yields (ϕ_9) on Concentration of Methanol[a]

[CH_3OH]/M	0.1	0.2	0.4	0.67	1.0	4.95	∞[b]
ϕ_9	0.0267	0.0526	0.0870	0.124	0.149	0.374	0.40
Intercept[c]				2.5			
Slope[c]/M				3.5			

[a] Degassed acetonitrile solutions; [DPE]= 0.1 M, [P]= 0.01 M, and [DCNB]= 0.1 M; at 313 nm. [b] Extrapolated value; see Figure 3. [c] Intercept and slope of the linear plot in Figure 3.

Table 4. Independence of Quantum Yields (ϕ_9) on Concentration of Phenanthrene[a]

[P]/M	0.1	0.09	0.08	0.06	0.05	0.035	0.02	0.01
ϕ_9	0.374	0.364	0.365	0.376	0.358	0.357	0.374	0.358

[a] Degassed 4:1-acetonitrile-methanol solution; [DPE]= 0.1 M and [DCNB]= 0.1 M; at 313 nm.

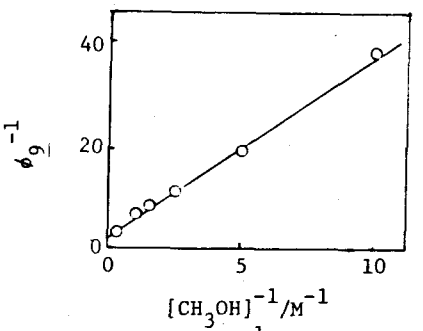

Figure 3. Plot of ϕ_9^{-1} *vs.* $[CH_3OH]^{-1}$ with least-squares fit; see footnotes in Table 3.

Quenching by Cation Radical Quenchers. The anti-Markownikowff addition of methanol to DPE by the redox-photosensitization was quenched by triethylamine (Q) (Table 5). The Stern-Volmer plot was linear up to ca. 2×10^{-3} M of Q (Figure 4). At higher concentration of Q, however, the plot deviates from the linearity (Figure 5). The curved Stern-Volmer plot could be

Table 5. Dependence of Quantum Yields (ϕ_9^Q) on Concentration of Triethylamine (Q)[a]

$[NEt_3]\times10^{-3}$/M	0.0	0.3	0.6	1.0	1.5	2.0	4.0	7.0	9.0	11	13	15
$\phi_9\ 10^2$	35.6	20.5	14.7	10.7	7.36	6.34	3.10	1.71	1.22	0.98	0.72	0.57

[a] Degassed 4:1-acetonitrile-methanol solution; [DPE]= 0.1 M, [P]= 0.01 M, [DCNB]= 0.1 M; at 313 nm.

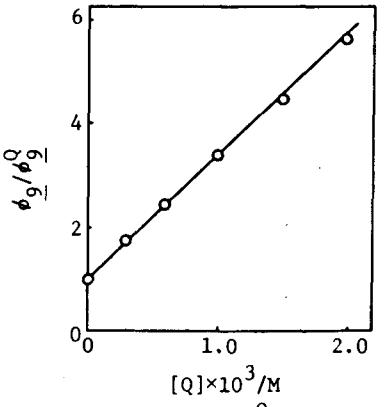

Figure 4. Plot of ϕ_9/ϕ_9^Q *vs.* [Q] (Q= triethylamine) with least-squares fit at $\leq 2.0\times10^{-3}$ M of Q; see footnotes in Table 5.

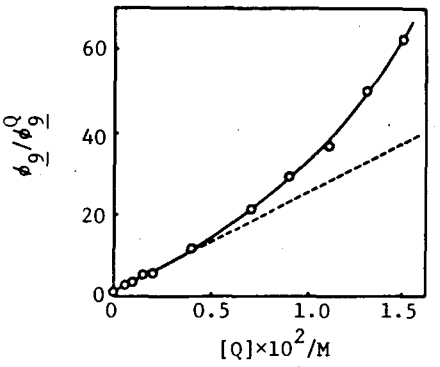

Figure 5. Plot of ϕ_9/ϕ_9^Q *vs.* [Q] (Q= triethyl amine) at $\geq 2\times10^{-3}$ M of Q; see footnotes in Table 5.

caused by either the formation of CT-complex in the ground state or the quenching of the fluorescence of P by Q. However, UV and fluorescence measurements eliminated these posibility. Thus, the curved plot clearly arises from the quenching of reaction intermediates by Q. With the other quenchers, linear Stern-Volmer plots were obtained at relatively low concentration of the quenchers, which no CT-absorption was observed. Table 6 lists the slopes of the plots together with the oxidation potentials of the quenchers. It was found that ϕ_9/ϕ_9^Q depends on concentration of DPE (Table 7 and Figure 6).

Table 6. Slopes in the Linear Region of Stern-Volmer Plots in the Quenching by Various Quenchers[a]

Quenchers	$E_{1/2}^{ox}$/V	$K_{SV}\times10^{-1}/M^{-1}$
Anisole	1.30	0.012
Hexamethylbenzene	1.16	47.0
o-Methylanisole	1.20	27.5
p-Methylanisole	1.11	16.5
1,3,5-Trimethoxybenzene	1.01	220
o-Dimethoxybenzene	0.97	300
p-Dimethoxybenzene	0.90	290
Triethylamine	0.37	242

[a] Degassed 4:1-acetonitrile-methanol solution; at 313 nm; [DPE]= 0.1 M, [P]= 0.01 M, and [DCNB]= 0.1 M.

Table 7. Dependence of Quantum Yields (ϕ_9 and ϕ_9^Q) on Concentration of DPE[a]

$[DPE]\times10^3/M$	$\phi_9\times10^2$	$\phi_9^Q\times10^2$	ϕ_9/ϕ_9^Q
5.0	18.4	4.82	3.82
6.3	20.5	5.45	3.76
7.7	21.3	5.87	3.63
10.0	23.0	6.39	3.60
15.0	25.1	7.05	3.56
20.0	28.6	8.31	3.44
35.0	30.9	8.33	3.37
100	35.6	10.7	3.33
Intercept[b]	3.25		
Slope[b]$\times10^3/M$	2.95		

[a] Degassed 4:1-acetonitrile-methanol solution; at 313 nm; [P]= 0.01 M, [DCNB]= 0.1 M; in the absence of Q (ϕ_9) and in the presence of Q ([Q]= 0.001 M) (ϕ_9^Q); Q= triethylamine. [b] Intercept and slope of the linear plot in Figure 6.

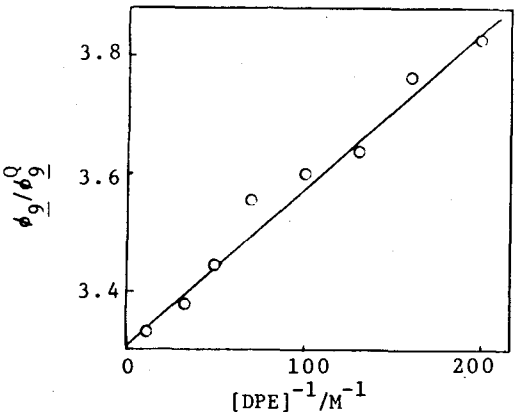

Figure 6. Plot of ϕ_9/ϕ_9^Q *vs.* $[DPE]^{-1}$ with least-squares fit; see footnote in Table 7.

2-3 DISCUSSION

Mechanism of Redox-Photosensitized Reactions. Since physical excitation transfer from excited S to either D or DCNB is highly endothermic (Table 8), the classical energy-transfer mechanism is very unlikely for the photosensitization by efficient S. In fact, the formations of products (1-5 and 8-12) were not quenched even by 1.0 M isoprene, a triplet mechanism being thus discarded. All the electron donors (D) used did neither quench the fluorescence of S nor form any CT-complexes with S and DCNB. The fluorescences of all S used were quenched by DCNB, though each S does not form any CT-complex with DCNB in polar and non-polar solvents. In benzene or ethyl acetate, the fluorescence quenching (S= P) was accompanied by the appearance of an exciplex emission with each isoemissive point at 387 or 393 nm, while exciplex emission could not be observed in acetonitrile or acetonitrile–methanol. However, an exciplex mechanism is unlikely, since the photosensitized reactions in benzene or ethyl acetate containing 10% methanol did not occur or were very slow.

In a variety of exciplex-forming systems; fluorescence quenching in very polar solvents has been established to occur *via* electron transfer between the fluorophor and the quencher.[9] In Table 9 are listed the fluorescence quenching rate constants and the calculated values of the free energy change (ΔG) associated with the electron-transfer process, using eq 1.[10] The diffusion-controlled fluorescence quenching and the negative values of ΔG

Table 8. Excited Singlet and Triplet Energies

Molecule	E_{0-0}/kcal mol^{-1}	
	Singlet	Triplet
Triphenylene (TR)	83.4[a]	66.5[a]
Naphthalene (NT)	92[a]	60.9[a]
Phenanthrene (P)	82.9[a]	62.0[a]
Chrysene (CR)	79.2[a]	57.3[a]
Pyrene (PR)	77.0[a]	48.1[a]
Anthracene (AN)	76.3[a]	42.7[a]
Furan (F)	120[b]	101[c]
1,1-Diphenylethylene (DPE)	95[b]	54.4[d]
Indene (IN)	92[b]	59[e]
Isoprene		60.1[a]
p-Dicyanobenzene (DCNB)[f]	98.6[a]	70.5[a]

[a] Values compiled in S. L. Murou, in "Handbook of Photochemistry," Marcel Dekker, New York, N. Y., 1973. [b] Estimated from the onset of the UV absorption. [c] M. Orloff and D. D. Fitts, J. Chem. Phys., 38, 2334 (1963). [d] E. F. Ullman and W. A. Henderson, J. Am. Chem. Soc., 89, 4390 (1967). [e] R. C. Hechman, J. Mol. Spectros., 2, 27 (1958). [f] Reduction potential was measured to be -1.91 V, determined by cyclic voltammetry.

Table 9. Rate Constants and Calculated ΔG Values for Fluorescence Quenching by *p*-Dicyanobenzene

Fluorophor	τ[a]/ns	k_q[a]$\times 10^{-10}$/M^{-1}s^{-1}	ΔG[b]/kcal mol^{-1}
TR	34±0.5[c]	1.4[c]	-9.1
NT	118[d,e]	1.2[e]	-21.1
P	60±1[e]	2.0[e]	
	17±1[c]	1.5[c]	-13.2
CH	48±0.5[c]	1.2[c]	-12.2

[a] For degassed solutions; concentration, 10^{-3}-10^{-4} M. [b] Calculated values in a acetonitrile, using eq 1 and the thermodynamic data in Table 8. Coulombic term is estimated to be 1.3 kcal/mol. [c] In 3:1-acetonitrile-methanol. [d] N. Mataga, M. Tamura, and H. Nishimura, Mol. Phys., 9, 367 (1965). [e] In acetonitrile.

$$\Delta G(\text{kcal/mol}) = 23.06[E(D/D^+)_V - E(A/A^-)_V - e^2/\varepsilon\alpha] - E_{0-0}(\text{kcal/mol}) \quad \cdots(1)$$

suggest that electron transfer from excited singlet S ($^1S^*$) to DCNB occurs to give cation radicals of S (S^+) and anion radical

of DCNB ($DCNB^{\cdot-}$).[11] From these results, therefore, a tentative mechanism for photosensitization by S is shown in Scheme 1; the initiation process is electron transfer from $^1S^*$ to DCNB and a key mechanistic pathway is the hole transfer $S^{\cdot+}$ to D, leading to the recovery of S and the formation of $D^{\cdot+}$ or its related species (*vide infra*). The final products were thus formed by the nucleophilic attack of methanol or other D on $D^{\cdot+}$ and the subsequent reaction of the intermediates. Evidence for the intermediacy of cation radicals was provided by the efficient quenching of the reactions with triethylamine or *p*-dimethoxybenzene possesing low oxidation potentials (Table 6). Moreover, it has been documented that anti-Markownikoff photoaddition of methanol DPE or IN in the presence of 1- or 2-cyanonaphthalene occurs *via* $DPE^{\cdot+}$[4a] $IN^{\cdot+}$[12], photodimerization of indene *via* $IN^{\cdot+}$.[5]

$$S \xrightarrow{h\nu} {}^1S^*$$

$$^1S^* + DCNB \longrightarrow S^{\cdot+} + DCNB^{\cdot-}$$

$$S^{\cdot+} + D \longrightarrow S + D^{\cdot+}$$

$$D^{\cdot+} + CH_3OH \longrightarrow \cdot D\text{-}OCH_3 + H^+$$

$$\cdot D\text{-}OCH_3 + DCNB^{\cdot-} \longrightarrow \underline{1}, \underline{2}, \underline{3}, \underline{4}, \underline{5}, \text{ or } \underline{12} + CN^-$$

$$\cdot D\text{-}OCH_3 + DCNB^{\cdot-} \longrightarrow {}^-D\text{-}OCH_3 + DCNB$$

$${}^-D\text{-}OCH_3 + H^+ \longrightarrow \underline{9} \text{ or } \underline{11}$$

$$D^{\cdot+} + D \longrightarrow DD^{\cdot+}$$

$$DD^{\cdot+} + DCNB^{\cdot-} \longrightarrow \underline{8} \text{ or indene dimers} + DCNB$$

$$DD^{\cdot+} + CH_3OH \longrightarrow \cdot DD\text{-}OCH_3 + H^+$$

$$\cdot DD\text{-}OCH_3 + DCNB^{\cdot-} \longrightarrow {}^-DD\text{-}OCH_3 + DCNB$$

$${}^-DD\text{-}OCH_3 + H^+ \longrightarrow \underline{11}$$

$$S^{\cdot+}, D^{\cdot+}, \text{ or } DD^{\cdot+} + Q \longrightarrow S, D, \text{ or } DD + Q^{\cdot+}$$

$$Q^{\cdot+} + DCNB^{\cdot-} \longrightarrow Q + DCNB$$

Scheme 1.

In the case of MF, DF, or IN, the formation of their cation radicals can occur since the hole transfer processes are isothermal or slightly endothermic. However, the complete hole transfer from $S^{\cdot+}$ to F and DPE is unfavarable since this process is highly (ca. 5-9 kcal/mol) endothermic (Table 1). A reasonable interpretation would be provided by assuming the intervention of of the π-complex $(S\cdot D)^{\cdot+}$;[13] methanol or other D attack the partially

developed positive charge or D side of the π-complex without complete hole transfer (eq 2). This mechanism is supported by the

$$S^{+\cdot} + D \rightleftharpoons (S\cdot D)^{+\cdot} \xrightarrow[DCNB^{-\cdot}]{CH_3OH \text{ or } D} S + \text{product(s)} \qquad (2)$$

curved Stern-Volmer plot in Figure 5 that demonstrates the existence of two different cation radical species as the reaction intermediated, *i.e.* $S^{+\cdot}$ and the π-complex. The formation of the π-complex is not surprising, since it has been reported that the cation radical of methylated benzenes forms π-complexes with neutral molecules of other methylated benzenes in vapor phase. Moreover, intermediacy of π-complex of $S^{+\cdot}$ and indene cyclobutane dimers will be elucidated in redox-photosensitized ring cleavage of the dimers (see chapter 3).

For mechanistic elucidation, the anti-Markownikoff addition of methanol to DPE by the redox-photosensitization was studies in detail. On the basis of the results, the possible mechanistic pathways are thus shown in Scheme 2; a key mechanistic pathway is formation of π-complex and the following attack of methanol on D side of the π-complex. In the presence of Q, hole transfer from either $S^{+\cdot}$ or $(S\cdot D)^{+\cdot}$ to Q should be considered as the quenching processes, since the oxidation potential of Q is very low. The cation radical intermediates are also quenched by impurities involving water. However, this process appears to be of minor importance, since their concentration is probably very low. Charge neutralization between the cation radicals and $DCNB^{-\cdot}$ and formation of dimer cation radicals of S $(S_2^{+\cdot})$[15] are not important, since $\phi_{\underline{9}}$ is independent of the light intensity and concentration of P (Figure 2 and Table 4). Since the fluorescences of S are completely quenched by 0.1 M of DCNB, unimolecular decay processes from $^1S^*$ can be neglected.

Analysis of Kinetics. In the absence of Q, steady-state analysis gives eq 17, where α and a represent the limiting quantum yield for $S^{+\cdot}$ formation and for 9 formation from the radical intermediate ($\cdot D\text{-}OCH_3$) respectively. From the intercepts and slopes

$$\frac{1}{\phi_{\underline{9}}} = \frac{1}{a\alpha}\left(1 + \frac{k_D^C[D] + k_N^C[X]}{k_M^C[CH_3OH]}\right)\left(1 + \frac{k_N[X]}{k_c[D]}\right) \qquad (17)$$

$$S \xrightarrow{h\nu} {}^1S^* \quad (3)$$

$${}^1S^* \xrightarrow{1/\tau} S \quad (4)$$

$${}^1S^* + DCNB \xrightarrow{\alpha} S^{+\cdot} + DCNB^{-\cdot} \quad (5)$$

$${}^1S^* + DCNB \xrightarrow{1-\alpha} S + DCNB \quad (6)$$

$$S^{+\cdot} + D \xrightarrow{k_c} (S\cdot D)^{+\cdot} \equiv C^{+\cdot} \quad (7)$$

$$S^{+\cdot} + X \xrightarrow{k_N} S \text{ and/or other(s)} \quad (8)$$

$$S^{+\cdot} + Q \xrightarrow{k_q} S + Q^{+\cdot} \quad (9)$$

$$C^{+\cdot} + CH_3OH \xrightarrow{k_M^c} S + \cdot D\text{-}OCH_3 \quad (10)$$

$$C^{+\cdot} + D \xrightarrow{k_D^c} S + DD^{+\cdot} \quad (11)$$

$$C^{+\cdot} + X \xrightarrow{k_N^c} S + D \text{ and/or other(s)} \quad (12)$$

$$C^{+\cdot} + Q \xrightarrow{k_q^c} S + D + Q^{+\cdot} \quad (13)$$

$$\cdot D\text{-}OCH_3 \xrightarrow[DCNB^{-\cdot}/\ H^+]{a} \underline{9} \quad (14)$$

$$DD^{+\cdot} \xrightarrow[DCNB^{-\cdot}/CH_3OH]{} \underline{10} \quad (15)$$

$$Q^{+\cdot} + X \longrightarrow Q \text{ and/or other(s)} \quad (16)$$

D= DPE, Q= triethylamine, and X= $DCNB^{-\cdot}$, H_2O, and impurities.

Scheme 2.

in Figures 2 and 3, the following rate ratios are obtained:

$$k_N[X]/k_c = 6.4\times10^{-3}\ M \quad (18)$$

$$(k_D^c[D] + k_N^c[X])/k_M = 1.4 \quad (19)$$

$$a\alpha = 0.43 \quad (20)$$

In the presence of Q, Stern-Volmer equation can be represented by eq 21, where [S]= 0.01 M. In eq 21, it has been

$$\frac{\phi_{\underline{9}}}{\phi_{\underline{9}}^Q} = 1 + \left(\frac{k_q^c}{k_M^c[CH_3OH]} + \frac{k_q}{k_c[D]}\right)[Q] + \frac{k_q k_q^c[Q]^2}{k_c k_M^c[D][CH_3OH]} \quad (21)$$

$$K_{SV} = k_q^c/k_M^c[CH_3OH] + k_q/k_c[D] \quad (22)$$

assumed that $k_M^C[CH_3OH] >> k_D^C[D] + k_N^C[X]$ and $k_C[D] >> k_N[X]$. This equation demonstrates that the plot of ϕ_9/ϕ_9^Q gives a linear at lower concentration of Q and a concave-curved line at higher concentration of Q, in accord with the observations (Figures 4 and 5). The plot of ϕ_9/ϕ_9^Q *vs.* reciprocals of concentration of D is a linear line at lower concentration of Q (10^{-3} M) and constant concentration of methanol (4.95 M) (Figure 6). From the intercept and the slope, the following rate ratios are obtained.

$$k_q^C / k_M^C = 1.1 \times 10^4 \quad (23)$$

$$k_q / k_C = 2.95 \quad (24)$$

Hole transfer from the cation radical of P to Q prbably occurs at a diffusion-controlled rate since this process is highly exothermic by 18.4 kcal/mol (0.80 eV). The plot of $\log K_{SV}$ *vs.* the difference between oxidation potentials of P and quenchers ($\Delta E_{1/2}^{ox} = E_{1/2}^{ox}(Q) - E_{1/2}^{ox}(P)$) is shown in Figure 7; $\log K_{SV}$ increases

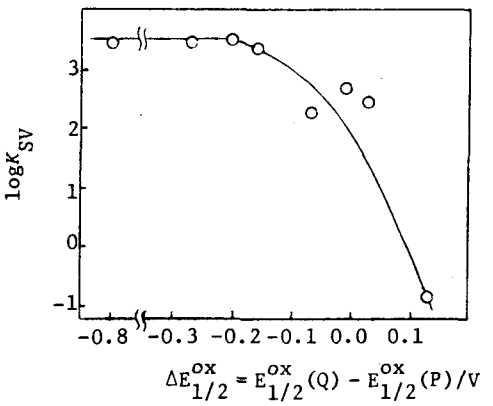

Figure 7. Plot of $\log K_{SV}$ *vs.* $\Delta E_{1/2}^{ox}$, using the data in Table 6.

with an increase of exothermic energy in hole transfer from $P^{\cdot+}$ to Q, and reaches the constant value (ca. 3.5) at $\Delta E_{1/2}^{ox} < -4$ kcal/mol. This suggests that hole transfer from $P^{\cdot+}$ and $(P \cdot D)^{\cdot+}$ to Q occurs at a diffusion-controlled rate. Therefore, it can be assumed reasonably that $k_q \simeq k_q^C \simeq 10^{10}$ $M^{-1}s^{-1}$. On the basis of this assumption, rate constants can be calculated using eqs 18, 19, 23, and 24. Table 10 lists the calculated rate constants.

Table 10. Rate Constants in Anti-Markownikoff Addition of Methanol to DPE by Redox-Photosensitization[a]

Process	Symbols	Values
Formation of $(P\cdot D)^{\pm\cdot}$	k_C	3.4×10^9 $M^{-1}s^{-1}$
Formation of $\cdot D\text{-}Och_3$ from $(P\cdot D)^{\pm\cdot}$ and methanol	k_M^C	9.0×10^5 $M^{-1}s^{-1}$
Decay of $P^{\pm\cdot}$	$k_N[X]$	2.2×10^7 s^{-1}
Decay of $(P\cdot D)^{\pm\cdot}$	$0.1k_D^C + k_N^C[X]$	1.3×10^6 s^{-1}
Limiting quantum yield of 9 formation	$a\alpha$	0.43

[a] See text.

An interesting point of the results is that the π-complex formation occurs very fast, being perhaps exothermic. On the other hand, the attack of methanol on the π-complex occurs very slow, compaired with the rate constant for reaction of cation radical of α-methylstyrene and ethanol (3.5×10^7 $M^{-1}s^{-1}$),[16] and therefore, competes processes of $(P\cdot D)^{\pm\cdot}$ formation and decay of the π-complex, suggesting that electrophilicity of the π-complex is relatively low. Thus, the redox-photosensitized reaction of DPE could be interpreted reasonably by the mechanism involving π-complex as key intermediate. Since ϕ_9 increases with an increase of $E_{1/2}^{ox}(S)$ (Table 1), the positive charge of the π-complex seems to increasingly develope on the side of D as $E_{1/2}^{ox}(S)$ increases, resulting in more fast attack of methanol on the π-complex.

$$(S\cdot D)^{\pm\cdot} \equiv \{(S^{\pm\cdot})\cdot D \leftrightarrow S\cdot(D^{\pm\cdot})\} \xrightarrow[CH_3OH]{} \text{Product(s)}$$

2-4 CONCLUSION

In the redox-photosensitized reactions, consequently, aromatic hydrocarbons can be considered to act as a redox carriers as shown in Scheme 3 simplified.

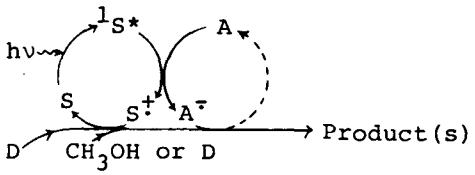

Scheme 3.

The redox-photosensitization is very similar to the catalytic nature of chlorophyll a molecules in the reaction center of photosynthesis; electronically excited chlorophyll molecules in the reaction center formed by receiving photoenergies from antena chlorophylls catalyze the pumping up of electron from electron donor to electron acceptor by acting as redox carriers, thus converting photoenergies into chemical energies.[17] Although the exact and whole mechanisms of photosynthesis have not been fully established, chlorophll a cation radicals are believe to play essential roles in the reaction center.[18] In this regard, the role of $S^{+\cdot}$ in the redox-photosensitization should be emphasized; $S^{+\cdot}$ is relatively stable to chemical reactions with weak nucleophiles such as furan, olefins, methanol, and water. This seems to be an important nature of $S^{+\cdot}$ for the occurrence of the redox-photosensitization and results in catalysis of $S^{+\cdot}$; $S^{+\cdot}$ forms π-complex with D, developes possitive charge on the D side, and causes the following reaction of D. The author believes that aromaticity of chlorophyll a cation radical has certain degree of connection with chemical stability of the cation radical which can be regenerated efficiently.

2-5 EXPERIMENTAL

Materials. Special grade acetonitrile was distilled three times from phosphorous pentoxide and then twice from calcium hydride before use. Methanol was distilled three times from magnesium methoxide before use. Benzene and ethyl acetate were distilled before use. Furan, 2-methylfuran, and 2,5-dimethylfuran were distilled from sodium before use. 1,1-Diphenylethylene, indene, anisole, hexamethylbenzene, *o*- and *p*-methylanisoles, 1,3,5-trimethoxybenzene, and *o*- and *p*-dimethoxybenzene were distilled from sodium in vacuo before use. Triethylamine was refluxed over and distilled from potassium hydroxide before use. Aromatic hydrocarbons and *o*-, *m*-, and *p*-dicyanobenzene were recrystallized three times from methanol or mixtures of ethanol-benzene and then sublimed. All other chemicals and solvents were reagent grade and purified by fractional distillation and/or recrystallization.

Analytical Methods. Melting points were taken on a hot stage and are uncorrected. Column chromatography was on silica

gel (70-230 mesh, Merck) or alumina (300 mesh, Nakarai Chemicals). Analytical gas-liquid chromatography (GLC) was performed on a Shimadzu GC-3BF dual column instrument with flame ionization detectors. The column used for quantitative analyses of 1,1-diphenylethylene, 1,1-diphenyl-2-methoxyethane (9), and 2-methoxyindan (11) was 75 cm × 4 mm of 10% Ucon Oil LB-550 X on Neopak-1A. GLC analyses of 1, 2, 8, 10, 12, indene dimers, the aromatic hydrocarbons, and *p*-dicyanobenzene were carried out with 75 cm × 4 mm columns of 5% PEG 20M on Shimalite W, 5% Ucon Oil LB-550 X on Shimalite W, 3% and 5% SE-30 on Shimalite W, 5% PEG-HT on Chromosorb WAW DMCS.

Spectroscopic measurements, quantum yields, and oxidation potentials were carried out as similar manners to in chapter 3.

Redox-Photosensitized Reaction of F in Preparative Scale. A solution of F (9.0 g, 132 mmol), P (0.18 g, 1 mmol), and DCNB (2.1 g, 16 mmol) in 4:1-acetonitrile–methanol (150 mL) was bubbled with an N_2-stream for 30 min and irradiated at >300 nm for 20 h under water-cooling at 20±1°C. After evaporation, the residure was refluxed in hexane, cooled to ambient temperature, and filtered. Solvent of the filtrate was evaporated to gave an oil, which was distilled fractionally to yield 2,5-dihydro-2-methoxy-5-*p*-cyanophenylfuran (1); 114°C (5 mmHg). Recrystallization from methanol gave pure 1 (1.58 g, 60% yield; based on unrecovered DCNB): mp 50-51°C; NMR δ 3.42 (s, 3H), 3.84 (dd, *J*= 2.0, 2.2 Hz, 1H), 5.04 (d, *J*= 2.9 Hz, 1H), 5.08 (dd, *J*= 2.0, 2.2 Hz, 1H), 6.50 (dd, *J*= 2.2, 2.9 Hz, 1H), 7.20-7.62 (AB_q, 4H); mass spectrum *m/e* 201 (M^+).

Anal. Calcd for $C_{12}H_{11}NO_2$: C, 71.62; H, 5.51; N, 6.96. Found: C, 71.58; H, 5.34; N, 7.04.

Chromatography of 1 on silica gel or alumina gave 6 in 30-60% yields; 1-*p*-cyanophenylfuran (6): mp 65-66°C; NMR δ (ppm) 6.42 (dd, *J*= 3.75, 1.9 Hz, 1H), 6.65 (d, *J*= 3.75 Hz, 1H), 7.43 (d, *J*= 1.9 Hz, 1H), 7.46-7.69 (AB_q, 4H); mass spectrum *m/e* 169 (M^+).

According to the above general procedure the redox-photosensitized reactions were carried out.

2-Methyl-2-methoxy-5-hydro-5-*p*-cyanophenylfuran (2). oil; bp 140°C (0.1 mmHg); NMR δ(ppm) 1.64 (s, 3H), 3.33 (s, 3H), 5.60(d, *J*= 2.3 Hz, 1H), 5.63 (d, *J*= 0.5 Hz, 1H), 6.08 (dd, *J*=2.3, 0.5 Hz, 1H), 7.4-7.5 (bs, 4H); mass spectrum *m/e* 215 (M^+).

2-Methyl-4-*p*-cyanophenyl-5-hydro-5-methoxyfuran (3). NMR δ (ppm) 1.16 (s, 3H), 3.33 (s, 3H), 3.77 (m, 1H), 4.89 (d, *J*= 2.7 Hz, 1H), 7.27 (AB_q, 4H).

2-Methyl-5-*p*-cyanophenylfuran (7). mp 82-83°C; NMR δ (ppm) 2.41 (s, 3H), 5.97 (bd, *J*= 3.0 Hz, 1H), 6.55 (d, *J*= 3.0 Hz, 1H), 7.50 (bs, 4H); mass spectrum *m/e* 183 (M^+).

Anal. Calcd for $C_{12}H_9NO$: C, 39.34; H, 2.48; N, 3.82. Found: C, 39.46, H, 2.33, N, 3.59.

1,1,4-Triphenyltetraline (8). mp 121-122°C; NMR δ (ppm) 1.60-2.10 (m, 2H), 2.64 (t, 2H), 4.16 (t, 1H), 6.88-7.40 (m, 19H); mass spectrum *m/e* 360 (M^+).

Anal. Calcd for $C_{28}H_{24}$: C, 93.29; H, 6.71. Found: C, 93.10, H, 6.55.

1,1-Diphenyl-2-methoxyethane (9). bp 130°C (10 mmHg); IR (CCl_4) 1110 cm^{-1} (C-O-C); NMR δ (ppm) 3.28 (s, 3H), 3.78 (d, 2H), 4.16 (t, 1H), 7.10 (m, 10H); mass spectrum *m/e* 212 (M^+).

Anal. Calcd for $C_{15}H_{16}O$: C, 84.87; H, 7.60. Found: C, 84.91; H, 7.61.

1,1,4,4-Tetraphenyl-1-methoxybutane (10). mp 135-136°C; IR (KBr) 1060 cm^{-1} (C-O-C); NMR δ (ppm) 1.90 (dt, 2H), 2.12 (t, 2H), 2.88 (s, 3H), 3.68 (t, 1H), 7.0-7.2 (m, 20 H).

Anal. Calcd for $C_{29}H_{28}O$: C, 88.73; H, 7.19. Found: C, 88.82; H, 7.16.

2-Methoxyindan (11). bp 90 °C (10 mmHg); NMR δ (ppm) 2.93 (dd, 4H), 3.23 (s, 3H), 4.10 (q, 1H), 7.00 (m, 4H). mass spectrum *m/e* 148 (M^+).

Anal. Calcd for $C_{10}H_{12}O$: C, 81.04; H, 8.16. Found: C, 80.98; H, 7.84.

1-*p*-Cyanophenyl-2-methoxyindan (12). bp 100°C (0.1 mmHg); NMR δ (ppm) 2.80-3.15 (m, 2H), 3.95 (q, 1H) 4.20 (d, 1H), 7.0 (m, 8H).

2-6 REFERENCES AND NOTES

[1] A. A. Lamola and N. J. Turro, in "Energy Transfer and Organic Photochemistry," Vol 14, A. Weissberger, Ed., Interscience, New York, N. Y., 1969.

[2] R. S. H. Liu and J. R. Edman, J. Am. Chem. Soc., 90, 213 (1968); R. S. H. Liu and D. M. Gale, *ibid.*, 90, 1897 (1968); R. S. H. Liu, *ibid.*, 90, 1899 (1968).

[3] N. C. Yang, J. I. Cohen, and A. Shani, J. Am. Chem. Soc., 90,

3264 (1968); I. E. Kochevar and P. J. Wagner, *ibid.*, 94, 3859 (1972); R. A. Caldwell, G. W. Sovocool, and R. P. Gajewski, *ibid.*, 95, 2549 (1973); A. Gupta and G. S. Hammond, *ibid.*, 98, 1218 (1976); I. G. Lopp, R. W. Hendren, P. D. Wildes, and D. G. Whitten, *ibid.*, 92, 6440 (1970); S. Murov and G. S. Hammond, J. Phys. Chem., 72, 3797 (1968); S. S. Hixon, J. Boyer, and C. CAlluci, J. Chem. Soc., Chem. Commun., 540 (1974).

[4] (a) R. A. Neunteunfel and D. R. Arnold, J. Am. Chem. Soc., 95, 4080 (1973); (b) Y. Shigemitsu and D. R. Arnold, J. Chem. Soc., Chem. Commun., 407 (1975); (c) D. R. Arnold and A. J. Maroulis, J. Am. Chem. Soc., 98, 5931 (1976); (d) A. J. Maroulis, Y. Shigemitsu, and D. R. Arnold, *ibid.*, 100, 535 (1978).

[5] S. Farid and S. E. Shealer, J. Chem. Soc. Chem. Commun., 677 (1973).

[6] A. Ledwith, Acc. Chem. Res., 5, 133 (1972).

[7] T. Asanuma, T. Gotoh, A. Tsuchida, M. Yamamoto, and Y. Nishijima, J. Chem. Soc., Chem. Commun., 485 (1977).

[8] For a review of cation radicals see "Radical Ions," E. T. Kaiser and L. Kevan, Ed., John Wiley & Sons, New York, N. Y., 1968.

[9] A. Weller, Pure Appl. Chem., 16, 115 (1968); P. Froehlich and E. L. Wehry, in "Modern Fluorescence Spectroscopy," Vol. 2, E. L. Wehry, Ed., Plenum Press, New York, N. Y., 1976, pp. 381-386.

[10] D. Rehm and A. Weller, Israel J. Chem., 8, 259 (1970).

[11] Mataga and his coworkers have detected pyrene cation radical and $DCNB^{\bullet-}$ in high yields by the laser flash photolysis of the pyrene-DCNB-acetonitrile system: T. Hino, H. Masuhara, and N. Mataga, Bull. Chem. Soc. Jpn., 49, 394 (1976).

[12] M. Yasuda, C. Pac, and H. Sakurai, Bull. Chem. Soc. Jpn., 53, No. 1 (1980).

[13] U. Svanholm and V. D. Parker, J. Am. Chem. Soc., 98, 2924 (1976).

[14] M. Moet-Ner, E. P. Hunter, and F. H. Field, J. Am. Chem. Soc., 100, 5466 (1978).

[15] Formation of $(PR)_2^{+}$ in dichloromethane has been reported: M. A. J. Rodgers, Chem. Phys. Lett., 9, 107 (1971); A. Kira, S. Arai, and M. Imamura, J. Chem. Phys., 54, 4890 (1971).

[16] K. Hayashi and M. Irie, European Polymer Journal, Vol. 13, 925 (1977).

[17] E. Rabinowitch and Govindjee, "Photosynthesis," John Wiley & Sons, New York, 1969.

[18] G. Tollin and G. Green, Biochem. Biophys. Acta, 60, 524 (1962).

CHAPTER 3 REDOX-PHOTOSENSITIZED RING CLEAVAGE OF CYCLOBUTANE COMPOUNDS

3-1 INTRODUCTION

Ring cleavage of cyclobutane compounds have been extensively discussed in terms of the conservation of orbital symmetry,[1] 1,4-biradical intermediates,[2-4] solar energy utilization,[5] and photoreactivation of damaged DNA.[6] Cleavage of the cyclobutane ring is usually carried out by means of thermolyses or photolyses and occasionally by metal ion catalyses.

Electron transfer is an important photochemical process of exciplex formation systems in polar solvents;[7,8] the chemistry of photo-generated ion radicals has now received considerable attention.[9-12] In chapter 2, the author described a novel type of photosensitization using aromatic hydrocarbon (S)—*p*-dicyanobenzene (DCNB)—acetonitrile systems, which causes ionic reactions of furan and olefins (D). The author now calls this photosensitization redox-photosensitization, since the initiation process is the photochemical electron transfer (photoredox) reaction from S to DCNB[13-15] and since an important intermediate is the cation radical of S ($S^{+\cdot}$) which may act as a redox-carrier. The redox-photosensitized reactions can occur, even when the oxidation potential of S is substantially lower than that of D; complete hole transfer from $S^{+\cdot}$ to D is thus endothermic, being perhaps unlikely. Therefore, the author assumed the intervention of a π-complex formed between $S^{+\cdot}$ and D as key intermediate.

Thus, redox-photosensitization is closely related with the chemical nature of photogenerated $S^{+\cdot}$ and has been applied to other reactions.[16,17] The author found that redox-photosensitization effects the cycloreversion of cyclobutane compounds. In this chapter, the author describes the redox-photosensitized ring cleavage of cyclobutane compounds which is a novel type of reaction without precident, being mechanically different from ring cleavage *via* the cation radical of cyclobutane compounds.[6a,18,19]

3-2 REDOX-PHOTOSENSITIZED RING CLEAVAGE OF 1,1a,2,2a-TETRAHYDRO-7H-CYCLOBUT[a]INDENE DERIVATIVES

3-2-1 INTRODUCTION

One of photochemical reactions so far proposed for solar energy utilization is valance isomerizations[20]; solar energy is stored by formation of high-strained cyclobutane compounds, which is followed at a later time by the reverse reaction, releasing thermal energy. In this category, development of effective catalysts for the reverse reaction is one of important problems.

In connection with this, it is of interest that $S^{+\cdot}$ generated in redox-photosensitised system acts as an efficient catalyst for cycloreversion of indene cyclobutane dimers.

In this section, the author descibes extensive kinetic studies to unveil the mechanism for the redox-photosensitized cycloreversion of *trans,syn*-indene dimer 1; the intermediacy of π-complex $(S \cdot 1)^{+\cdot}$ is strongly suggested. Moreover, redox-photosensitization has been applied to a dozen of 1,1a,2,2a-tetrahydro-7*H*-cyclobut[*a*]-indene derivatives 1-12 to see the structure-reactivity relationship in redox-photsensitized ring cleavage.

3-2-2 RESULTS

Preparation of Cyclobutane Compounds. All the cyclobutane compounds were prepared by known methods; the synthetic route are delinated in Scheme 1. The spectral properties of 1-12 are in accord with the structures. The *endo* configuration of the hydroxyl group of 4, 5, and 8 was deduced from the well-known fact that hydride reduction[21] and Grignard reactions[22] of bicyclic ketones usually occur by the dominant attack of the reagents to the sterically less hindered side. Irradiation of a benzene solution containing *trans*-β-nitrostyrene and indene gave 6 in good yield in a similar manner to the photocycloaddition of *trans*-β-nitrostyrene to styrene.[23] The *endo* location of the phenyl group of 6 and 7 was indicated from the nmr spectra; one of aromatic protons shows the signal at unusually high field.

Quantum Yield for Indene Formation in Redox-Photosensitized Cycloreversion of 1. For mechanistic investigation, the cycloreversion of *trans,syn*-cyclobut[*a*]diindene 1 using phenanthrene (P) as S was employed as the typical reaction. Irradiation of a dry acetonitrile solution containing P, DCNB, and 1 at 313 nm gave indene (IN) as the only detectable product in 75-80% isolated

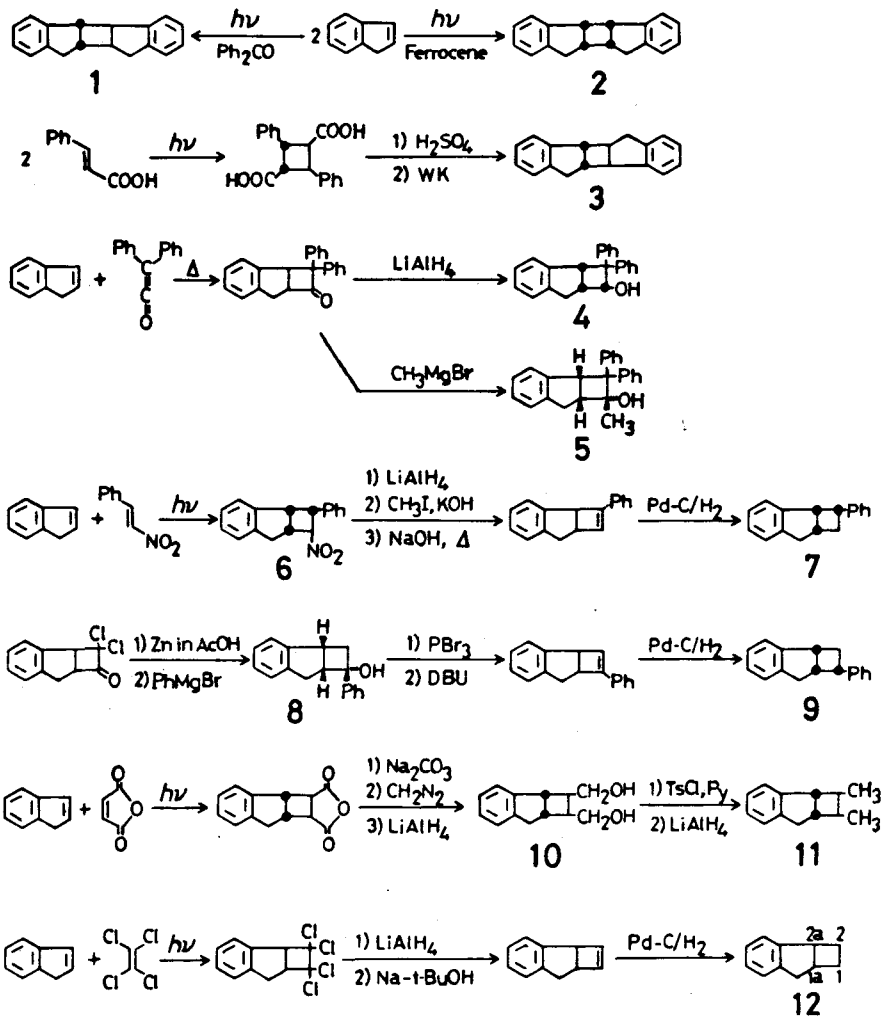

Scheme 1.

yield (based on 2 mol formation of IN per 1 mol of 1 used). On the other hand, P and DCNB were recovered in 85 and 90% yields respectively. In the absence of either P or DCNB, no photoreaction occured at all.

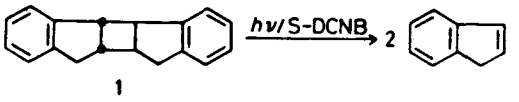

The formation of IN increased linearly with irradiation time up to ca. 8% conversion (Figure 1). Quantum yields for indene

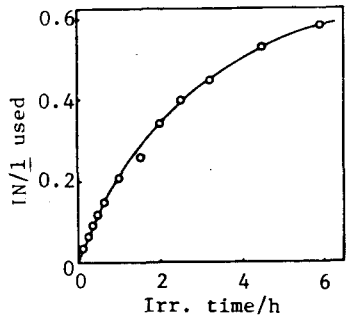

Figure 1. Formation curve of IN [mol per mol of 1 used] irradiation time in the redox-photosensitized ring cleavage of 1; degassed acetonitrile solutions; 313 nm irradiation; [1]= 0.05 M, [P]= 0.01 M, and [DCNB]= 0.1 M.

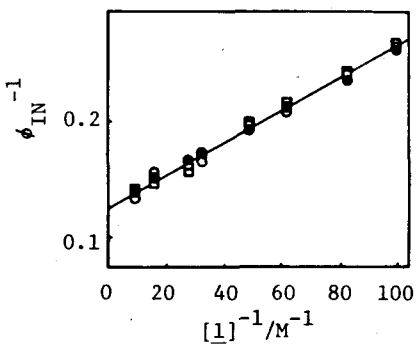

Figure 2. Plots of ϕ_{IN}^{-1} *vs.* $[1]^{-1}$ with least-squares fit; 313 nm irradiation with light intensities of 2.7×10^{-8} (-○-), 1.2×10^{-7} (-●-), and 6.4×10^{-7} (-□-) einstein/min; see footnotes in Table 1.

Table 1. Dependence of Quantum Yields (ϕ_{IN}) on Concentration of 1 and Light Intensity[a]

$[1]\times10^{3}$/M	ϕ_{IN} Light intensity[b]		
	2.74×10^{-8}	1.1×10^{-7}	6.4×10^{-7}
10	3.68	3.68	3.60
12	3.92	4.02	3.89
16	4.69	4.63	4.17
20	4.98	5.03	4.81
30	6.02	5.75	5.92
34	6.04	5.90	6.09
60	6.25	6.33	6.58
100	7.25	6.33	6.85
∞		8.2[c]	
Slope[d]$\times10^{3}$/M		1.54	

[a] Degassed dry acetonitrile solution; [P]= 0.01 M and [DCNB]= 0.1 M; at 313 nm. [b] Einstein/min.
[c] Extrapolated value (ϕ_{IN}^{∞}); see text and Figure 2.
[d] Slope of the linear plot in Figure 2.

formation (ϕ_{IN}) were determined at less than 3% conversion (Table 1). The plot of ϕ_{IN}^{-1} *vs.* reciprocals of concentration of 1 is linear and independent of the intensity of the incident light at 313 nm (Figure 2). It was found that ϕ_{IN}^{-1} depends on either concentration of P or dryness of solution as is shown in Table 2 and Figure 3.

Table 2. Dependence of Quantum Yields (ϕ_{IN}) on Concentration of Phenanthrene[a]

[P]/M	ϕ_{IN}	
	Dry solution[b]	Wet solution[c]
0.10	2.41	2.36
0.09	2.65	-
0.08	-	2.64
0.072	2.90	-
0.06	3.67	3.30
0.045	4.17	-
0.04	-	3.98
0.03	4.90	-
0.02	6.25	4.83
0.01	6.85	5.81
0.00[d]	9.4	7.6
(Slope/M^{-1})[e]	3.06	3.02

[a] Degassed acetonitrile solution; [1]= 0.05 M, and [DCNB]= 0.1 M; at 313 nm. [b] See Experimental. [c] A drop of water was addes into 1000 mL of dry acetonitrile. [d] Extrapolated values. [e] Slope of the linear plot in Figure 3.

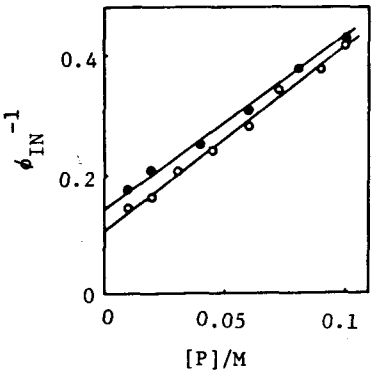

Figure 3. Plots of ϕ_{IN}^{-1} *vs.*[P] with least-squares fit for dry (-O-) and wet (-●-) solutions; see footnotes in Table 2.

Quenching by Cation Radical Quenchers. The redox-photosensitized cycloreversion of 1 was quenched by *p*-dimethoxybenzene (Q) (Table 3). The Stern-Volmer plot was linear up to ca. 10^{-3} M of Q (Figure 4). At higher concentration of Q, however, the plot deviates from the linearity (Figure 5). It was found that the end absorption of DCNB (0.1 M) shifted very slightly to longer wavelength in the presence of relatively high concentration of Q, while the absorption of P was identical to that in the absence of Q. A CT-complex is perhaps formed between Q and DCNB in the ground state. The deviation from the linearity at higher concentration of Q would arise from the absorption of the incident light at 313 nm

Table 3. Dependence of Observed and Calculated Quantum Yields (ϕ^{Q}_{IN}) on Concentration of *p*-Dimethoxybenzene (Q)[a]

$[Q]\times10^{2}$/M	ϕ^{Q}_{IN}		$(\phi^{Q}_{IN})^{-1}$			
			Obsd	Calcd[b]		
	at 334 nm	at 313 nm		α= 0.1	0.2	0.3
0.000	3.60	3.62	0.276	0.276	0.276	0.276
0.010	-	0.89	1.12	1.01	1.01	1.01
0.025	0.51	0.53	1.90	2.11	2.11	2.11
0.040	-	0.35	2.88	3.22	3.21	3.22
0.055	0.24	0.24_5	4.08	4.33	4.32	4.34
0.070	-	0.18	5.53	5.43	5.42	5.45
0.085	0.15_5	0.15_6	6.39	6.54	6.54	6.58
0.10	0.130	0.13_3	7.50	7.06	7.65	7.70
0.40	-	0.32_4	30.9	30.2	30.6	31.2
0.50	0.030	-	-	-	-	-
0.80	-	0.016	62.2	61.1	63.1	65.32
1.00	0.013	-	-	-	-	-
1.10	-	0.011_5	87.0	85.2	88.9	93.0
1.30	0.010	-	-	-	-	-
1.40	-	0.0086	116.1	109.8	115.9	122.5
1.60	0.0078	-	-	-	-	-
1.70	-	0.0070	143.0	134.6	144.2	153.8
1.80	0.0066	-	-	-	-	-
2.00	0.0056	0.0057	176.0	161.1	173.7	186.9

[a] Degassed dry acetonitrile solution; [1]= 0.01 M, [P]= 0.01 M, and [DCNB]= 0.1 M. [b] Calculated from eq 21; see text.

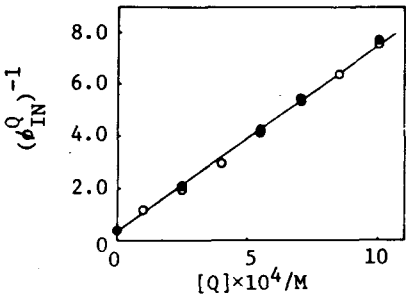

Figure 4. Plots of $(\phi^{Q}_{IN})^{-1}$ *vs.* [Q] with least-squares fit at $\leq 10^{-3}$ M of Q; 313 nm (-○-) and 334 nm (-●-) irradiation; see footnotes in Table 3.

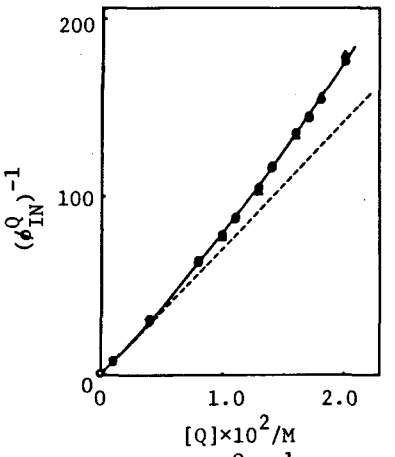

Figure 5. Plots of $(\phi_{IN}^{Q})^{-1}$ *vs.* [Q]; values for 313 nm (-○-) and 334 nm (-△-) irradiation and calculated values (-●-) with α = 0.2; see footnotes in Table 3.

by the CT-complex. Even at the maximum concentration of Q used (2×10^{-2} M), however, the absorbance of the CT-complex at 313 nm is only 0.1% that of P. Moreover, an identical curved Stern-Volmer plot was again obtained at 334 nm, where the absorbance of the CT-complex is absent (Table 2). It was confirmed that the fluorescence of P is not quenched even by 0.1 M of Q. Thus, the curved plot clearly arises from the quenching of reaction intermediates by Q. With the other quenchers, linear Stern-Volmer plots were obtained at relatively low concentration of the quenchers, where no CT-absorption was observed. Table 4 lists the slopes of the plots together with the oxidation potentials of the quenchers.

Table 4. Slopes in the Linear Region of Stern-Volmer Plots in the Quenching by Various Quenchers[a]

Quenchers	$E_{1/2}^{ox}$/V	$K_{SV}\times10^{-3}/M^{-1}$
p-Dimethoxybenzene	0.90	7.11
m-Dimethoxybenzene	1.01	6.34
p-Methylanisole	1.11	1.27
o-Methylanisole	1.20	0.80
Triethylamine	0.37	6.10

[a] Degassed dry acetonitrile solution; [1]= 0.01 M, [P]= 0.01 M, and [DCNB]= 0.1 M; at 313 nm.

Redox-Photosensitized Cycloreversion of 1 Using Other Aromatic Hydrocarbons. The photosensitized cycloreversion of 1 was effected by the other aromatic hydrocarbons involving triphenylene (TR), naphthalene (NT), chrysene (CR), and dimethylnaphthalenes, while pyrene (PR) and anthracene (AN) were not effective. Similarly, ϕ_{IN} was determined for each S was linear. Table 5 lists the intercepts and slopes of the plots and ϕ^{∞}_{IN} together with the oxidation potentials of S.

Table 5. Intercepts and Slopes of Linear Plots of ϕ_{IN}^{-1} *vs.* $[1]^{-1}$ for Various Aromatic Hydrocarbons (S)[a]

S	$E^{ox}_{1/2}(S)$/V	Slope×10^3/M	Intercept	ϕ^{∞}_{IN}
Triphenylene (TR)	1.29	1.32	0.110	9.1
Naphthalene (NT)	1.22	1.47	0.116	8.5
Phenanthrene (P)	1.17	1.54	0.112	8.2
1,4-Dimethylnaphthalene	1.10	171	2.00	0.50
1,2-Dimethylnaphthalene	1.06	184	3.23	0.31
Chrysene (CR)	1.05	90.0	1.41	0.71
1,3-Dimethylnaphthalene	1.02	163	3.70	0.27
2,3-Dimethylnaphthalene	0.99	203	3.76	0.27
Pyrene (PR)	0.78	[b]	[b]	0.00[b]
Anthracene (AN)	0.75	[b]	[b]	0.00[b]

[a] Degassed dry acetonitrile solution; [S]= 0.01 M and [DCNB]= 0.1 M; at 313 nm; see text. [b] Lack of ring cleavage.

Redox-Photosensitized Cycloreversion of Other Cyclobutane Compounds. Among the compounds investigated, the reactive cyclobutanes are 2, 4, 5, and 7 (Scheme 2). The cycloreversion of *cis,syn*-dimer 2 occurred more efficiently than that of 1, giving IN in 85% isolated yield. In the case of 7, IN and styrene were formed in a 1:1-ratio; other products could not be detected. The photosensitized ring cleavage of 4 and 5 gave IN along with diphenylacetaldehyde and 1,1-diphenylacetone respectively; the carbonyl compounds are evidently formed by the keto,enol-rearrangement of the corresponding enols which are initially formed by ring cleavage. However, the formation of the carbonyl compounds was much less than that of IN, even at low conversions. It was confirmed that the carbonyl compounds are relatively stable upon irradiation in the presence of P and DCNB at 313 nm. Therefore,

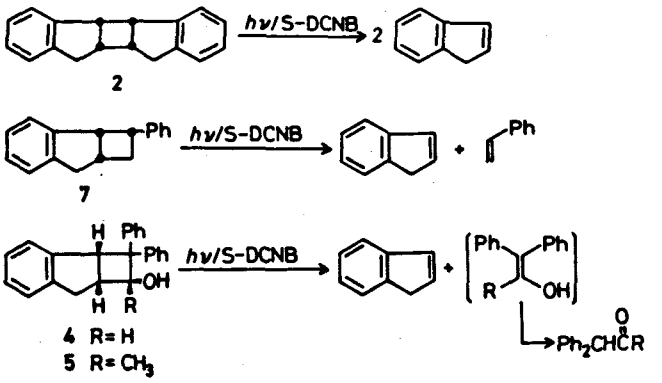

Scheme 2.

Table 6. Redox-Photosensitized Ring Cleavage of 1-12 and Limiting Quantum Yields (ϕ_{IN}^{∞})[a]

Cyclobutanes	$E_{1/2}^{ox}$/V	S[b]			
		TR	NT	P	CR
1	1.32	9.1	8.5	8.2	0.71
2	1.32	12.1	11.8	11.3	0.92
3	1.49	×	×	×	×
4	1.43	ND[c]	ND[c]	0.19	×
5	1.41	0.20	ND[c]	0.12	×
6	1.70	×	×	×	×
7	1.44	0.08	0.047	0.033	×
8	1.50	×	×	×	×
9	1.58	×	×	×	×
10	1.60	×	×	×	×
11	1.69	×	×	×	×
12	1.73	×	×	×	×

[a] Extrapolated values from linear plots of ϕ_{IN}^{-1} *vs.* reciprocals of concentration of the cyclobutanes; [S]= 0.01 M and [DCNB]= 0.1 M; at 313 nm. The cross mark indicates the lack of ring cleavage. [b] See abbreviation in Table 5. [c] Ring cleavage occured but the values were not determined.

unreclaimed reactions appear to consume the enols; other product could not be detected by GLC. In contrast, the other cyclobutanes are entirely unreactive; irradiation for long time resulted only in the complete recovery of the starting materials. The results are summarized in Table 6.

3-2-3 DISCUSSION

Mechanism of Redox-Photosensitized Cycloreversion of 1.

All the cyclobutane compounds used did neither quench the fluorescence of S nor form any CT-complexes with S and DCNB. Moreover, the cycloreversion of 1 was not sensitized by such typical triplet photosensitizers as benzophenone and acetophenone, whose triplet excitation energies are higher than those of S. Therefore, neither triplet excitation nor singlet exciplex mechanism can be accepted as the mechanism of the redox-photosensitization. As has been discussed in the previous chapter, electron transfer from the excited singlet state of S ($^1S^*$) to DCNB is responsible for the initiation process, giving the cation radical of S ($S^{+\cdot}$) and the anion radical of DCNB ($DCNB^{-\cdot}$). Since ϕ_{IN}^{∞} decreases with a decrease of the oxidation potential of S (Table 3), $S^{+\cdot}$ is perhaps a reactive species for the cycloreversion. This is strongly supported by the observation that the cycloreversion of 1 is quenched by the compounds possessing low oxidation potentials.

It has been reported that some cyclobutane compounds undergo the ring-cleavage reaction *via* the cation radicals.[6a,18,19] Therefore, complete hole transfer from $S^{+\cdot}$ to 1 would occur to give the cation radical of 1, which subsequently undergoes the cycloreversion, *i.e.* $S^{+\cdot} + 1 \longrightarrow S + 1^{+\cdot} \longrightarrow S + IN + IN^{+\cdot}$. If this were the case, irradiation in the presence of methanol would yield 2-methoxyindan as an initial product, since there is knwon the *anti*-Markownikoff photoaddition of methanol to phenyl-substituted olefins *via* the cation radicals.[10] In fact, it has been confirmed that 2-methoxyindan is formed upon irradiation of a 10:1-acetonitrile–methanol solution containing IN and 1-cyanonaphthalene.[24] However, when the redox-photosensitized cycloreversion was carried out in 3:1-acetonitrile–methanol, only IN was formed as the initial product at low conversion (Figure 6). On the other hand, 2-methoxyindan was formed only when IN was accumulated to significant extents. This clearly demonstrates that 2-methoxyindan is a secondary product from the redox-photosensitized addition of methanol to initially formed IN, as has been described in chapter 2. Moreover, methanol adducts of 1 or related compounds could not be detected. The results require that the redox-photosensitized cycloreversion must occur by means of a mechanism which involves neither cation radical of 1 nor IN. In this regard, it should be pointed out that the

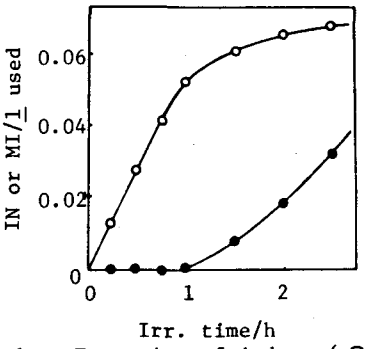

Figure 6. Formation of indene (-O-) and 2-methoxyindan (MI) (-●-) *vs.* irradiation time. Degassed 3:1-acetonitrile–methanol solutions; 313 nm irradiation; [1]= 0.05 M, [P]= 0.01 M, and [DCNB]= 0.1 M.

oxidation potential of P is considerably lower than that of 1; complete hole transfer from $P^{+\cdot}$ to 1 is endothermic, being thus unlikely for the occurrence of the efficient (chain) cycloreversion.

In order to interpret reasonably the results obtained, the possible mechanistic pathways are thus shown in Scheme 3; a key mechanistic pathway is the catalytic cycloreversion of 1 by $S^{+\cdot}$ *via* π-complex $(S\cdot 1)^{+\cdot}$, which results in the formation of two neutral indene molecules and the recovery of $S^{+\cdot}$ without complete hole transfer. This mechanism is supported by the curved Stern-Volmer plot in Figure 5 that demonstrates the existence of two different cation radical species as the reaction intermediates, *i.e.* $S^{+\cdot}$ and the π-complex. The formation of the π-complex is not surprising, since it has been reported that the cation radical of methylated benzene forms π-complexes with neutral molecules of other methylated benzenes in vapor phase.[25] The π-complex may collapse into S and/or other products as a chain termination process. The formation of dimer cation radical $S_2^{+\cdot}$ should be taken into account as another chain termination process, since ϕ_{IN} decreases with an incerease of concentration of S; the dimer cation radical of pyrene is known to be formed.[26] In the presence of Q, hole transfer from either $S^{+\cdot}$ or $(S\cdot 1)^{+\cdot}$ to Q should be considered as the quenching processes, since the oxidation potential of Q is relatively low. The cation radical intermediates are also quenched by impurities involving water. However, this process appears to be of minor importance, since their concentration is probably very low.

$$S \xrightarrow{h\nu} {}^1S^* \quad (1)$$

$${}^1S^* \xrightarrow{1/\tau} S \quad (2)$$

$${}^1S^* + DCNB \xrightarrow{\alpha} S^{+\cdot} + DCNB^{-\cdot} \quad (3)$$

$${}^1S^* + DCNB \xrightarrow{1-\alpha} S + DCNB \quad (4)$$

$$S^{+\cdot} + \underline{1} \xrightarrow{k_c} (S\cdot\underline{1})^{+\cdot} \equiv C^{+\cdot} \quad (5)$$

$$S^{+\cdot} + S \xrightarrow{k_s^c} S_2^{+\cdot} \quad (6)$$

$$C^{+\cdot} \xrightarrow{k_r^c} S^{+\cdot} + 2\ IN \quad (7)$$

$$C^{+\cdot} \xrightarrow{k_d^c} S \text{ and/or others} \quad (8)$$

$$C^{+\cdot} + S \xrightarrow{k_s^c} S_2^{+\cdot} + \underline{1} \quad (9)$$

$$S^{+\cdot} + Q \xrightarrow{k_q} S + Q^{+\cdot} \quad (10)$$

$$C^{+\cdot} + Q \xrightarrow{k_q^c} S + \underline{1} + Q^{+\cdot} \quad (11)$$

$$S^{+\cdot} + X \xrightarrow{k_x} S \text{ and/or others} \quad (12)$$

$$C^{+\cdot} + X \xrightarrow{k_x^c} S + \underline{1} \text{ and/or others} \quad (13)$$

$$S_2^{+\cdot} + Q \longrightarrow 2\ S + Q^{+\cdot} \quad (14)$$

$$S_2^{+\cdot} + X \longrightarrow 2\ S \text{ and/or others} \quad (15)$$

(X= $DCNB^{-\cdot}$, H_2O, and impurities)

Scheme 3.

neutralization between the cation radicals and $DCNB^{-\cdot}$ is not important, since ϕ_{IN} is independent of the light intensity. The complete quenching of the fluorescence of S by 0.1 M of DCNB indicates that the unimolecular decay processes from $^1S^*$ can be neglected.

Analysis of Kinetics. In the absence of Q, steady-state analysis gives eqs 16 and 17, where α represents the limiting quantum yield for $S^{+\cdot}$ formation. In eq 16 it has been assumed that $(k_s^c[S] + k_d^c) >> k_x^c[X]$ and $k_s[S] >> k_x[X]$. In eq 17 the term of $[S]^2$ has been neglected since the plot of ϕ_{IN}^{-1} *vs.* [P] is linear.

$$\frac{1}{\phi_{IN}} = \frac{1}{2\alpha}\left(\frac{k_s^c[S] + k_d^c}{k_r^c}\right)\left(1 + \frac{k_s[S]}{\beta k_c[\underline{1}]}\right) \quad (16)$$

$$\beta = \frac{k_s^c[S] + k_d^c}{k_r^c + k_s^c[S] + k_d^c} \quad ; \ [S] = 0.01\ M$$

$$\frac{1}{\phi_{IN}} = \frac{1}{2\alpha}\left(\frac{k_d^c}{k_r^c}\right)\left[1 + \left\{\frac{k_s^c}{k_d^c} + \frac{(k_r^c + k_s^c)k_s}{k_d^c k_c[\underline{1}]}\right\}[S]\right] \quad (17)$$

$[\underline{1}] = 0.05$ M

From the intercepts and slopes in Figures 2 and 3, the following rate ratios are obtained.

$$\alpha k_r^c / k_d^c = 4.72 \quad (18)$$

$$k_s / \beta k_c = 1.26 \quad (19)$$

$$k_d^c / k_s^c = 6.6\times10^{-2} \quad (20)$$

In the presence of Q, Stern-Volmer equation can be represented by eq 21, where [S]= 0.01 M. In this equation it has been assumed that $k_q \approx k_q^c$ (*vide infra*).

$$\frac{1}{\phi_{IN}^Q} = \frac{1}{\phi_{IN}} + \frac{k_q[Q]}{2\alpha k_r^c}\left(1 + \frac{k_r^c + k_d^c + k_s^c[S] + k_s[S]}{k_c[\underline{1}]} + \frac{k_q[Q]}{k_c[\underline{1}]}\right) \quad (21)$$

The slope (κ_{SV}) in the linear region of the plot of $(\phi_{IN}^Q)^{-1}$ *vs.* concentration of Q should depend on concentration of $\underline{1}$ as is represented by eq 22.

$$\kappa_{SV} = \frac{k_q}{2\alpha k_r^c}\left(1 + \frac{k_r^c + k_d^c + k_s^c[S] + k_s[S]}{k_c[\underline{1}]}\right) \quad (22)$$

In similar manner to Figure 4, linear Stern-Volmer plots at several points of concentration of $\underline{1}$ were obtained; the slopes (κ_{SV}) are listed in Table 7. The plot of κ_{SV} *vs.* $[\underline{1}]^{-1}$ is linear as is shown in Figure 7; the intercept and slope give the following rate ratios.

$$k_q / 2\alpha k_r^c = 24.53 \quad (23)$$

$$\frac{k_r^c + k_d^c + k_s^c[S] + k_s[S]}{k_c} = 2.97 \quad (24)$$

Table 7. Dependence of Quantum Yields (ϕ_{IN}^{Q}) on Concentration of Either 1 or *p*-Dimethoxybenzene (Q)[a]

$[Q]\times10^4$/M	ϕ_{IN}^{Q} at $[1]\times10^2$/M				
	1.3	1.8	3.0	5.0	10.0
0.0	4.15	4.81	5.75	6.58	7.14
1.5	1.00	1.35	2.43	2.77	7.55
3.0	0.48	0.55	1.21	1.67	3.44
4.5	0.38	0.41	0.76	1.21	2.43
6.0	0.28	0.30	0.61	1.08	2.02
8.0	0.20	0.26	0.43	0.81	1.96
10.0	0.17	0.19	0.37	0.63	1.41
$(K_{SV}\times10^{-3}/M^{-1})$[b]	5.76	4.18	2.54	1.36	0.53

[a] See footnotes in Table 1. [b] Slopes of linear Stern-Volmer plots.

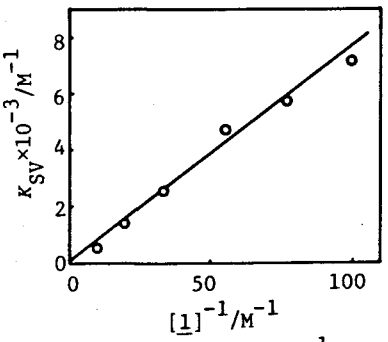

Figure 7. Plot of K_{SV} *vs.* $[1]^{-1}$ with least-squares fit. The slope and intercept are 72.8 and 24.53 M^{-1} respectively.

Hole transfer from the cation radical of P to Q probably occurs at a diffusion-controlled rate since this process is exothermic by 6.2 kcal/mol (0.27 eV). In regard with k_q^c, it should be noted that K_{SV} for triethylamine which possesses a very low oxidation potential is quite similar to that for Q. Therefore, it is reasonable to assume that $k_q \simeq k_q^c \simeq 10^{10}$ $M^{-1}s^{-1}$. On the basis of this assumption, k_s^c and k_d^c can be calculated to be 6.6×10^8 $M^{-1}s^{-1}$ and 4.3×10^7 s^{-1} respectively, using eqs 18, 20, and 23. In the quenching by *o*- and *p*-methylanisoles, however, k_q^c may not be equal

to k_q and/or k_q may be less than the rate constant for a diffusion-controlled process.

If α is given, the other rate constants can be also calculated. The author has estimated the value of α and the rate constants as follows: (1) presumption of an appropriate value for α; (2) k_r^c from eq 18 and then k_c and k_s from eqs 19 and 24; (3) quantum yields $(\phi_{IN}^Q)_{cal}$ from eq 21; (4) repeated computation of $(\phi_{IN}^Q)_{cal}$ using various values of α until they agree with the observed quantum yields. Consequently the best fit values were obtained when α= 0.2 (Table 3). This value seems to be reasonable, since it has been reported that α is 0.38 for the pyrene—DCNB—acetonitrile system.[27] Table 8 lists the calculated rate constants.

Table 8. Rate Constants in Redox-Photosensitized Cycloreversion of 1[a]

Processes	Symbols	Values
Formation of $(P\cdot\underline{1})^+$	k_c	3.6×10^8 $M^{-1}s^{-1}$
Formation of P_2^+ from P^+ and P	k_s	2.1×10^7 $M^{-1}s^{-1}$
Formation of P_2^+ from $(P\cdot\underline{1})^+$ and P	k_s^c	6.6×10^8 $M^{-1}s^{-1}$
Ring cleavage of 1 from $(P\cdot\underline{1})^+$	k_r^c	1.0×10^9 s^{-1}
Unimolecular decay of $(P\cdot\underline{1})^+$	k_d^c	4.3×10^7 s^{-1}
Efficiency for formation of P^+	α	0.2
Fraction of ring cleavage from $(P\cdot\underline{1})^+$	$1-\beta$	0.953[b]

[a] See text. [b] Value at [P]= 0.01 M.

An interesting point of the results is that the π-complex is very short-lived to collapse into two neutral indene melecules and P^+ within 1 ns, suggesting a low energy barrier for the cycloreversion of 1 *via* the π-complex. On the other hand, the π-complex formation occurs at a rate two orders of magnitude less than a diffusion-controlled process, being perhaps only slightly exothermic or nearly isothermal. This seems to be reasonable since the oxidation potential of 1 is considerably higher than that of P.

Although k_s is very small compared with the reported rate constant for the formation of pyrene dimer cation radical in dichloromethane,[26] it should be noted that the reversible dissociation of S_2^+ was not taken into account in the calculation. If S_2^+ is reversibly formed, k_s should be replaced by $\gamma k_s'$; $\gamma = k_s^s/(k_{-s} + k_d^s)$. The loss of the positive charge of S_2^+ would be

caused by the reactions with $DCNB^{\cdot-}$, water, and other impurities. Therefore, k_d^S might be very small compared with k_{-s}. Moreover,

$$S^{\cdot+} + S \underset{k_{-s}}{\overset{k_s'}{\rightleftharpoons}} S_2^{\cdot+} \xrightarrow{k_d^S} 2\ S \text{ and/or others}$$

it can be expected that k_s' is more or less smaller in acetonitrile than in dichloromethane since more polar solvents can more shield cation radicals than less polar ones.

Dependency of ϕ_{IN} on Oxydation Potentials of S. Both ϕ_{IN}^{∞} and $\beta k_c/k_s$ depend on the oxidation potentials of S ($E_{1/2}^{ox}(S)$) as is shown in Figure 8; the plots sharply change in the vicinity of 1.1-1.15 V. The dependencies reflect all the changes of the rate constants involved. However, it is not unreasonable to assume that the dimer cation radicals of S are formed at similar rates since the structures of S are similar. Moreover, it is known that α does not remarkably change for exciplex formation systems of similar electron donor-acceptor pairs where photochemical electron transfer is exothermic.[27] Therefore, it appears that the

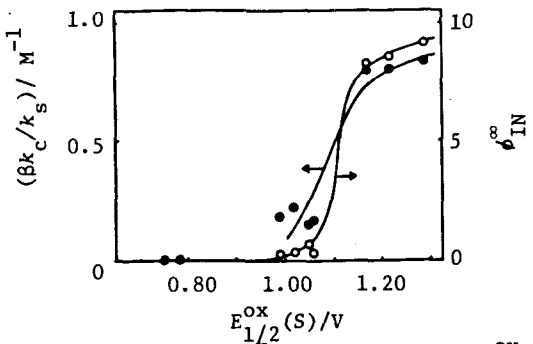

Figure 8. Plots of ϕ_{IN}^{∞} and $\beta k_e/k_d$ *vs.* $E_{1/2}^{ox}(S)$ (see Table 5).

dependency of ϕ_{IN}^{∞} on $E_{1/2}^{ox}(S)$ mainly reflects that of k_r^c. Since β decreases with an increase of k_r^c, the plot of $\beta k_c/k_s$ *vs.* $E_{1/2}^{ox}(S)$, suggesting that bonding of the π-complex $(S\cdot\underline{1})^{\cdot+}$ might arise from charge resonace.

$$(S\cdot\underline{1})^{\cdot+} \equiv \{(S^{\cdot+})\cdot\underline{1} \leftrightarrow S\cdot(\underline{1}^{\cdot+})\}$$

If this is the case, the positive charge of the π-complex will increasingly develope on the side of 1 as $E^{ox}_{1/2}(S)$ increases. Therefore, the dependency of ϕ^{∞}_{IN} on $E^{ox}_{1/2}(S)$ implies that energy barriers for the cycloreversion of 1 decrease with increasing development of the positive charge on 1. When $E^{ox}_{1/2}(S)$ is over about 1.15 V, the energy barriers would be low enough for the catalytic cycloreversion of 1 by $S^{+\cdot}$ to occur much faster than the other processes.

Structure-Reactivity Relationship in Redox-Photosensitized Ring Cleavage of Cyclobutanes. As has been discussed above, it can be expected that smaller differences of oxidation potential between S and the cyclobutanes appear to be more favorable for ring cleavage. However, this is not true in every case. For example, even chrysene is effective to the cycloreversion of 1, while ring cleavage of 3 did not occur by the redox-photosensitization using triphenylene; the difference of oxidation potential of the latter pair is greater than that of the former pair.

In this regard, the following facts should be pointed out; (1) the requirement of phenyl substitution at C_2 for the occurrence of redox-photosensitized ring cleavage of the cyclobutanes investigated, (2) the lower oxidation potentials of the reactive cyclobutanes (*e.g.* 1 and 7) compared with the unreactive cyclobutanes (*e.g.* 3 and 9), and (3) the relatively high oxidation potential and unreactive nature of 6 which possesses the phenyl group at C_2 but the nitro group at C_1.

In order to interpret the lower oxidation potential of the reactive cyclobutanes, the author assumes interactions between the two π-electron systems through the C_2–C_{2a} σ bond of the cyclobutane ring; a relatively strong through-bond interaction between the n-orbitals of 1,4-diazabicyclo[2.2.2]octane (DABCO) has been demonstrated.[28] The two benzene rings of 1 and 2 are fixed and much more favorably located for the through-bond interaction than those of the other reactive cyclobutanes 4, 5, and 7; the lowest oxidation potential of 1 and 2 can be reasonably understood.

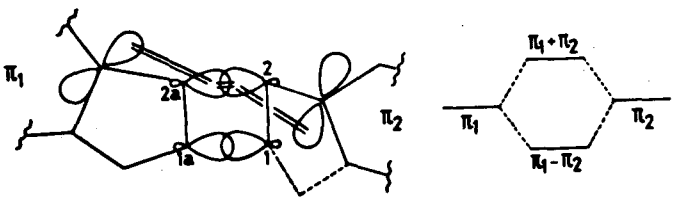

From the structures of the reactive cyclobutanes, therefore, it is suggested that the through-bond interaction is essential for the occurrence of redox-photosensitized cleavage of the cyclobutane ring. In the π-complex of a reactive cyclobutane with $S^{+\cdot}$, the positive charge might develope, even in part, on the C_2–C_{2a} bond because of the through-bond interaction, thus leading to weakening of this bond; the degree of bond weakening perhaps depends on either the difference of oxidation potential between S and the cyclobutane or the degree of the through-bond interaction.

Since the oxidation potential of 6 is much higher than that of 7, the nitro group at C_1 perhaps purturbs the highest occupied molecular orbital of the two π-electron systems interacting through the C_2–C_{2a} bond; interactions between the C_1–C_{1a} and C_2–C_{2a} σ bonds might play significant roles in anodic one-electron oxidation of the cyclobutanes. This interpretation would be in line with the observation that the oxidation potentials of 3 and 9 are lower than those of the parent cyclobutane 12 and its methylated compound 11.

Although it is not clear at the present time whether redox-photosensitized ring cleavage is concerted or stepwise, the author believes that it is energetically unlikely to assume the intervention of the discrete 1,4-diradical arising from initial cleavage of the C_2–C_{2a} bond.[26] Since the cycloreversion of 1 occurs very fast *via* the π-complex with $P^{+\cdot}$, a concerted mechanism might, at least in part, participate in this reaction.[27] A speculative mechanism can be delighted by assuming that the σ orbitals of the C_1–C_{1a} bond interact more and more with those of the C_2–C_{2a} bond as the latter bond is breakingly during the lifetime of the π-complex.

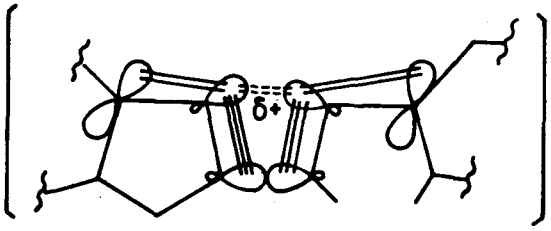

Finally, it should be, of couse, noted that ring-strain energies and steric repulsion affect the efficiency of ring cleavage; the highly reactive nature of 1 and 2 appears to be caused by ring strain in part. Moreover, the *cis* configuration of 2 makes this compound more reactive. It can be reasonably inter-

preted in terms of steric repulsion that 4 is 6 times more efficiently cleaved than 7 by the redox-photosensitization using phenanthrene, though their oxidation potentials are nearly identical.

3-2-4 CONCLUSION

The photo-generated cation radical of aromatic hydrocarbons can act as an efficient catalyst for ring cleavage of the cyclobutane compounds which possess the structures capable of through-bond interactions. In the redox-photosensitized cycloreversion of 1, the intermediacy of the π-complex with the cation radical of phenanthrene (or other aromatic hydrocarbons) has been demonstrated and a concerted nature has been suggested from the value of k_r^c. Thus, redox-photosensitization can provide another route for ring cleavage of cyclobutane compounds.

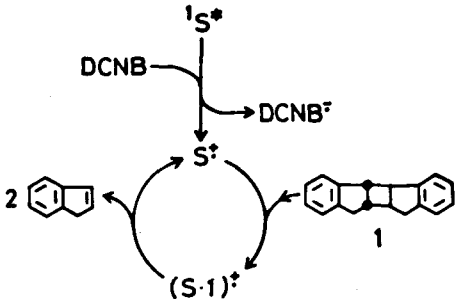

3-2-5 EXPERIMENTAL

Materials. Spectral grade acetonitrile was distilled three times from phosohrous pentoxide then twice from calcium hydride before use. Indene, *o*- and *p*-methylanisoles, and *m*-dimethoxybenzene were distilled from sodium in vacuo before use. Triethylamine was refluxed over and distilled from potassium hydroxide before use. *p*-Dimethoxybenzene was distilled from sodium in vacuo and then recrystallized from a mixture of hexane-benzene. The dimethylnaphthalene except the 2,3-isomer were purified by fractional distillation. The other aromatic hydrocarbons were recrystallized three times from methanol or mixtures

of ethanol-benzene and then sublimed. *p*-Dicyanobenzene was purified by recrystallization from benzene and sublimation. The following compounds were prepared by the reported methods; β-nitrostyrene,[28] tetramethylammonium tetrafluoroborate,[29] and diphenylacetaldehyde.[30] 1,1-Diphenylacetone was prepared by chromic acid oxidation[31] of 1,1-diphenylpropan-2-ol which had been obtained from diphenylacetaldehyde and methylmagnesium iodide. All other chemicals and solvents were reagent grade and purified by fractional distillation and/or recrystallization.

Analytical Methods. Melting points were taken on a hot stage and are uncorrected. Column chromatography was on silica gel (70-230 mesh, Merck). Analytical gas-liquid chromatography (GLC) was perfomed on a Schimadzu GC-3BF dual instrument with flame ionization detectors. The column used for quantitative analyses of indene, 2-methoxyindan, and styrene was 75 cm ×4 mm of 10% Ucon Oil LB-550 X on Neopak-1A and n-tridecane was used as internal standard. GLC analyses of the cyclobutanes, the aromatic hydrocarbons, *p*-dicyanobenzene, diphenylacetaldehyde, and 1,1-diphenylacetone were carried out with 75 cm × 4 mm columns of 5% SE-30 on Schimalite W, 5% Ucon Oil LB-550X on Schimalite W, and 10% PEG 20M on Shimalite W. Preparative GLC was on a Hitachi 023 instrument with thermal conductivity detectors, using a 2 m × 7 mm column of 10% Ucon Oil LB-550X on Neopak 1A.

Proton nuclear magnetic resonance (NMR) spectra were recorded at 100 MHz on a JEOL JNM-PS-100 spectrometer or at 60 MHz on a JEOL JNM-60 spectrometer. The solvent was carbon tetrachloride of chloroform-*d*. The chemical shifts are δ values (ppm) measured downfield from tetramethylsilane which was the internal standard. Infrared (IR) spectra were obtained on a Shimadzu IR-400 spectrophotometer as nujor mull or solutions in carbon tetrachloride or chloroform. Ultraviolet spectra were recorded on a Hitachi 124 specrophotometer. Fluorescence measurements were carried out on a Hitachi MPF-2A fluorometer. Mass spectra were obtained on a Hitachi RMU-6E on a Hitachi RMU-6E instrument.

Elemental analyses were performed at the Elemental Analysis Center of the Institute of Scientific and Industrial Research, Osaka University

Quantum Yields. All the volumetric flasks and pipettes used were dried in a desicator in vacuo and the irradiation tubes

(Pyrex, 8 mm i.d.) were heated under high vacuum before use. Aliquots (4 mL) of solutions of samples and 2-hexanone actinometer[32] were introduced into the tubes, degassed by freeze-pump-thaw method (five cycles) to a reduced pressure $<5\times10^{-5}$ Torr, and then irradiated using a "merry-go-round" apparatus, in the center of which there was placed on Eikosha PIH-300 high-pressure mercury lamp surrounded by a double-cylindrical Pyrex vessel filled with a filter solution. All of them was immersed in a water bath kept at 20±1°C. Potassium chromate solutions of different concentration were used for isolation of the 313 nm light and change of the light intensity. In the quenching experiments at 334 nm, relative quantum yields were obtained using the above equipment and a hexan solution of naphthalene (0.1 M) as the light filter. The quantum yields in the absence and presence of 1×10^{-3} M and 1×10^{-2} M of *p*-dimethoxybenzene were determined using a Shimdzu-Bosch & Romb high-intensity monochromator and a potassium ferrioxalate actinometer.[33] In all the runs, conversions were kept below 3%, usually 0.5-1%. Each value was averaged for three runs.

Oxidation Potentials. The oxidation potentials were determined in acetonitrile by cyclic voltammetry using a two-compartment cell in which a reference electrode with an agar bridge was separated from the platinum anode and the cathode by a glass frit. A platinum circle (5 mm i.d.) seeled into glass (Beckman) was used as working electrode, a platinum sheet (10 mm × 10 mm) as the counter electrode, an Ag/Ag^+ (0.1 M silver nitrate in acetonitrile) as the reference electrode, and 0.1 M tetraethylammonium tetrafluoroborates as supporting electrolyte. A Hokuto Denko HB-107A voltage scanner, a Hokuto Denko HA-104 potentiostat, and a Yokogawa Type 3083 XY recorder were used. All the measurements were carried out at a constant scan speed (0.2 V/s) at 23±0.1°C under a nitrogen atmosphere. In most cases, voltammograms showed no cathodic peaks corresponding to reversible reduction of cation radicals. Therefore, half-peak potentials were employed as the half wave oxidation potentials ($E^{ox}_{1/2}$). Experimental errors were confirmed to be less than 0.015 V.

trans,syn-Cyclobut[*a*]diindene (1). This compound was prepared by the benzophenone-sensitized dimerization of indene[34] and recrystallized from methanol: mp 111-112°C (lit.[34] 110-112°C).

Anal. Calcd for $C_{18}H_{16}$: C, 93.06; H, 6.94. Found: C, 92.91; H, 6.88.

cis,syn-Cyclobut[*a*]diindene (2). An acetonitrile solution of indene (10 g, 0.17 mol) and ferrocene (1 g, 5.4 mmol) placed in a Pyrex vessel was flushed by a nitrogen stream for 30 min and irradiated for 15 h with a high-pressure mercury lamp. After removal of one half of the solvent, the remaining was added into 300 mL of diethyl ether. The ether solution was washed with several portions of cold 0.1 M nitric acid and then with water and dried. Filtration and evaporation left a brownish oil, which was chromatographed on silica gel. Elution with hexane gave 2 (3.2 g, 32% yield) as colorless crystals: mp 60.5-62°C (lit.[34] 61-62°C).

Anal. Calcd for $C_{18}H_{16}$: C, 93.06; H, 6.94. Found: C, 92.91: H, 6.80.

trans,anti-Cyclobut[*a*]diindene (3). To a solution prepared by dissolution of sodium (1.5 g, 65 mmol) into 70 mL of dry triethylene glycol were added 3 g of α-truxone[35] (12 mmol) and 6 mL of 85% hydrazine hydrate. The mixture was heated at about 200°C for 20 h, cooled to room temperature, added into 200 mL of 0.1 M hydrochloric acid under ice-cooling, and extracted with 100 mL of diethyl ether. The ether extract was washed with saturated sodium bicarbonate and brine, dried, and filtered. The ether was removed to give 0.76 g of colorless solids. Recrystallization from ethanol gave pure 3: mp 141-142°C (lit.[34] 142-144°C).

Anal. Calcd for $C_{18}H_{16}$: C, 93.06; H, 6.94. Found: C, 92.84; H, 6.79.

endo-1-Hydroxy-2,2-diphenyl-1,1a,2,2a-tetrahydro-7*H*-cyclobut[*a*]indene (4). To lithium aluminum hydride (4.8 g, 128 mmol) in 100 mL of diethyl ether was added dropwise 2,2-diphenyl-1,1a,-2,2a-tetrahydro-7*H*-cyclobut[*a*]inden-1-one[36] (5 g, 16 mmol) in 50 mL of diethyl ether under ice-cooling and the mixture was stirred at an ambient temperature for 10 h. After careful addition of saturated ammonium chloride, the ether solution was decanted, washed with 0.1 M hydrochloric acid, saturated sodium bicarbonate, and brine, dried, and filtered. Evaporation left an oil, which was tritulated in hexane to give solids. Recrystallization from hexane-benzene gave pure 4 (3.0 g, 60% yield): mp 91-92°C; IR 3590 cm^{-1} (OH); NMR δ 1.66 (s, 1H), 2.90 (dd, *J*= 16.6, 9.4 Hz, 1H), 3.30 (m, 1H), 3.31 (dd, *J*= 16.6, 1.8 Hz, 1H), 4.50 (dd, *J*= 7.8, 2.2 Hz, 1H), 4.78 (dd, *J*= 7.4, 2.2 Hz, 1H), 6.80-7.50 (m, 14H); mass spectrum *m/e* 312 (M^+).

Anal. Calcd for $C_{23}H_{20}O$: C, 88.42; H, 6.45. Found: C, 88.18, H, 6.18.

endo-1-Hydroxy-*exo*-1-methyl-2,2-diphenyl-1,1a,2,2a-tetrahydro-7*H*-cyclobut[*a*]indene (5). To a solution of methylmagnesium iodide prepared from methyl iodide (8 g, 56 mmol) and magnesium shots (1.8 g, 74 mmol) in 100 mL of dry diethyl ether was added dropwise 2,2-diphenyl-1,1a,2,2a-tetrahydro-7*H*-cyclobut[*a*]inden-1-one (7.2 g, 23 mmol) in 50 mL of dry diethyl ether under ice-cooling. After stirring for 3 h, the mixture was treated with saturated ammonium chloride. The ether solution was decanted, washed with 0.1 M hydrochloric acid, saturated sodium bicarbonate, and brine, dried, and filtered. Evaporation left white solids. Recrystallization from hexane-benzene gave pure 5 (7.0 g, 92% yield): mp 155-156°C; IR 3590 cm^{-1} (OH); nmr δ 0.95 (s, 3H), 1.64 (bs, 1H), 2.96 (dd, *J*= 16.4, 7.6 Hz, 1H), 3.23 (dd, *J*= 16.4, 1.6 Hz, 1H), 3.29 (ddd, *J*= 7.6, 7.2, 1.6 Hz, 1H), 4.72 (d, *J*= 7.2 Hz, 1H), 6.80-7.60 (m, 14H); mass spectrum *m/e* 326 (M^+).

Anal. Calcd for $C_{24}H_{22}O$: C, 88.31; H, 6.79. Found: C,88.08; H, 6.55.

exo-1-Nitro-*endo*-2-phenyl-1,1a,2,2a-tetrahydro-7*H*-cyclobut[*a*]indene (6). A solution of indene (100 g, 0.86 mol) and β-nitrostyrene (40 g, 0.27 mol) in 200 mL of benzene was flushed with a nitrogen stream for 30 min and irradiation for 16 h with a high-pressure mercury lamp. After evaporation of the benzene, the residue was chromatographed on silica gel. Elution with 30% benzene in hexane gave yellow solids. Recrystallization from methanol gave pure 6 (55 g, 78% yield): mp 75-78°C; IR 1540, 1370 cm^{-1}; NMR δ 3.20 (m, 2H), 3.63 (m, 1H), 4.03 (t, *J*= 8 Hz, 1H), 6.35 (d, *J*= 15 Hz, one of aromatic protons), 6.80-7.40 (m, 8H); mass spectrum *m/e* 265 (M^+).

Anal. Calcd for $C_{17}H_{15}NO_2$: C,72.96; H, 5.70; N, 5.28. Found: C, 76.89; H, 5.48; N; 5.21.

endo-2-Phenyl-1,1a,2,2a-tetrahydro-7*H*-cyclobut[*a*]indene (7). Reduction of 6 with lithium aluminum hydride gave the corresponding amine in 92% yield. This amine was converted into the methiodide with methyl iodide and sodium hydroxide.[37] A mixture of the methiodide (15 g, 37 mmol) and 15 mL of water placed in a stainless steel vessel was heated and then 50 g of sodium hydroxide in 40 mL of water was added with vigorous stirring. The temperature was raised to 200°C while stirring was continued and water was added from time to time to replace that lost by evaporation. During the reaction, yellow solids were distilled azeotropically

together with water and collected. After the completion of the reaction, the residue was extracted with 300 mL of diethl ether. The ether solution was combined with the yellow solids, washed with 0.1 M hydrochloric acid, saturated sodium bicarbonate, and brine, dried, and filtered. After evaporation of the ether, the residue was chromatographed on silica gel. Elution with 10% benzene in hexane gave colorless solids. Recrystallization from methanol gave 3.5 g of 2-phenyl-1a,2a-dihydro-*7H*-cyclobut[*a*]indene (44% yield): mp 105-106°C; NMR δ 2.96 (m, 2H), 3.52 (m, 1H), 4.56 (m, 1H), 6.28 (dd, *J*= 2.1, 1.9 Hz, 1H), 6.93-7.46 (m, 9H): mass spectrum *m/e* 218 (M^+).

Anal. Calcd for $C_{17}H_{14}$: C, 93.54; H, 6.46. Found: C, 93.78; H, 6.47.

This olefin was hydrogenated over 5% palladium carbon to afford 7 in 80% yield: mp 49-50°C; NMR δ 2.06 (m, 1H), 2.46 (m, 1H), 3.05 (m, 3H), 3.98 (m, 2H), 6.03 (d, *J*= 15 Hz, one of aromatic protons), 6.60-7.23 (m, 8H); mass spectrum *m/e* 220 (M^+).

Anal. Calcd for $C_{17}H_{16}$: C, 92.68; H, 7.32. Found: C, 92.45; H, 7.18.

endo-1-Hydroxy-*exo*-1-phenyl-1,1a,2,2a-tetrahydro-*7H*-cyclobut[*a*]indene (8). The cycloadduct of indene and dichloroketene[38] was reduced with activated zinc dust to afford 1,1a,2,2a-tetrahydro-*7H*-cyclobut[*a*]inden-1-one in 77% yield: mp 41-42°C. The IR and NMR spectra were in accord with those reported.[38]

In a similar way to the preparation of 5, the reaction of this ketone with phenylmagnesium bromide gave 8 in 93% yield; mp 61-63°C; IR 3590 cm^{-1} (OH); NMR δ 1.62 (s, 1H), 2.07 (ddd, *J*= 25.4, 7.8, 2.0 Hz, 1H), 3.05 (m, 2H), 3.51 (m, 2H), 3.51 (m, 3H), 6.95-7.44 (m, 9H); mass spectrum *m/e* 236 (M^+).

Anal. Calcd for $C_{17}H_{16}O$: C, 86.41; H, 6.82. Found: C, 86.13;H,6.88.

endo-1-Phenyl-1,1a,2,2a-tetrahydro-*7H*-cyclobut[*a*]indene (9). Bromination of 8 with phosphorous tribromide gave the corresponding bromide as an oil in 88% yield: bp 105-110°C (0.01 mmHg). A hexamethylphosphoric triamide solution (50 mL) of the bromide (12.7 g, 43 mmol) and 1,8-diazabicyclo[5.4.0]undec-7-ene (13 g, 86 mmol) was heated at 80°C for 10 h under a nitrogen atomosphere, cooled to room temperature, and then added to 200 mL of diethyl ether. The ether solution was washed with 0.1 M hydrochloric acid, saturated sodium bicarbonate, and brine, dried, and filtered. After evaporation of the ether, fractional distillation of the residual oil gave a colorless oil: bp 103-104°C (0.01 mmHg). This

oil solidified and was recrystallized from methanol to give pure 1-phenyl-1a,2a-dihydro-7*H*-cyclobut[*a*]indene (5.8 g, 70% yield): mp 55-57°C; NMR δ 3.06 (m, 2H), 3.88 (m, 1H), 4.22 (m, 1H), 6.50 (s, 1H), 6.80-7.31 (m, 9H); mass spectrum *m/e* 218 (M^+).

Anal. Calcd for $C_{17}H_{14}$: C, 93.54; H, 6.46. Found: C, 93.29; H, 6.25.

Catalytic hydrogenation of this olefin over 5% palladium carbon gave 9 as a colorless oil in 82% yield: bp 81-82°C (0.01 mmHg); NMR δ 2.25 (m, 1H), 2.78 (m, 2H), 2.98 (m, 1H), 3.53 (m, 1H), 3.88 (m, 2H), 6.80-7.32 (m, 9H); mass spectrum *m/e* 220 (M^+).

Anal. Calcd for $C_{17}H_{16}$: C, 92.68; H, 7.32. Found: C, 92.39; H, 7.26.

exo,cis-1,2-Di(hydroxymethyl)-1,1a,2,2a-tetrahydro-7*H*-cyclobut[*a*]indene (10). The dimethyl ester of the photocycloadduct of indene and maleic anhydride[39] was reduced with lithium aluminum hydride to afford dialcohol 10 in 55% yield. This compound was recrystallized from hexane: mp 80-81°C; IR 3580 cm^{-1} (OH); NMR δ 2.09 (s, 2H), 2.80 (m, 2H), 3.14 (m, 2H), 3.63 (m, 2H), 3.86 (s, 4H), 7.06 (s, 4H); mass spectrum *m/e* 204 (M^+).

Anal. Calcd for $C_{13}H_{16}O_2$: C, 76.44; H, 7.90. Found: C, 76.20; H, 7.64.

exo,cis -1,2-Dimethyl-1,1a,2,2a-tetrahydro-7*H*-cyclobut[*a*]indene (11). Dialcohol 10 was converted into the corresponding ditosylate in 62% yield by the published method.[40] This ditosylate was reduced with lithium aluminum hydride to afford 11 in 49% yield. This compound was purified by preparative GLC and fractional distillation: bp 58-60°C (0.01 mmHg); NMR δ 0.98 (d, 3H), 1.23 (d, 3H), 2.40-4.12 (m, 6H), 6.80-7.25 (m, 4H); mass spectrum *m/e* 172 (M^+).

Anal. Calcd for $C_{13}H_{16}$: C, 90.64; H, 9.36. Found: C, 90.90; H, 9.12.

1,1a,2,2a-Tetrahydro-7*H*-cyclobut[*a*]indene (12). To lithium aluminum hydride (3.9 g, 110 mmol) in 300 mL of dry diethyl ether was added dropwise the photocycloadduct of indene and tetrachloroethylene[41] (15 g, 53 mmol) in 200 mL of dry diethyl ether under ice-cooling and the mixture was refluxed for 8 h. After careful addition of saturated ammonium chloride, the ether solution was decanted, washed with 0.1 M hydrochloric acid, saturated sodium bicarbonate, and brine, dried, and filtered. Evaporation left colorless solids. Recrystallization from methanol gave pure 1,2-dichloro-1a,2a-dihydro-7*H*-cyclobut[*a*]indene (9.5 g, 85% yield): mp 48-49°C (lit.[41] 49-50°C). The NMR spectrum was in good agreement with that reported.[42]

This dichloroolefin was dechlorinated by sodium in t-butyl alcohol according to the published method[43] to give 1a,2a-dihydro-7*H*-cyclobut[*a*]indene in 40% yield. This compound was purified by purified by preparative GLC and fractional distillation: bp 37-38 °C (0.1 mmHg). The NMR spectrum was in good agreement with that reported.[42]

The catalytic hydrogenation of this olefin over 5% palladium carbon gave 12 in 80% yield. This compound was purified by preparative GLC and fractional distillation: bp 81-82°C (18 mmHg); mass spectrum *m/e* 144 (M^+). The NMR spectrum was in good agreement with that reported.[42]

Anal. Calcd for $C_{11}H_{12}$: C, 91.61; H, 8.39. Fuond; C, 91.29; H,8.67.

3-3 REDOX-PHOTOSENSITIZED CHAIN MONOMERIZATION OF CIS,SYN-DIMETHYLTHYMINE CYCLOBUTANE DIMER AND UNUSUAL EFFECT OF MOLECULAR OXYGEN

3-3-1 INTRODUCTION

Photosensitized monomerization of thymine cyclobutane dimers is of biological interest with regard to enzymatic photoreactivation (PR) of damaged DNA and has been investigated for understanding of known molecular mechanisms of PR.[6a,44,45] Even in typical photosensitized reactions, however, quantum yields for monomerization are usually low,[44,45] 0.5 at best.[6a] Since PR is thought to be very efficient,[46] a model reaction should meet, at least, the requirement that efficiencies be high. In this section the author describes that *cis,syn*-dimethylthymine cyclobutane dimer (DMT◇DMT) is efficiently monomerized by the redox-photosensitization using aromatic hydrocarbon (S)—*p*-dicyanobenzene (DCNB)—acetonitrile systems, which has been described in chapter 2 and the previous section, and that oxygen molecules remarkably enhance efficiencies of the photosensitized monomerization.

3-3-2 RESULTS AND DISCUSSION

Irradiation of an air-saturated dry acetonitrile solution containing phenanthrene (P), DCNB, and DMT◇DMT at 313 nm gave N,N'-dimethylthymine (DMT) in nearly quantitative yield (<97%) (based on

2 mol formation of DMT per 1 mol of DMT◇DMT) even at ca. 100% conversion (Figure 9), whereas both P and DCNB were completely recovered. In the absence of either P or DCNB, the monomerization did not occur at all. Table 9 lists quantum yield for formation of DMT (ϕ_{DMT}) and oxidation potentials of S and DMT◇DMT.

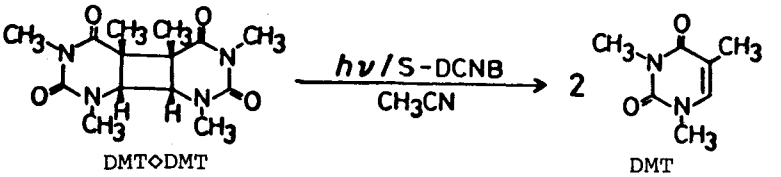

DMT◇DMT DMT

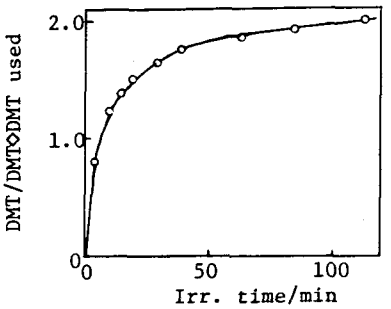

Figure 9. Formation curve of DMT [mol per mol of DMT◇DMT] *vs.* irradiation times in the redox-photosensitized monomerization of DMT◇DMT. Air-saturated solutions; 313 nm irradiation; [DMT◇DMT]= 0.01 M, [P] = 0.01 M, and [DCNB] = 0.1 M.

Table 9. Quantum yield for redox-Photosensitized monomerization of DMT◇DMT and oxidation potentials of S and DMT◇DMT[a]

S	$E^{ox}_{1/2}$ [b]/V	ϕ_{DMT}
Triphenylene	1.29	10.68
Naphthalene	1.22	8.83
Phenanthrene (P)	1.17	8.36
Chrysene	1.05	0.11
Pyrene	0.78	0.00
Anthracene	0.75	0.00
DMT◇DMT	1.45	-

[a] Air-saturated dry acetonitrile solutions containing S (0.01 M), DCNB (0.1 M) and DMT◇DMT (0.01 M) were irradiated at room temperature using the 313 nm light.
[b] Oxidation Potentials were determined *vs.* Ag/Ag^+ in acetonitrile by cyclic voltammetry.

As is shown in Table 10, quantum yields remarkably depend on concentration of dissolved O_2; the maximum value was obtained with air-saturated solution. It is notable that quantum yields are over 2 except that for thoroughly degassed solution, demonstrating the occurrence of a chain reaction. Surprisingly, the limiting quantum yields for air-saturated solution using P as S is 205! The effect of O_2 is extremely unusual and has not been observed in

Table 10. Effect of Molecular Oxygen to Redox-Photosensitized Monomerization of DMT◇DMT[a]

	ϕ_{DMT}		ϕ^{∞}_{DMT}
[DMT◇DMT]=	0.01 M	0.04 M	(∞)
Degass	0.039	0.14	1.20
CO_2-saturatn	1.88	-	-
N_2-saturatn	-	3.1	-
Air-saturatn	8.66	30.1	205
O_2-saturatn	3.66	6.6	38

[a] In all the runs, 0.01 M of P and 0.1 M of DCNB were used. Degassing was carried out by five freeze-pump-thaw cycles under vacuum ($<10^{-5}$ mmHg). Each gas-saturated solution was obtained by bubbling with a stream of the corresponding gas for 20 minutes. The limiting quantum yields were from the intercept of liniear plots of ϕ_{DMT}^{-1} *vs.* $[DMT◇DMT]^{-1}$ (Figure 10).

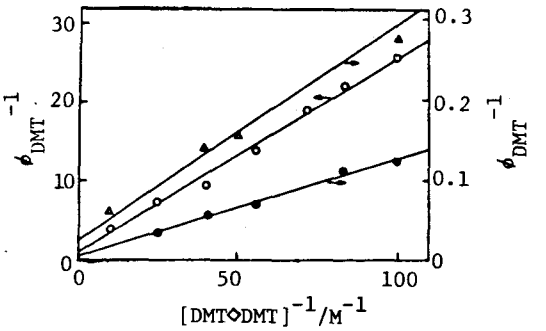

Figure 10. Plots of ϕ_{DMT}^{-1} *vs.* $[DMT◇DMT]^{-1}$ with least-squares fit; degassed(-○-), O_2-saturated (-△-), and air-saturated (-●-) acetonitrile solution; see footnote in Table 10.

the redox-photosensitized cycloreversion of non-boilogical cyclobutane compounds,[47] implying specific interactions of O_2 with DMT◇DMT.

In fact, it was found that a CT-complex is formed between O_2 and DMT◇DMT (Figure 11). Air-saturation of a thoroughly degassed acetonitrile solution of DMT◇DMT caused a slight but significant bathochromic shift of the end absorption, which was considerably

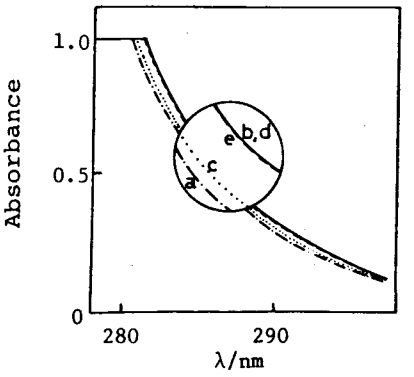

Figure 11. UV-spectra of DMT◇DMT (0.01 M) (a) in a thoroughly degassed acetonitrile solution (—·—), (b) after air-bubbling for 20 min (——), (c) after purging dissolved air from (b) by argon-bubbling for 20 min (···), (d) after air-saturated of (c) by air-bubbling for 20 min (——), and (e) after O_2-saturation of (d) by O_2-bubbling for 20 min (---).

but not completely reduced by subsequent argon-bubbling. When the argon-saturated solution was again aerated, the spectrum of the original air-saturated solution was recovered. The alternate shifts between the spectra of the air- and argon- saturated solutions were repeated several times, thus showing reversible formation of the CT-complex between O_2 and DMT◇DMT, though the complexed O_2 can not be completely removed by argon-bubbling. It should be noted that the spectrum of O_2-saturation was identical to that of air-saturated solution, suggesting that air-saturation can provide enough amounts of O_2 for the maximum formation of the CT-complex. Thus, the spectral changes are in line with the results in Table 10. The remarkable enhancement of ϕ_{DMT} by air-saturation is clearly due to formation of the CT-complex. On the other hand, O_2-saturation results only in an increase of uncomplexed O_2. Therefore, ϕ_{DMT} for O_2-saturated solution is lower than that for air-saturated solution, since uncomplexed O_2 perhaps deactivates such reaction intermediates as excited molecules and ion radicals.

$$DMT\diamond DMT + O_2 \rightleftharpoons DMT\diamond DMT\cdot O_2$$

It is of interest to note that the CT-complex still exists in part even after bubbling with argon.

As discussed in the previous section, the redox-photosensitized monomerization is initiated by electron transfer from excited singlet state of S ($^1S^*$) to DCNB, since DMT◇DMT did neither quench the fluorescence of S nor form CT-complexes with S and DCNB. The mechanism involving the catalytic monomerization by the cation radical of S ($S^{+\cdot}$) without the intervention of DMT◇DMT$^{+\cdot}$ (Scheme 4) is suggested from the following reasons: (1) The photosensitized monomerization did not occur in ethyl acetate. (2) The ϕ_{DMT} increases with an increase in oxidation potentials of S. (3) Oxidation potentials of S are considerably lower than that of DMT◇DMT. (4) The ϕ_{DMT} depends on concentration of DMT◇DMT (Figure 10). (5) The plot of ϕ_{DMT}^{-1} *vs.* concentration of P is linear (Figure 12).[48] (6) The monomerization was quenched by *p*-dimethoxybenzene (Q). The Stern-Volmer plot was linear at low concentration ($<1.5\times10^{-2}$ M) of Q. At higher concentration of Q, however, the plot deviates from the linearity (Figure 13).[49] (7) A similar mechanism is demonstrated for the redox-photosensitized cycloreversion of indene dimers, as discussed in the previous section. According to this mechanism, $P^{+\cdot}$ can monomerize more than

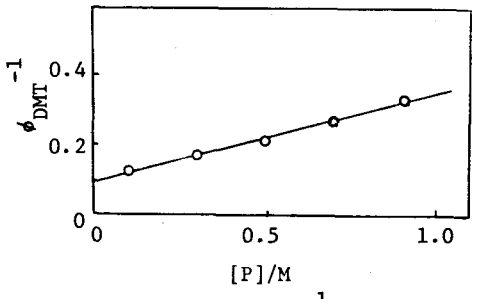

Figure 12. Plot of ϕ_{DMT}^{-1} *vs.* [P] with least-squares fit; 313 nm irradiation; air-saturated acetonitrile solutions; [DMT◇DMT]= 0.01 M and [DCNB]= 0.1 M.

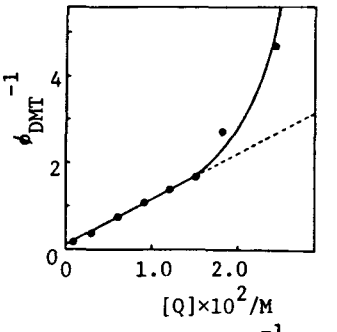

Figure 13. Plot of ϕ_{DMT}^{-1} *vs.* [Q] (Q= *p*-dimethoxybenzene); 313 nm irradiation; air-saturated acetonitrile solutions; [DMT◇DMT]= 0.01 M, [P]= 0.01 M, and [DCNB]= 0.1 M.

one hundred molecules of the dimer complexed with O_2. However, it can not be reasonably interpreted why the complexation with O_2

makes the dimer much more feasible to the catalytic monomerization by S^{+}.

$$S \xrightarrow{h\nu} {}^{1}S^{*}$$

$${}^{1}S^{*} + DCNB \longrightarrow S^{+} + DCNB^{-}$$

$$S^{+} + DMT\diamond DMT\cdot O_2 \xrightarrow{fast} S^{+} + 2\ DMT + O_2^{+}$$

$$S^{+} + DMT\diamond DMT \xrightarrow{slow} S^{+} + 2\ DMT$$

$$S^{+} + X \longrightarrow S \text{ and/or others}$$

(X= $DCNB^{-}$, H_2O, and so on)

Scheme 4.

In summary, the redox-photosensitized monomerization of DMT◇DMT *via* the CT-complex with O_2 is extremely efficient, thus providing a possible model reaction for PR. The author belives that roles of O_2 in PR, especially complexation of UV-damaged DNA with O_2, should not be overlooked. Although, the lack of O_2-effects to PR of UV-irradiated *E. coli*[50] and yeast[51] has been reported, it can not be regarded that the oxygen molecules complexed with damaged DNA may be easily removed by usal methods, *e.g.* N_2-bubbling or simple evacuation.

Finally, it should be noted that *cis,anti*-dimer of DMT was not monomerized at all by the redox-photosensitization.[52,53] Since the oxidation potential of *cis,anti*-dimer (1.82 V) is much higher than that of *cis,syn*-dimer (1.45 V), the importance of through-bond interaction between two n-orbitals of nitrogen atoms at 3- and 3'-positions through C_1–C_1, σ bond of the cyclobutane ring in this monomerization is again emphasized, as discussed in the redox-photosensitized ring cleavage of indene dimers.

3-3-3 EXPERIMENTAL

Materials. Acetonitrile, aromatic hydrocarbons, *p*-dicyanobenzene, and *p*-dimethoxybenzene were purified as described in the privious section. The following compounds were prepared by the reported methods; N,N'-dimethylthymine[54] and *cis,syn*- and *cis,anti*-dimers of N,N'-dimethylthymine.[55]

Analytical Methods. Analytical gas-liquid chromatography (GLC) was performed on a Shimadzu GC-3BF dual column instrument with flame ionization detectors. The column used for quantitative

analyses of N,N'-dimethylthymine was 75×cm 4 mm of 5% Ucon Oil LB-550X on Neopak-1A and methyl palmitate was used as internal standard. GLC analyses of dimers of N,N'-dimethylthymine, the aromatic hydrocarbons, and *p*-dicyanobenzene were carried out with 75 cm×4mm columns of 5% SE-30 on Schimalite W and PEG 20M on Shimalite W.

Ultraviolet spectra were recorded on a Hitachi 323 spectrophotometer. Fluorescence measurements were carried out with a Hitachi MPF-2A fluorometer.

Quantum yields were determined and oxidation potentials were measured in similar manners described in the previous section.

3-4 REFERENCES AND NOTES

[1] R. B. Woodward and R. Hoffmann, "The Conservation of Orbital Symmetry," Verlag Chemie, GmbH, Weinheim/Bergstr., 1970.

[2] H. R. Gerberich and W. D. Walters, J. Am. Chem. Soc., 83, 4884 (1961); L. A. Paqeutte and G. L. Thompson, *ibid.*, 94, 7127 (1972); L. M. Stephenson and J. I. Brauman, *ibid.*, 93, 1988 (1971); L. M. Stephenson and T. A. Gibson, *ibid.*, 96, 5624 (1974); M. J. S. Dewar, S. Kirschner, H. W. Kollmar, and L. E. Wade, *ibid.*, 96, 5242, 5246 (1974).

[3] R. Hoffman, S. Swaminathan, B. G. Odell, and R. Gliter, J. Am. Chem. Soc., 92, 7091 (1970); G. Jones,II, and M. H. Williamson, Jr., *ibid.*, 96, 5617 (1974); G. Jones, II, J. Chem. Educ., 51, 175 (1974).

[4] L. Salem and C. Rowland, Angew. Chem., Int. Ed., 11, 92 (1972); R. E. Bergman, in "Free Radicals," J. K. Kochi, Ed., John Wiley & Sons, Vol. 1, New York, 1973, p. 191.

[5] M. D. Archer, "Photochemical Aspects of Solar Energy Conversion," in Photochemistry, Vol. 6, A Special Periodical Report, Chemical Society Pubblications, London, 1975, p. 739.

[6] (a) A. A. Lamola, Mol. Photochem., 4, 107 (1972); (b) J. C. Sutherland, Photochem. Photobiol., 25, 435 (1977).

[7] A. Weller, Pure Appl. Chem., 16, 115 (1968).

[8] M. Ottolenghi, Accounts Chem. Res., 6, 153 (1973); P. Froelich and E. L. Wehry, in "Modern Fluorescence Spectroscopy," Vol. 2, E. L. Wehry, Ed., Plenum Press, New York, N. Y., 1976, pp. 381-386.

[9] C. Pac and H. Sakurai, Tetrahedron Lett., 3829 (1969); K. Mizuno, C. Pac, and H. Sakurai, J. Chem. Soc., Chem. Commun., 553 (1975); K. Mizuno, H. Okamoto, C. Pac, and H. Sakurai, *ibid.*, 839 (1975).

[10] R. A. Neunteufel and D. R. Arnold, J. Am. Chem. Soc., 95,4080 (1973); D. R. Arnold and A. J. Maroulis, *ibid*., 99, 7355 (1977) and references cited therein.

[11] J. A. Bartrop, Pure Appl. Chem., 33, 179 (1973).

[12] A. Ledwith, Accounts Chem. Res., 5, 133 (1972); S. Farid, S. H. Hartman, and T. R. Evans, in "The Exciplex," M. Gordon and W. R. Ware, Ed., Academic Press, New York, N. Y., 1975, P. 327; T. R. Evans, R. Wake, and O. Jaeckie, *ibid*., p. 345; K. Mizuno, R. Kaji, H. Okada, and Y. Otsuji, J. Chem. Soc., Chem. Commun., 594 (1978).

[13] C. Pac, A. Nakasone, and H. Sakurai, J. Am. Chem. Soc., 99, 5806 (1977).

[14] T. Asanuma, T. Gotoh, A. Tsuchida, Y. Yamamoto, and Y. Nishijima, J. Chem. Soc., Chem. Commun., 485 (1977).

[15] S. Tazuke and N. Kitamura, J. Chem. Soc., Chem. Commun., 515 (1977).

[16] T. Majima, C. Pac, and H. Sakurai, Chem. Lett., 1133 (1979).

[17] S. Tazuke and N. Kitamura, Nature, 275, 301 (1978).

[18] P. Bersford, M. C. Lambert, and A. Ledwith, J. Chem. Soc., (c), 2508 (1970).

[19] S. Takamuku and W. Schnabel, private communication.

[20] G. S. Hammond, N. J. Turro, and A. Fischer, J. Am. Chem. Soc., 83, 4647 (1961); D. S. Kabakoff, J. C. G. Bünzli, J. F. M. Oth, W. B. Hammond, and J. A. Berson, *ibid*., 97, 1510 (1975); K. C. Bishop III, Chem. Rev., 76, 461 (1976); T. Tezuka, Y. Yamashita, and T. Mukai, J. Am. Chem. Soc., 98, 6051 (1976).

[21] H. C. Brown and H. D. Deck, J. Am. Chem. Soc., 87, 5620 (1965).

[22] E. C. Ashby and J. T. Laemmile, Chem. Rev., 75, 521 (1975).

[23] O. L. Chapman, A. A. Griswald, E. Hoganson, G. Lenz, and J. Reasoner, Pure Appl. Chem., 9, 585 (1964).

[24] M. Yasuda, C. Pac, and H. Sakurai, Bull. Chem. Soc. Jpn., 53, No. 1 (1980).

[25] M. Meot-Ner, E. P. Hunter, and F. H. Field, J. Am. Chem. Soc., 100, 5466 (1978).

[26] M. A. J. Rodgers, Chem. Phys. Lett., 9, 107 (1971); A. Kira, S. Arai, and M. Imamura, J. Chem. Phys., 54, 4890 (1971).

[27] T. Hino, H. Akazawa, H. Masuhara, and N. Mataga, J. Phys. Chem., 80, 33 (1976).

[28] P. Bischof, J. A. Hashmal, E. Heilbronner, and V. Hornung, Tetrahedron Lett., 4025 (1969); E. Heilbronner and K. A. Muszkat,

J. Am. Chem. Soc., 92, 3818 (1970).

[26] The activation energy for the thermal cleavage of *tras*-1,2-diphenylcyclobutane into styrene has been reported to be 35.6 kcal/mol and a partial participation of a concerted mechanism has been suggested.[26a] Since 1 is very stable even at 170°C, the activation energy for the thermal cycloreversion of 1 is roughly estimated to be ~30 kcal/mol. If thermolyses of cyclobutane compounds would occur by way of 1,4-diradicals in a ~10 kcal/mol shallow minimum of the potential surface,[26b,c] activation energies for the cycloreversion of 1 *via* the 1,4-diradical should be over ~20 kcal/mol. (a) G. Jones, II and V. L. Chow, J. Org. Chem., 39, 1447 (1974); (b) L. M. Stephenson and J. I. Braunman, J. Am. Chem. Soc., 93, 1988 (1971); (c) MO calculations predict that there are no minima for intermediates but a large flat region of a potential surface; R. Hoffmann, S. Swaminathan, B. G. Odell, and R. Gleiter, J. Am. Chem. Soc., 92, 7091 (1970).

[27] Redox-photosensitized ring cleavage of 13-*cis* and 13-*trans* gave 14-*cis* and 14-*trans* respectively along with 15 in a 1:1-ratio, clearly demonstrating the stereospecific nature of the cycloreversion. Therefore, it has been that the cycloreversion would occur either in a concerted mechanism or *via* very short-lived singlet 1,4-diradicals; T. Majima, C. Pac, and H. Sakurai, unpublished results.

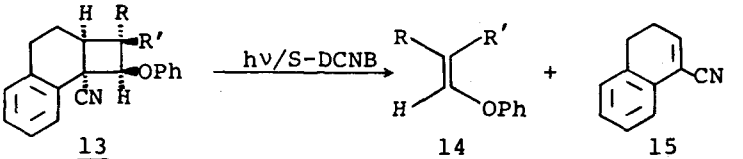

13 14 15

cis: R = H, R′ = CH_3

trans: R = CH_3, R′ = H

[28] D. E. Worrall, Org. Synth., Coll. Vol. 1, 413 (1941).

[29] H. O. House, E. Feng, and N. P. Peet, J. Org. Chem., 36, 2731 (1971).

[30] D. J. Rief and H. O. House, Org. Synth., Coll. Vol. 4, 375 (1963).

[31] E. J. Eisenbraun, Org. Synth., Coll. Vol. 5, 310 (1973).

[32] P. J. Wagner, Tetrahedron Lett., 5795 (1968).

[33] C. G. Hatchard and C. A. Parker, Proc. Roy. Soc. (London), A235, 518 (1956).

[34] W. Metzner and D. Wendisch, Liebigs Ann. Chem., 730 111 (1969).

[35] C. Lieberman and O. Bergami, Chem. Ber., 22, 784 (1889).

[36] N. Campbell and H. G. Heller, J. Chem. Soc., 933 (1967).

[37] D. E. Applequist and J. D. Roberts, J. Am. Chem. Soc., 78, 4012 (1956).

[38] L. Ghosez, R. Montaigne, A. Roussel, H. Vanlierde, and P. Mollet, Tetrahedron, 27, 615 (1971).

[39] W. Metzner, H. Partale, and C. H. Krauch, Chem. Ber., 100, 3156 (1967).

[40] C. S. Marvel and V. S. Sekera, Org. Synth. Coll. Vol. 3, 366 (1955).

[41] W. Metzner and W. Hartmann, Chem. Ber., 101, 4099 (1968).

[42] W. Wendisch and W. Metzner, Chem. Ber., 101, 4106 (1968).

[43] P. G. Gassman and J. L. Marshall, Org. Synth., Coll. Vol. 5, 424 (1973).

[44] G. J. Fisher and H. E. John, in "Photochemistry and Photobiology of Nucleic Acids," Vol. 1, Ch. 5, Academic Press, New York, 1976.

[45] C. Helene and M. Charlier, Photochem. Photobiol. 25 429 (1977).

[46] H. Harm, in "Photochemistry and Photobiology of Nucleic Acids," Vol. 2, Ch. 6, Academic Press, New York, 1976.

[47] In the case of photosensitized ring cleavages of 1,1a,2,2a-tetrahydro-*7H*-cyclobut[*a*]indene which has been described in section 3-2, quantum yields for formation of olefins in air-saturated solution are significantly lower than in degassed solution.

[48] The linear plot can not be explained by a mechanism involving DMT◇DMT^{+} and/or DMT$^{+\cdot}$ in which the plot must be a curved line with a minimum value or a line with a negative slope.

[49] The curved Stern-Volmer plot demonstrates the existence of two different cation radicals as the reaction intermediates, *i.e.* S$^{+\cdot}$ and the π-complex between S$^{+\cdot}$ and DMT◇DMT.

[50] F. H. Johnson, E. A. Flagler, H. F. Blum, Proc. Soc. Exptl. Biol. Med., 74, 32 (1950).

[51] A. C. Giese, R. M. Iverson, and R. T. Sanders, J. Bacteriol. 74, 271 (1957).

[52] The end absorption of *cis,anti*-dimer of DMT was found to be correspondingly shifted, similarly to *cis,syn*-dimer, when a thoroughly degassed solution was in turn saturated with air, argon, and air. However, the degree of the bathochromic shift

cis,anti-dimer was less than that of *cis,syn*-dimer.

[53] The monomerization of *trans,syn*-dimer of DMT occured by the redox-photosensitization, although the efficiency of the monomerization was lower than that of *cis, syn*-dimer; ϕ^{∞}_{DMT} = 11.8 (air-saturated) and 0.082 (degassed), in acetonitrile solutions containing 0.01 M of P and 0.1 M of DCNB.

[54] D. Davidson and O. Baudisch, J. Am. Chem. Soc., 48, 2379 (1926).

[55] D. L. Wulff and G. Fraenkel, Biochem. Biophys. Acta, 51, 332 (1961).

CHAPTER 4 REDOX-PHOTOSENSITIZED STEREOMUTATION OF 1-PHENOXYPROPENE; CATALYSIS BY THE CATION RADICAL OF AROMATIC HYDROCARBONS

4-1 INTRODUCTION

Numerous studies have been done on *cis,trans*-isomerism of olefins in either the ground state[1] or the electronically excited state.[2] However, only a few papers on stereomutations of olefins *via* the ion radicals have been published so far. Recently, radiation-induced isomerization of *cis*-2-butene is reported to occur *via* the cation radical by means of a chain reaction mechanism,[3] while the *trans*-isomer does not isomerize. Likewise, *cis*-stilbene efficiently isomerizes to the *trans*-isomer upon γ-radiation of benzene solution;[4] a chain mechanism involving the anion radical is suggested. In this chapter, the author describes redox-photosensitized stereomutation of 1-phenoxypropene, using aromatic hydrocarbon–*p*-dicyanobenzene–acetonitrile systems, which has been described in foregoing chapters.

4-2 RESULTS AND DISCUSSION

Irradiation of an acetonitrile solution containing an aromatic hydocarbon (S), *p*-ducyanobenzene (DCNB), and *cis*- or *trans*-1-phenoxypropene (c-P or t-P) at 313 nm resulted in loss of stereointegrity of the starting olefin, ultimately giving rise to a photostationary mixture of c-P and t-P in 1:1-ratio (Figure 1). At a photostaionary state, the material balance was over 95%. Further irradiation of a photostationary mixture led to a slow consumption of the olefins, forming other products which appear to be dimers of the olefin, whereas S and DCNB were completely recovered. When benzene or ethyl acetate was used as solvent, the photoisomerization did not occur at all. The coexistence of S and DCNB was found to be essential for the photosensitized isomerization. Notably, quantum yields for the *cis,trans*-isomarization (Table 1) increase with an increase in oxidation potentials of S.

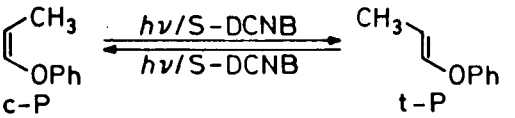

Table 1. Quantum Yields for *cis,trans*-Isomerization of c-P and t-P by Redox-Photosensitization[a]

S	$E^{ox}_{1/2}$[b]/V	$\phi_{c\to t}$	$\phi_{t\to c}$
Anthracene	0.75	~0.0	~0.0
Pyrene	0.78	~0.0	~0.0
Chrysene	1.05	0.58	0.33
Phenanthrene	1.17	0.66	0.41
		(0.95)[c]	(0.58)[c]
Naphthalene	1.20	0.74	0.54
Triphenylene	1.29	0.81	0.58
		(1.19)[c]	(0.81)[c]

[a] [S]= 1.0×10^{-2} M, [DCNB]= 1.0×10^{-1} M, and [c-P or t-P]= 1.0×10^{-4} M in acetonitrile; irradiation at 313 nm. [b] Half-wave values of oxidation potentials *vs.* Ag/Ag^{+} determined by cyclic voltammetry. $E^{ox}_{1/2}$ of c-P and t-P = 1.38 V. [c] Limited quantum yields ($\phi^{\infty}_{c\to t}$ or $\phi^{\infty}_{t\to c}$) extrapolated to infinite concentration of c-P and t-P.

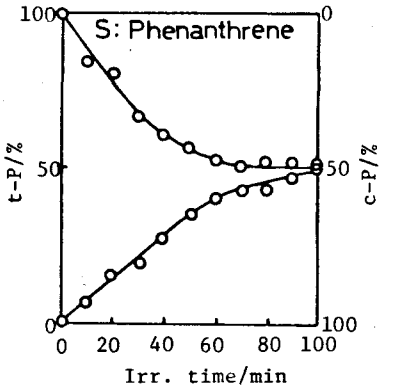

Figure 1. Plots of c-P or t-P % *vs.*irradiation time; [S]= 1.0×10^{-2} M, [DCNB]= 1.0×10^{-1} M, and [c-P or t-P]= 1.0×10^{-4} M; at 313 nm.

Triplet mechanisms for the photosensitized isomerization can be safely excluded, since 1.0 M isoprene did not quench the isomerization at all. UV spectra revealed that charge transfer complexes are not formed in the ground state. Moreover, the fluorescence of S was not quenched by c-P and t-P at all. Thus, the olefins do not interact with S in either the ground or excited singlet state and with DCNB in the ground state.

As stated foregoing chapters, electron transfer from excited singlet S ($^1S^*$) to DCNB is responsible for the initiation process, being in accord with the requirements for the occurrence of the photosensitized isomerization that aprotic solvent and the co-existence of S and DCNB are essential. For mechanistic elucidation, it should be noted that the values of $\phi_{c\to t}$ plus $\phi_{t\to c}$ are over unity,[5] and that quantum yields depend on oxidation potentials of S. This suggested that the isomerization proceeds by means of a chain reaction mechanism involving the cation radical of S ($S^{+\cdot}$). However, the oxidation potentials of S are considerably lower than those of c-P and t-P. Therefore, it is suggested that the cation

radical of S forms π-complexes with the olefins which act as key intermediates; partial development of the positive charge on the olefin side would lead to a decrease in bond order of the olefinic double bond, thus making the double bond capable of bond rotation. Simplified reaction pathways are shown in Scheme 1. Chain termination processes would involve loss of the positive charge of cation radicals, formation of other products and so on.

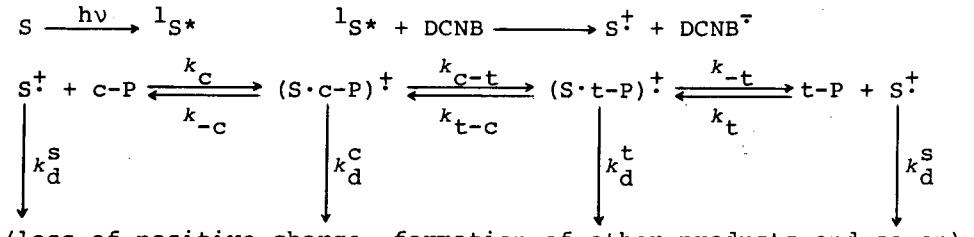

Scheme 1.

At photostationary state, $[c\text{-P}]/[t\text{-P}] \simeq (k_t/k_{-t}) \times (k_{-c}/k_c) \times (k_{t-c}/k_{c-t}) = K_t/(K_c \cdot K_{c-t}) = 1.0$, provided $k_{-c} >> k_d^c + k_{c-t}$, $k_{-t} >> k_d^t + k_{t-c}$, and $k_c[c\text{-P}]$ or $k_t[t\text{-P}] >> k_d^s$. If $k_d^c \simeq k_d^t$, $\phi_{c-t}^{\infty}/\phi_{t-c}^{\infty} \simeq k_{c-t}/k_{t-c} = K_{c-t} = 1.5$ (S = triphenylene) or 1.65 (S = phenanthrene), from which K_t/K_c can be calculated to be 1.5 or 1.65. These values suggest that the isomerization of $(S\cdot c\text{-P})^{+\cdot}$ to $(S\cdot t\text{-P})^{+\cdot}$ slightly predominates over the reverse reaction, whereas formation of $(S\cdot c\text{-P})^{+\cdot}$ from $S^{+\cdot}$ and c-P is correspondingly less favorable than that of $(S\cdot t\text{-P})^{+\cdot}$ from $S^{+\cdot}$ and t-P.

Alternatively, the complete hole transfer from $S^{+\cdot}$ to c-P or t-P would occur to form $c\text{-P}^{+\cdot}$ or $t\text{-P}^{+\cdot}$, which would lose stereointegrity. Electron transfer from S to $c\text{-P}^{+\cdot}$ and $t\text{-P}^{+\cdot}$ would regenerate $S^{+\cdot}$ along with the stereomutation of the olefin. However, this mechanism apperars to be unfavorable since the hole transfer process is considerably endothermic.

Finally, it should be noted that the redox-photosensitized isomerization of *trans*-β-methylstyrene and *trans*-anethole was found to occur in either the absence or presence of isoprene, giving again photostationary mixtures of the *cis*- and *trans*-isomers in 1:1-ratio.[6] The redox-photosensitization would thus provide another route for stereomutation of olefins.

4-3 EXPERIMENTAL

Acetonitrile, aromatic hydrocarbons, and *p*-dicyanobenzene were purified as described in chapter 3. 1-Phenoxypropene were prepared according to the published method[7] and separated to *cis*- and *trans*-isomers by preparative gas-liquid chromatography. *trans*-Anethole and *trans*-β-methylstyrene (Tokyo Kasei Co., Ltd.) were distilled from sodium under a pure nitrogen stream before use.

Analytical gas-liquid chromatography, spectroscopic studies, quantum yields, and oxidation potentials were carried out as descibed in chapter 3. The column used for quantitative analyses of 1-phenoxypropene was 75 cm × 4 mm of 5% Ucon Oil LB-550X on Neopak-1A and n-tridecane was used as internal standard.

4-4 REFERENCES AND NOTES

[1] K. Mackenzie, in "The Chemistry of Alkenes," Ed by S. Patai, Interscience, 1964, p. 387 and Vol. 2, 1970, p. 115.

[2] J. Saltiel, J. D'Agostino, E. D. Megarity, L. Metts, K. R. Neuberger, M. Wrighton, and O. C. Zafiriou, in "Organic Photochemistry," Ed. by O. L. Chapman, Marcel Dekker, Vol. 3, 1973, p. 1.

[3] Y. Harata, M. Matsui, and M. Imamura, Chem. Lett., 199 (1977).

[4] R. R. Hentz, K. Shima, and M. urton, J. Phys. Chem., 71, 461 (1967).

[5] The values do not necessarily indicate the true chain length, since quantum yields of reactive cation radicals of S are probably less than unity; the quantum yield was determined to be 0.2 in the redox-photosensitized ring cleavage of indene dimers (see chapter 3).

[6] *cis*- and *trans*-1-Methoxypropene and 2-butene were not isomerized by the redox-photosensitization, suggesting the requirement of aryl substituents for the occurrence of redox-photosensitized stereomutation of olefins.

[7] S. M. McElvain and B. Fajardo-Pinzon, J. Am. Chem. Soc., 67, 650 (1945).

CHAPTER 5 RADIATION-INDUCED CYCLOREVERSION OF INDENE CYCLOBUTANE DIMERS IN N-BUTYL CHLORIDE BY A CHAIN REACTION MECHANISM

5-1 INTRODUCTION

Ion radicals are important intermediates in radiation chemistry and can be selectively formed by radiolyses of organic solutions.[1] However, radiolytic chain reactions which involve ionic species as chain carriers have been scarcely published except polymerization reactions; radiation-induced chain isomerizations of *cis*-butene and *cis*-stilbene occur *via* the cation radical and the anion radical respectively.[2,3] In chapter 3 the author described redox-photosensitized ring cleavage of indene cyclobutane dimers involving catalytic cleavage by cation radical of aromatic hydrocarbons. In this regard, cycloreversion of the dimers *via* cation radical of the dimers is of interest. Thus the author studied γ-radiolysis of the dimers in n-butyl chloride. In this chapter, the author describes that chain cycloreversion of 1 and 2 occurs upon γ-radiation of n-butyl chloride solutions, while the other similar compounds, 3, 4, and 5 are stable to the γ-radiolysis.

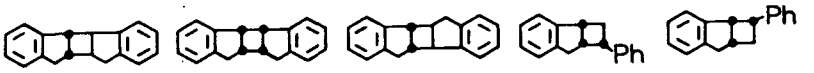

1 2 3 4 5

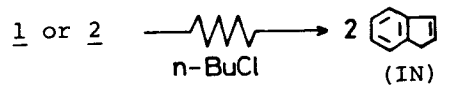

5-2 RESULTS AND DISCUSSION

Solutions of 1 in n-butyl chloride were degassed by freeze-pump-thaw cycles under a high vacuum and irradiated with 4 KCi ^{60}Co at room temperature. Gas-liquid chromatography showed that indene (IN) was the only detectable product and that the formation increased linearly with irradiation time up to ca. 20% conversion (Figure 1). The significantly dose dependency of G(IN) seems to be caused by efficient competitive scavenging of the active species by IN formed. Addition of 1- and 2-butene had no effects

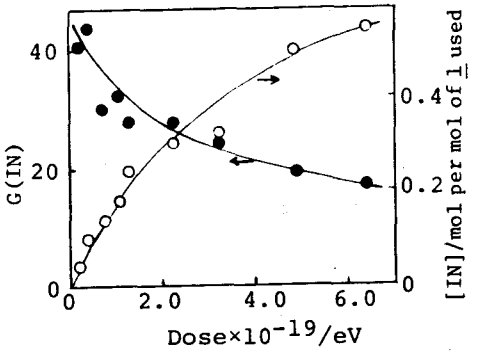

Figure 1. Radiation-induced formation of IN in n-butyl chloride solution of 1; [1]= 1.0×10^{-2} M.

Table 1. Effects of Additives and Dose Rate in γ-Radiolysis of 1 in n-Butyl Chloride[a]

	G(IN)
Additives[b]	
None	40.0
1-Butene[c]	39.3
2-Butene[c]	40.2
O_2[d]	39.6
CH_3OH	<0.1
Indene (10^{-3} M)	18.8
Indene (5×10^{-3} M)	10.6
Dose rate ($\times10^{19}$ eV/g·h)	
6.19	42.6
1.29	40.9
0.976	37.9

[a] [1]= 10^{-2} M. [b] Dose rate, 1.29×10^{19} eV/g.h. [c] Bubbling for 5 min. [d] Air-saturated.

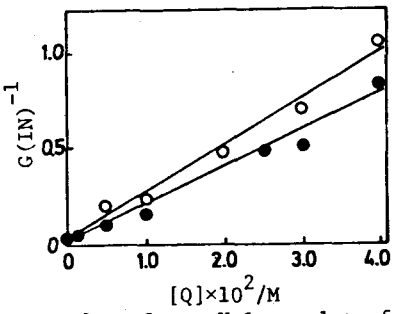

Figure 2. Stern-Volmer plots for quenching by 1,4-dimethoxybenzene (-o-) and 1,1-dimethylindene (-●-); [1]= 10^{-2} M; dose rate, 1.29×10^{19} eV/g·h.

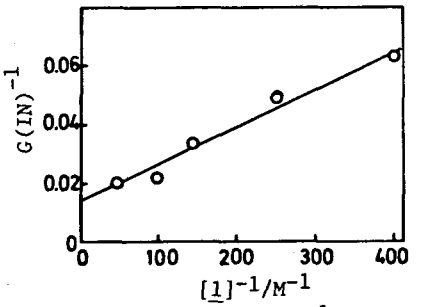

Figure 3. Plot of $G(IN)^{-1}$ *vs.* $[1]^{-1}$; dose rate, 1.29×10^{19} eV/g·h.

on this reaction. This reaction was, however, completely quenched by 0.1 M of either methanol or 1,4-dimethoxybenzene, but not at all by molecular oxygen. The G(IN) is independent of the dose rate. The results are summarized in Table 1 and Figure 2. These results clearly demonstrate that the cycloreversion proceeds by means of a cation radical mechanism and that neither excited species not free radicals participate in the reaction at all. In Figure 3 is shown a linear plot of $G(IN)^{-1}$ *vs.* $[1]^{-1}$, from which the limiting G value (G^{∞}) was determined to be 67.

γ-Radiation of n-butyl chloride solution is known to give n-

butyl chloride cation ($BuCl^{+\cdot}$)[1,4] in the G value of ca. 3,[1] which decays within 80 μs at 113 K to give butene cations.[4] Therefore, G^{∞} clearly demonstrates the occurrence of a chain reaction. As has been discussed in the redox-photosensitized cycloreversion of 1,[5] it is suggested that the cycloreversion of 1 is catalyzed by cation radicals without hole transfer. For mechanistic elucidation, therefore, the author proposes the following mechanistic pathways (Scheme 1), where $S^{+\cdot}$ and Q represent the cation carrier and 1,4-dimethoxybenzene respectively.

$$BuCl \xrightarrow{\sim} BuCl^{+\cdot} + e^{-} \quad (G_0 \simeq 3)$$

$$BuCl + e^{-} \longrightarrow Bu\cdot + Cl^{-}$$

$$BuCl^{+\cdot} \xrightarrow{k_d} C_4H_8^{+\cdot} \text{ (+ other products)}$$

$$S^{+\cdot} + 1 \xrightarrow{k_r} S^{+} + 2\,IN$$

$$S^{+\cdot} + 1 \xrightarrow{k_{ht}} S + 1^{+\cdot}$$

$$S^{+\cdot} + Q \xrightarrow{k_q} S + Q^{+\cdot}$$

$$1^{+\cdot} \xrightarrow{k_c} IN^{+\cdot} + IN$$

$$IN^{+\cdot} \longrightarrow \text{Other product(s)}$$

Scheme 1.

As the cation carrier, indene cation $IN^{+\cdot}$, can be safely discarded, since the cycloreversion was quenched by either 1,1-dimethylindene or indene. For $1^{+\cdot}$ to act as the chain carrier, the lifetime should be longer than 100 ns,[6] being unusally long compared with that of tetraphenylcyclobutane cation; it is estimated to be much shorter than 20 ns.[7] Therefore, $1^{+\cdot}$ appears to be unfavorable for the chain carrier. If $BuCl^{+\cdot}$ is the chain carrier, eq 1 can be derived, being in accord with the linear relationships of $G(IN)^{-1}$ *vs.* $[1]^{-1}$ and [Q] in Figures 2 and 3.

$$\frac{1}{G(IN)} = \frac{1}{G_0}\left(\frac{k_{ht}}{2k_r + k_{ht}}\right)\left(1 + \frac{k_d + k_q[Q]}{k_{ht}[1]}\right) \qquad (1)$$

Provided $k_q \simeq 10^{10}\ M^{-1}s^{-1}$ and $G_0 \simeq 3$, the following rate constants are obtained from the intercepts and slopes in Figures 2 and 3; $k_r \simeq 10^{10}\ M^{-1}s^{-1}$, $k_{ht} \simeq 10^{9}\ M^{-1}s^{-1}$, and $k_d \simeq 8\times10^{6}\ s^{-1}$. The value of k_r suggests that the catalytic cleavage occurs on

every collision. However, detailed discussion requires further investigation. For example, $S^{+\cdot}$ may be a "vibrationally excited" hole[4] or a relaxed hole; hole capture by Q or by 1 may occur by a hole migration process or a charge transfer process.

Equation 1 can be transformed to eq 2, where $G(IN)_0$ and $G(IN)_Q$ are G-values for IN formation in the absence and in the presence of Q respectively. The $G(IN)_Q$ values were determined for various

$$\log\left(\frac{G(IN)_0}{G(IN)_Q} - 1\right) = \log\left(\frac{k_q[Q]}{k_{ht}[1] + k_d}\right) \equiv (\log k_q)_{rel} \qquad (2)$$

compounds as Q. The plot of $(\log k_q)_{rel}$ *vs.* oxidation potentials of Q ($E^{ox}_{1/2}(Q)$) gave a curved line which is interpreted by the Marcus theory[8] for electron transfer reactions (Figure 4). This

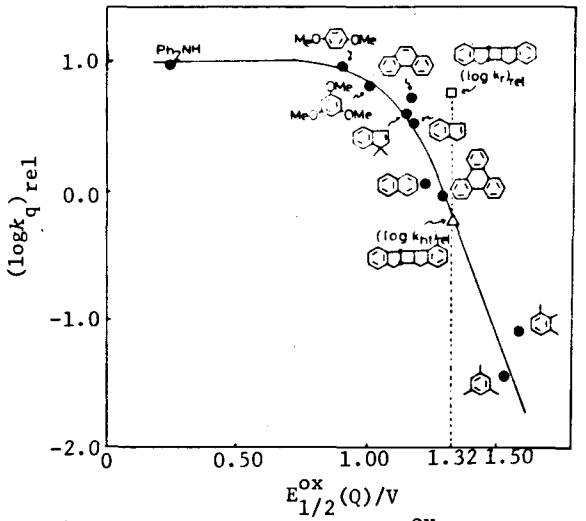

Figure 4. Plot of $(\log k_q)_{rel}$ *vs.* $E^{ox}_{1/2}(Q)$ for quenching of the radiolytic cycloreversion of 1 by various compounds (Q); $[1] = 10^{-2}$ M; dose rate, 1.29×10^{19} eV/g·h.

demonstrates that Q acts as a quencher of the chain carrier, *i.e.* $BuCl^{+\cdot}$, of the cycloreversion, that relative rate constant for the quenching process depends on $E^{ox}_{1/2}(Q)$, and that hole transfer from $BuCl^{+\cdot}$ to Q with lower oxidation potentials than 0.9 V occurs at a diffusion-controlled rate. From the rate constants obtained above the relative rate constant for hole transfer from $BuCl^{+\cdot}$ to 1 $\log\{k_{ht}[1]/k_{ht}[1] + k_d)\} = (\log k_{ht})_{rel}$ and for the cyclorever-

sion process $\log\{k_r[\underline{1}]/(k_{ht}[\underline{1}] + k_d)\} = (\log k_r)_{rel}$ can be calculated. Interestingly, plot of $(\log k_{ht})_{rel}$ *vs.* $E^{ox}_{1/2}(\underline{1})$ was found to be on the curved line, while the plot of $(\log k_r)_{rel}$ *vs.* $E^{ox}_{1/2}(\underline{1})$ deviated significantly. This suggests that the mechanism of the cycloreversion is distinct from a mechanism of hole transfer.

The radiolytic cycloreversion of $\underline{2}$ was more efficiently than that of $\underline{1}$; the G(IN) value at 10^{-2} M of $\underline{2}$ was 56.7. This can be reasonably understood, since $\underline{2}$ is more strained owing to the *cis*-configuration than $\underline{1}$. In contrast, $\underline{3}$, $\underline{4}$, and $\underline{5}$ were not radiolytically cleaved in n-butyl chloride.[9] The occurrence of radiolytic cycloreversion of cyclobutane compounds in n-butyl chloride would thus depend on stereoelectronic structures of compounds. For example, a through-bond interaction between two π-electron systems can occur in $\underline{1}$ and $\underline{2}$ but not in $\underline{3}$. In this regard, it should be noted that the oxidation potential of $\underline{1}$ (1.32 V) is identical to that of $\underline{2}$ by significantly lower than that of $\underline{3}$ (1.49 V). Moreover, ring strain energies should be also taken into consideration; the inertness of $\underline{4}$ and $\underline{5}$ to the catalytic cycloreversion would arise mainly from the less strained structure.[10]

5-3 EXPERIMENTAL

n-Butyl chloride (Wako Pure Chemical Ind.) was repeatedly shaken with concentrated sulfuric acid and washed water and solution of sodium bicarbonate. Then the butyl chloride was shaken with a solution of sodium hydroxide, washed with water, dried with calcium chloride, and fractionally distilled three times from phosphorous pentoxide. 1,1-Dimethylindene was prepared according to the published method.[11] Indene and *p*-dimethoxybenzene were purified as described in chapter 3. All other chemicals were reagent grade and purified fractional distillation and/or recrystallization.

Analytical gas-liquid chromatography and measurements of oxidation potentials were carried out as descibed in chapter 3.

5-4 REFERENCES AND NOTES

1 W. H. Hamill, in "Radical Ions," Ed by E. T. Kaiser and L. Kevan, John Wiley & Sons, New York, N. Y. 1968, p. 321.

2 Y. Harata, M. Matsui, and M. Imamura, Chem. Lett., 199 (1977).

[3] R. R. Hentz, K. Shima, and M. Burton, J. Pys. Chem., 71, 461 (1967).

[4] S. Arai, A. Kira, and M. Imamura, J. Phys. Chem., 80, 1968 1976).

[5] See chapter 3.

[6] If $\underline{1}^{+\cdot}$ is the chain carrier, the rate equation does not agree with the results in Figures 2 and 3. However, eq 2 can be obtained by taking into account of the process, $\underline{1}^{+\cdot} + \underline{1} \xrightarrow{k_t}$ $IN^{+\cdot}$ + 3 IN, and assuming that $k_{ht}[\underline{1}] >> k_d$ and $2k_r[\underline{1}] >> k_c$. If $k_r \simeq 10^{10}$ $M^{-1}s^{-1}$, k_c is 8.5×10^6 s^{-1}; this is the maximum value.

$$\frac{1}{G(IN)} = \frac{1}{G_0}\left(\frac{k_t}{2k_r + 3k_t}\right)\left(1 + \frac{k_c + k_q[Q]}{k_t[\underline{1}]}\right) \qquad (2)$$

[7] S. Takamuku, S. Miki, and H. Sakurai, unpublised results.

[8] R. A. Marcus, J. Chem. Phys., 24, 966, 979 (1956); 44, 679 (1965); Annu. Rev. Pys. Chem., 15, 155 (1964).

[9] Radiolytic cycloreversion of 6 and 7 in n-butyl chloride did not occur at all. However, 8 and 9 cleaved to give indene in 4.6 and 3.0 G(IN) respectively (at [8 or 9]= 10^{-2} M; dose rate, 1.29×10^{19} eV/g·h).

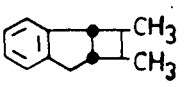

6

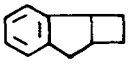

7

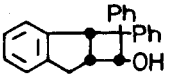

8

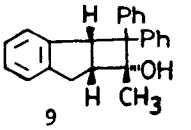

9

[10] Oxidation potentials of 10 and 11 are 1.58 and 1.44 V respectively.

[11] L. L. Miller and R. F. Boyer, J. Am. Chem. Soc., 93, 645 (1971).

CONCLUSION

The results obtained from the present investigation may summarized as follows;

Chapter 1: Pyridine, methylated pyridines, and methylated imidazoles quenched the exciplexes of aromatic nitrile–2,5-dimethylfuran or 2,5-dimethyl-2,4-hexadiene, and the rate constants for the exciplex quenching were obtained. The exciplex quenching by 2-methyl and 2,6-dimethylpyridines was much less efficient than that by the other quenchers. The exciplex quenching was discussed in terms of the interaction of the n-orbital of the quenchers with the positive charge developed on the electron-donor side of the exciplexes. Curved Stern-Volmer plots were obtained in the quenching of aromatic nitrile fluorescence by 1-methylimidazole and/or 1,2-dimethylimidazole. On the basis of the kinetic results, the mechanism was discussed in terms of a termolecular interaction between excited singlet aromatic nitrile, the methylated imidazole as the π-donor, and the second one as the n-donor.

Chapter 2: The redox-photosensitized using aromatic hydrocarbon–dicyanobenzene–acetonitrile systems caused ionic reactions of electron donors such as furan, 2-methyl- and 2,5-dimethylfuran, 1,1-diphenyl ethylene, and indene to give the ionic products. It was found that the initiation process was photoredox reaction, an important intermediate was the cation radical of S acting as a redox carrier, and the π-complex of the electron donor with the cation radical of aromatic hydrocarbons was a key intermediate. The analysis of kinetics of anti-Markownikoff addition of methanol to 1,1-diphenylethylene, was investigated in detail. The rate constants for the formation of the π-complex and for the attack of methanol on the π-complex were determined to be 3.4×10^{9} $M^{-1}s^{-1}$ and 9.0×10^{5} $M^{-1}s^{-1}$ respectively. The importance of chemically stable cation radicals for the occurrence of the redox-photosensitized reactions was discussed.

Chapter 3: Selective photoexcitation of aromatic hydrocarbon in the aromatic hydrocarbon–dicyanobenzene–*trans,syn*-indene dimer–acetonitrile system resulted in the ring cleavage of the dimer to give indene in a limiting quantum yield of >8. The mechanistic aspects in the redox-photosensitized chain cycloreversion of the dimer were investigated in detail. The π-complex of the dimer with the cation radical of aromatic hydro-

carbons which was generated by photochemical electron transfer with dicyanobenzene was shown to be a key intermediate, by way of which the cycloreversion of 1 rapidly occurred without the formation of its cation radical; the rate constant for the cycloreversion was determined to be 1×10^{9} s^{-1}. Redox-photosensitization was applied to the other related compounds and it was found that the cyclobutanes which could undergo redox-photosensitized ring cleavage possessed the phenyl group at C_2. The importance of through-bond interactions between the two π-electron systems was discussed.

cis,syn-Dimethylthymine dimer was monomerized by means of a chain reaction upon selective photoexcitation of aromatic hydrocarbonds in aerated acetonitrile in the presense of *p*-dicyanobenzene. It was found that remarkable enhancement of quantum yields by air-saturation was clearly due to formation of the CT-complex which was confirmed by UV spectra.

Chapter 4: The stereomutation of 1-phenoxypropene occurred by the redox-photosensitization using aromatic hydrocarbons–dicyanobenzene–acetonitrile systems, giving rise to a photostationary mixture of the *cis*- and *trans*-isomers in 1:1-ratio. The quantum yields for the *trans*→*cis* and *cis*→*trans* isomerizations were over unity. The mechanism was discussed in terms of catalysis by the cation radical of aromatic hydrocarbons.

Chapter 5: The cycloreversion of *trans,syn*- and *cis,syn*-indene dimers occurred upon γ-radiation of n-butyl chloride solutions. The effects of additives and high G values for formation of indene demonstrated that the cycloreversion proceeds by means of a chain reaction mechanism involving cation radicals as chain carriers.